UNIVERSITI TEKNOLOGI MALAYSIA

BORANG PENGESAHAN
LAPORAN AKHIR PENYELIDIKAN

TAJUK PROJEK :　**DEVELOPMENT OF LOW NOx LIQUID FUEL BURNER**

Saya _____**MOHAMMAD NAZRI MOHD JAAFAR**_____
(HURUF BESAR)

Mengaku membenarkan **Laporan Akhir Penyelidikan** ini disimpan di Perpustakaan　Universiti Teknologi Malaysia dengan syarat-syarat kegunaan seperti berikut :

1.　Laporan Akhir Penyelidikan ini adalah hakmilik Universiti Teknologi Malaysia.

2.　Perpustakaan Universiti Teknologi Malaysia dibenarkan membuat salinan untuk tujuan rujukan sahaja.

3.　Perpustakaan dibenarkan membuat penjualan salinan Laporan Akhir Penyelidikan ini bagi kategori TIDAK TERHAD.
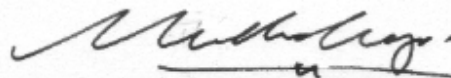
4.　* Sila tandakan (/)

☐　SULIT　(Mengandungi maklumat yang berdarjah keselamatan atau Kepentingan Malaysia seperti yang termaktub di dalam AKTA RAHSIA RASMI 1972).

☐　TERHAD　(Mengandungi maklumat TERHAD yang telah ditentukan oleh Organisasi/badan di mana penyelidikan dijalankan).

[√]　TIDAK TERHAD

TANDATANGAN KETUA PENYELIDIK

MOHAMMAD NAZRI MOHD JAAFAR
Ketua Projek
Vot 74069
Fakulti Kejuruteraan Mekanikal
Universiti Teknologi Malaysia
81310 UTM Skudai, Johor

Nama & Cop Ketua Penyelidik

Tarikh : _____20/5/05_____

CATATAN :　　***Jika Laporan Akhir Penyelidikan ini SULIT atau TERHAD, sila lampirkan surat daripada pihak berkuasa/organisasi berkenaan dengan menyatakan sekali sebab dan tempoh laporan ini perlu dikelaskan sebagai SULIT dan TERHAD.*

DEVELOPMENT OF LOW NO$_X$ LIQUID FUEL BURNER

RESEARCHERS:

PROF. MADYA DR. MOHAMMAD NAZRI MOHD. JAAFAR (HEAD)
DR. AZEMAN MUSTAFA
PROF. MADYA HAMIDON MUSA
WAN ZAIDI WAN OMAR
DR. MOHD. ZAMRI YUSOFF
IR. DR. HJ. KAMSANI ABDUL MAJID
MOHAMAD SHAIFUL ASHRUL ISHAK

RESEARCH VOTE NO:
74069

FACULTY OF MECHANICAL ENGINEERING
UNIVERSITI TEKNOLOGI MALAYSIA

2005

"I declared that this report entitled "**DEVELOPMENT OF LOW NO$_X$ LIQUID FUEL BURNER**" is the results of our own research except as cited in references".

Signature   : _____

Name   : Mohammad Nazri Mohd. Jaafar

Date   : 20th May 2005

DEVELOPMENT OF LOW NO$_X$ LIQUID FUEL BURNER

(Keywords: Combustion, Air Swirlers, Exhaust Gas, NO$_x$ emission)

ABSTRACT

Recently, most of the gas turbine combustion research and development involves in lowering the emissions emitted from the combustor. Emission causes adverse affect to the world and mankind especially. Main concern of the present work is to reduce the NO$_x$ emission since the CO emission could be reduced through homogeneous mixing of fuel and air. Homogeneous mixing of fuel and air is also needed in order to reduce NO$_x$ emission. A liquid fuel burner system with radial air swirler vane angle of 30°, 40°, 50° and 60° has been investigated using 163mm inside diameter combustor. Orifice plates with three different sizes of 20mm, 25mm and 30mm were inserted at the back plate of swirler outlet. All tests were conducted using diesel as fuel. Fuel was injected at two different positions, i.e. at upstream and downstream of the swirler outlet using central fuel injector with single fuel nozzle pointing axially outwards. Experiment has been carried out to compare the three emissions NO$_x$, CO and SO$_2$. NO$_x$ reduction of about 53 percent was achieved for orifice plate of 20mm with downstream injection compared to orifice plate of 20mm with upstream injection. CO$_2$ and SO$_2$ was reduced about 26 percent and 56 percent respectively for the same configuration. This comparison was taken using swirler vane angle of 60°. The overall study shows that larger swirler vane angle produces lower emission results compared to the smaller ones. Smaller orifice plates produce better emission reduction. Meanwhile, downstream injection position significantly decreases the emission levels compared to upstream injection position. Combination of smallest orifice plate and largest swirler vane angle with downstream injection produce widest and shortest flame length.

Key researcher:

Prof. Madya Dr. Mohammad Nazri Mohd. Jaafar (head)
Dr. Azeman Mustafa
Prof. Madya Hamidon Musa
Wan Zaidi Wan Omar
Dr. Mohd. Zamri Yusoff
Ir. Dr. Hj. Kamsani Abdul Majid
Mohamad Shaiful Ashrul Ishak

Email: nazri@fkm.utm.my
Tel. No.: 607-5534661
Fax. No.: 607-5566159

PEMBANGUNAN PEMBAKAR BAHAN API CECAIR RENDAH NO$_X$

(Katakunci: Pembakaran, Pemusar udara, Gas ekzos, Emisi NO$_x$)

ABSTRAK

Masa kini, kebanyakan kajian dan pembangunan ke atas pembakaran turbin gas melibatkan pengurangan emisi dari pembakar. Pencemaran memberi kesan negatif kepada dunia dan manusia khususnya. Dalam projek ini, perhatian diberikan kepada pengurangan emisi NO$_x$ kerana emisi CO dapat dikurangkan melalui percampuran yang baik di antara bahan api dan udara. Percampuran yang baik juga diperlukan untuk mengurangkan emisi NO$_x$. Pembakar berbahan api cecair menggunakan pemusar udara aliran jejarian bersudut 30°, 40°, 50° dan 60° dikaji menggunakan pembakar berdiameter dalam 163mm. Tiga plat orifis bersaiz 20mm, 25mm dan 30mm dipasang di bahagian keluar pemusar udara. Ujikaji dijalankan menggunakan bahan api diesel. Bahan api dibekalkan pada dua kedudukan pancitan, yakni di belakang dan di hadapan pemusar udara menggunakan pemancit bahan api berlubang tunggal menghala arah paksi. Ujikaji dijalankan ke atas tiga jenis pencemar iaitu NO$_x$, CO dan SO$_2$. Emisi NO$_x$ dapat dikurangkan sebanyak 53 peratus bagi plat orifis 20mm menggunakan pancitan di hadapan pemusar udara berbanding plat orifis 20mm menggunakan pancitan di belakang pemusar udara. CO dan SO$_2$ pula dapat dikurangkan sebanyak 26 dan 56 peratus masing-masing untuk konfigurasi yang sama. Ujikaji menunjukkan emisi yang rendah bagi pemusar udara bersudut besar berbanding pemusar udara bersudut kecil. Plat orifis bersaiz kecil memperoleh nilai emisi yang rendah. Pancitan di hadapan pemusar udara menunjukkan pengurangan emisi yang lebih baik berbanding pancitan di belakang pemusar udara. Saiz api yang pendek dengan bukaan yang besar diperoleh apabila pemusar udara besudut besar, plat orifis yang kecil dan pancitan di hadapan pemusar udara digunakan.

Penyelidik utama:

Prof. Madya Dr. Mohammad Nazri Mohd. Jaafar (ketua)
Dr. Azeman Mustafa
Prof. Madya Hamidon Musa
Wan Zaidi Wan Omar
Dr. Mohd. Zamri Yusoff
Ir. Dr. Hj. Kamsani Abdul Majid
Mohamad Shaiful Ashrul Ishak

Email: nazri@fkm.utm.my
Tel. No.: 607-5534661
Fax. No.: 607-5566159

ACKNOWLEDGEMENTS

TABLE OF CONTENTS

LIST OF TABLES

LIST OF FIGURES

LIST OF ABREVIATIONS

A	-	cross sectional area
C_c	-	contraction coefficient
C_D	-	discharge coefficient
d_o	-	Initial jet diameter
d	-	hub diameter
D	-	diameter
et al.	-	and others
g	-	acceleration due to gravity (9.81 m/s^2)
G_θ	-	axial flux of angular momentum
G_x	-	axial flux of axial momentum
h	-	height
HP	-	horse power
i.e.	-	id est (that is)
I_e	-	intensity of rotation
L	-	length
$\dot{m}$	-	mass flow rate
m	-	mass
M	-	Airflow Mach number
n	-	quantity
P	-	pressure
q	-	volumetric flow rate
r	-	radius
R	-	gas constant (8.31 J/ mol K)
Re	-	Reynolds number
s	-	vane thickness

S	-	swirl number
T	-	temperature
vs.	-	versus
V	-	Volume
V	-	velocity
We	-	Weber number
x	-	distance
Z	-	Z number
^{o}C	-	degree Celsius
^{o}	-	degree
Σ	-	summation
Δ	-	differential
α	-	vane angle
σ	-	stress
π	-	phi $\left(\dfrac{22}{7}\right)$
λ	-	wavelength
θ	-	angle
ρ	-	density
μ	-	dynamic viscosity
γ	-	ratio of specific heat
C	-	carbon
CH	-	methylidyne
CH_2	-	methylene
CH_4	-	methane
CHO	-	formyl radical
CN	-	cyano radical
CO	-	carbon monoxide
CO_2	-	carbon dioxide
$C_{12.5}H_{22.2}$	-	Diesel
H	-	hydrogen
H_2	-	Hydrogen
HCN	-	hydrogen cyanide

H_2CN	-	amidogen, methylene-
HO_2	-	hydrogen dioxide
NCO	-	isocyanato radical
N	-	nitrogen
N_2	-	nitrogen
NO	-	nitrogen oxide
NO_2	-	nitrogen dioxide
N_2O	-	nitrous oxide
NO_x	-	oxides of nitrogen
O	-	oxygen (atom)
O_2	-	oxygen (Gas)
OH	-	hydroxyl radical
O_3	-	ozone
SO_2	-	sulphur dioxide
AFR	-	air fuel ratio
ASME	-	American Society of Mechanical Engineers
CFC	-	chlorofluorocarbon
EGR	-	exhaust gas recirculation
EQR	-	equivalence ratio
FAR	-	fuel air ratio
FGR	-	flue gas recirculation
FLR	-	filter, lubricator and regulator
HHV	-	higher heating value
ppm	-	part per million
RQL	-	rich-burn quench lean-burn
SMD	-	Sauter mean diameter
SCR	-	selective catalytic reduction
SNCR	-	selective non-catalytic reduction
UHC	-	unburned hydrocarbon

LIST OF APPENDICES

CHAPTER I

INTRODUCTION

1.1   Background

Global environmental problems such as global warming, acid rain, ozone layer depletion and photochemical smog have become serious problems all over the world. Pollution and environmental degradation are discussed in a great deal today, but it is often spoken of in a way that is disconnected from its cause. Conventional energy processes can cause major problems to the environment, and it is important to consider energy issues alongside environmental issues in order to seek solution effectively.

The increasing use of gas turbine power plants for electricity generation, motor vehicles and other industrial application causes atmospheric pollution. For several decades, the gas turbine has been the prime movers for aircrafts, due to the tremendous advantages in term of speed, fuel economy and passenger comfort.

The combustion of fossil fuels is also a major contributor of four main environmental concerns. These environmental problems are caused by air pollution that contains oxides of nitrogen, carbon monoxide and oxides of sulphur. These environmental problems concern has prompted many governing bodies to legislate new regulations regarding emissions from combustion process in the hope that these environmental problems will be reduced.

1.2   Review of Previous Works

Past researchers who studied on the effect of varying the swirl strength were mainly interested on the flow pattern and temperature profiles resulted from varying the swirl strength. They were emphasizing the effect of swirl on the generation of torroidal central recirculation zones and flame geometry rather than the effect of swirl strength on emissions formation.

Mikus, T. and Heywood, J.B. (1971) in their work on automotive gas turbine concluded that leaning out the primary zone or reducing the residence time of conventional combustor designs using conventional fuel injection techniques was unlikely to reduce NO emissions enough to meet emissions standard. This was due to the presence of stoichiometric fuel and air ratio in parts of the flow within the primary zone even if the excess air was present. To achieve a significant reduction in NO emissions, combustors need to be developed with both a leaner and more homogeneous fuel and air ratio distribution in the primary zone that is attainable in conventional designs.

Mestre (1974) compared the effect of swirling and non-swirling system on combustion. He demonstrated that swirl helps to improve combustion efficiency, decreases all pollutants and increases flame temperature. He also observed that during the present of swirl, a shorter blue flame was observed indicating good mixing while non-swirling system showed a longer yellow flame indicating that there is still some fuel left unvapourized.

A series of combustor tests were conducted by Mularz et. al. (1975) to evaluate three improved designs of swirl-can combustor modules, using axial swirlers and their objectives were to obtain low levels of exhaust pollutants while maintaining high combustion efficiency at combustor operating conditions. He came with an opinion that swirl-can modules consisted of three components; a carburettor, an inner swirler and a flame stabiliser. The functions of the module were to mix fuel and air, swirl the mixture, stabilise combustion in its wake and provide large interfacial mixing areas between the bypass air around the module and combustion gases in its wake. They found that swirl-can combustor model performed with high

combustion efficiency at all conditions tested but the NO_x emissions were still higher than the maximum allowable level of 20ppm which was needed to achieve the 1979 Environmental Protection Agency (EPA) emissions standards.

Meanwhile, Ballal and Lefebvre (1979), in their study, stressed that for a premixed flame, the weak extinction limits were governed mainly by inlet air temperature, to a lesser extent by air velocity and turbulence level and were almost independent of pressure.

Past researchers also have studied the effect of varying the vane angle, which in turn vary the swirl number, on combustion performance. Claypole and Syred (1981) investigated the effect of swirl strength on the formation of NO_x. At swirl number of 3.04, much of the NO_x in the exhaust gases was recirculated into the flame front. The total emissions of NO_x were reduced, however, at the expense of reduced combustion efficiency.

Noyce and Sheppard (1982) investigated the influence of equivalence ratio on air and fuel mixing. They suggested that at low and high power conditions the high CO emissions could be minimised by better mixing.

Al-Kabie (1989), on the other hand, studied the effect of radial swirler on emission reduction in gas turbine combustor. In his study, he imposes swirler expansion ratio of 1.8 to achieve adequate combustion efficiency. Al-Kabie, in his study, showed that high efficiency was not achieved in weak region until there was a significant outer expansion and associated recirculation zone. However, there was a little influence of the expansion ratio on the weak extinction limit. Alkabie have shown that if fuel is injected into the outer recirculation zone, in the corner of the dump expansion region, then NO_x emission are high as this recirculation zone has a high residence time and low refreshment rate with air. To minimise this effect for burner application, the use of an orifice restriction at the outlet of the wall fuel injector was used. The intention was to deflect any fuel in the wall region radially inwards into the shear layer. Various non-conventional fuel injection methods was studied such as swirler vane passage, radial central and wall injection were used with gaseous propane and natural gas and liquid kerosene and gas oil. The test was

conducted using lean-lean two-stage combustion concept. He demonstrated that there is no significant effect on NO_x emissions by varying the vane angle from 20° to 60°, hence varying the swirl number from 0.41 to 3.25, respectively. However, he found that at very high swirl number of 3.25, NO_x emissions were considerably higher than the rest at all associated equivalence ratios for two different inlet air temperature of 400 K and 600 K. This may be due to increased residence time in the rich stabilizing shear layer and hence increased NO_x emissions. The same effect was demonstrated when he switched from natural gas to propane. Another way to increase the strength of swirl without changing the vane angle is to decrease the vane depth of the swirler. Combustion efficiencies were also improved as the swirl strength increased. Increasing the swirl strength also extends the lean flammability limits.

Bicen et. al. (1990), have reported temperature and species measurements for annular and tubular combustors using the same axial swirler for flame stabilisation. The annular combustor was operated at an air/fuel ratio of 29 and fuelled by natural gas; it displayed a marked improvement in combustion efficiency, 94% compared to 69%, when the inlet air temperature was raised from 315K to 523K. This improvement was observed to be a result of improved fuel and air mixing. Meanwhile, the tubular combustor was operated at a leaner fuel/air ratio of 57 and fuelled by propane, showed a more modest improvement in combustion efficiency, 97.7% compared to 98.8%, when the inlet air temperature was raised from 315K to 523K. They then concluded that from detailed measurements, the increase in efficiency was due to improved mixing in the combustor. Whitelaw commented that combustor aerodynamics was more dominant characteristic compared to chemical kinetics in the primary zone combustion (Bicen, A.F. et. al, 1990).

Escott, N.H. (1993) studied the combusting flow of three method of swirling generation namely single, coswirl and counterswirl. He used three basic fuel injection modes of swirler vane passage, central and wall injection. Escott finds that low NO_x emission was achievable through central fuel injection mode, but the lowest emission results were shown by wall injection method. However, Escott insisted that the results were strongly dependent on the input temperature and pressure provided to the flow. Escott also run an experiment on simple fuel staged injection system and concluded that there was no improvement in either emission or stability compared to

non-staged modes. Coswirl and counterswirl combustion system with passage fuel injection into half of the air flow improved the flame stability but with unacceptable increase in NO_x emissions. From his observation, he concluded that lower NO_x emission was generated by counterswirl system with deteriorated flame stability due to more vigorous air mixing and consequently leaner fuel occurring in the interjet shear layer.

Kim, M.N. (1995), in his study, stresses on curved blade radial swirlers with wall injection and vane passage injection. The fuels were natural gas, propane and gas oil. He concluded that vane passage injection mode produce lower emission results compared to 76mm wall injection because of wall injections mode injects the fuel in the high residence time corner recirculating zone. This created locally rich zone and high thermal NO_x. He also find that natural gas produce lower emission compared to propane due to the better fuel and air mixing between natural gas and air since natural gas has a lower molecular weight than propane which means high diffusivity action and natural gas can be quickly dispersed into turbulent region of shear layer and hence low NO_x formation.

Mohd. Radzi Mohamed Yunus (2002), studied the effect of varying swirler vane angles on emissions reduction. He found that optimum swirler vane angle for NO_x emission found to be 60°; for CO was 80° and for SO_2 was 70°. He suggested that recirculation zone size and turbulence flow affects emissions significantly.

1.3   Problem Statement

Current researchers hastily moved their intension to post combustion methods as they found out that post combustion methods could possibly reduce emissions twice of the pre combustion methods. But, take note that this would heavily increase the cost which would discourage the industries to venture in. Besides that, post combustion methods at present situation were almost impossible to apply in aircraft engines as it would increase the engine weight which opposes the aircraft applications requirement of producing low weight-high trust engines. This research

concerns on the above mentioned problems and carried out a study to discover a better solution on reducing emission from gas turbine, mainly for aircraft applications.

1.4   Objective of Research

The main objectives of this project are as follows:

a. To investigate and select a method of reducing pollutions from liquid fuel burner.
b. To design the liquid fuel burner system that incorporates the chosen method.
c. To fabricate the prototype, an efficient and environmental friendly liquid fuel burner.
d. To evaluate the performance of the prototype burner.

1.5   Scopes of Research

The scope of the research is as follows:

a. Literature survey on existing liquid fuel burner and emissions reduction techniques.
b. Preliminary design and dimensioning of liquid fuel burner.
c. Preliminary design of burner components such as air swirler, atomiser, etc.
d. Preliminary design analysis based on experimental data of the existing burner and from simulation results.
e. Detail design of the liquid fuel burner including technical drawings for fabrication.
f. Construction of the liquid fuel burner prototype, including other components.
g. Testing of liquid fuel burner performance:
    (i) Combustion stability
    (ii) Flame development and propagation

(iii) Emissions production/reduction

(iv) Temperature and pressure profiles across the burner

1.6 Limitation of the Study

(i) The research will be conducted using four different swirler vane angles of 30°, 40°, 50° and 60°.

(ii) Three orifice plate diameters of 20mm, 25mm and 30mm will be used for experimental testing to study the effect of orifice plate insertion.

(iii) Fuel injection is placed at two positions that is at 15mm upstream or downstream from the swirler exit.

(iv) Diesel fuel used was supplied by Universiti Teknologi Malaysia, which is obtained bulkily from Petronas fuel station.

(v) The geometry of combustion chamber, fuel injector, orifice plates and swirlers are as designed.

(vi) Fuel and injection air are pressurized constantly at 2 bar.

(vii) Flow rate of injection air is constant at 170 ℓ/m.

(viii) Swirling air flow rate will be varied from 24 CFM to 9 CFM, which is from 679.608 LPM to 254.853 LPM.

1.7 An Outline of the Report

This report consists of seven chapters. Chapter one describes briefly on the problem statement of current research. Problem statement reveal lacks of previous researches and illustrates the significant of this research. However, there were some limitations in the study that has been expressed.

Chapter two discusses thoroughly on the literature study. Four main items of gas turbine combustor; combustion chamber, flame stabilizer, fuel injector and air-fuel system has been discussed fundamentally. The impact of the emissions towards environment and human was explained in detail. The requirement that to be fulfilled on producing a good combustion chamber, flame stabilizer, fuel injector and air-fuel supply has been discussed for better understanding. Besides that, varieties of these four items have been highlighted in this section to study the availability and manufacturability of these items.

Meanwhile, chapter three concerns on the emissions behaviour and emissions controlling methods. Main concern of this research is to improve the NO_x emissions as CO emissions could be reduced through good mixing of air and fuel. NO_x emission control techniques have been described briefly.

Chapter four, on the other hand, emphasize on the burner design concepts. This chapter explains the requirement required to build a burner. All four main items of combustor; combustion chamber, swirler, fuel injector and air fuel system design concepts has been discussed.

Chapter five elaborates on the experimental testing setup. This chapter describes clearly on the equipments and instrumentations used for the entire experimental testings. There were also guidelines on how the experiment has been conducted.

Chapter six confers about the experimental results and discussion on the combustion performance of that carried out in the experimental testing. Results has been compared between four different swirler vane angle of 30°, 40°, 50° and 60° using three different orifice plate sizes of 20mm, 25mm and 30mm at upstream and downstream injection position. The behaviour of the emission results and temperature profiles was discussed thoroughly.

Chapter seven concludes the emission results and temperature profiles discussions. Recommendation for future work has been stressed in this chapter to

provide inspiration for future researchers to continue delivering improvement in emission reduction from pre combustion burners.

CHAPTER II

LITERATURE REVIEW

2.1   Introduction

Gas turbine technology has developed gradually and continuously over the past fifty years. Despite continued advances in the technology of gas turbine combustors, the need to protect the environment from combustion gaseous has led to considerable demand to improve the combustor design.

Combustion chamber, flame stabilizer, injector and air-fuel mixture system are the components in a combustor that should be carefully studied in order to achieve a low emission burner system. In this thesis, the research will focus more on the swirler vane angles as the main parameter is on lowering burner emission.

2.2   Environmental Problems

The use of fossil fuels is a major source of air pollution, in particular, emissions of oxides of nitrogen, oxides of carbon and oxides of sulphur. Fossil fuels combustion is a major contribution of four pressing environmental concerns, which is, global warming, acid rain, photochemical smog and ozone depletion. This concern has prompted many governing bodies to legislate regulations on emissions from combustion process in the hope that these environmental problems will be reduced.

2.2.1 Acid Rain

Acid rain has several damaging effects on ecological system. Acid rain falls and polluted the lakes, river and sea. Lake acidification tends to reduce the population of its inhabitants. Many lakes around the world are losing their fish population due to the lake acidification. Acid rain also causes damage to plants and human health. The main source of acid rain is oxides of sulphur and nitrogen, predominantly from the combustion processes. In general SO_2 contributes about 60 percent of such precipitation, whereas NO_x contributes about 35 percent. SO_2 content can be reduced by desulphurization process in the combustion chamber but this process will tend to increase the NO_x in the combustion chamber (Mellor, A.M., 1990).

2.2.2 Ozone Depletion

Ozone layer has the ability to absorb ultra-violet (UV) radiation from the sun. A direct UV ray can kill plants and animal cells. It also can cause skin cancer to human. As the ozone layer absorbs ultra-violet, it may change the temperature structure of the atmosphere and hence alter the atmospheric circulation. Ozone in the troposphere is a greenhouse gas. It absorbs the infrared radiation and will trap heat hence cause the earth to become warmer. The formation and destruction of the ozone layer should always be in equilibrium to preserve the ozone layer that is protecting the earth. However, the increased in the concentration of pollution gases in the atmosphere such as oxides of nitrogen from the combustion processes has led to an imbalance in this equilibrium. The destruction of the ozone layer occurs at the faster rate then its formation. The clear sign of ozone depletion was the 'ozone hole' that was reported in 1984 (Mellor, A.M., 1990). Since then, ozone hole was reported each year.

2.2.3   Global Warming

Global warming or known as greenhouse effect is a phenomenon described by a rise in the earth atmospheric temperature. This rise of temperature is caused by the imbalance of the energy of the earth. Greenhouse gases play an important role to reflect back the ultraviolet radiation that penetrates the earth's atmosphere as infrared radiation. Greenhouse gases are carbon dioxide (CO_2), methane (CH_4), ozone (O_3), nitrous oxide (N_2O) and chlorofluorocarbon (CFC).

Atmosphere emits less energy into space than the earth's surface. This is because the atmosphere's average temperature is lower, roughly -18°C. The different between the energy emitted by the earth and the atmosphere is absorbs by the atmosphere. This energy trapping process is called the greenhouse effect. The greenhouse effect keeps the global temperature at a habitable 15°C rather than a hostile -18°C (Mellor, A.M., 1990). However, if the concentration in the atmospheric carbon dioxide increases, the global temperature will be higher. This phenomenon will cause global climate change. CO_2 is the biggest contributor to global warming. The effect of the doubling in carbon dioxide concentration will raise the global average surface temperature by 2 ± 1 K (Mellor, A.M., 1990).

2.2.4   Photochemical Smog

Photochemical smog is a phenomenon that happened when there are air stagnation, abundant sunlight and high concentration of hydrocarbon and oxides of nitrogen in the atmosphere (Escott, N.H., 1993).

Smog arises from photochemical reactions in the lower atmosphere by the interaction of hydrocarbons and nitrogen dioxide released by the exhausts of motors and combustion processes. This interaction results in a series of more complex reactions producing secondary pollutants such as ozone, aldehydes, ketones and peroxyacyl nitrates.

2.3   Combustor Exhaust Emissions

Generally there are four major pollutants from any combustion processes. These are oxides of nitrogen (NO_x), carbon monoxide (CO), unburned hydrocarbon (UHC) and smoke. Sulphur dioxide (SO_2) is present if the fuel used during the combustion processes contained sulphur. In this research, concern was on the three hazardous pollutants that are oxides of nitrogen, carbon monoxide and sulphur dioxide since these pollutants has detrimental effect on the health and environment. Table 2.1 shows the amount these emissions form varies sources.

Table 2.1: Source of Atmospheric emissions (Jabatan Alam Sekitar, 1997)

(unit: ton/year)

Pollutants	Pollution Source	Present (1992)	Future (2005)	
			Without Measures	With Measures
	Factories			
SO_x	Power Stations	19,522	30,041	12,759 (58)
	General Factories	11,047	11,283	5,345 (53)
	Sub-total	30,569	41,324	18,104 (56)
	Motor Vehicles	3,117	7,079	5,755 (19)
	Air Planes	416	360	360 (0)
	Ships	1,552	2,836	2,836 (0)
	Households	0	0	0 (-)
	Total	35,654	51,599	27,055 (48)
	Factories			
NO_x	Power Stations	12,792	26,054	22,758 (13)
	General Factories	2,979	4,415	4,364 (1)
	Sub-total	15,571	30,469	27,122 (11)
	Motor Vehicles	36,212	82,199	55,728 (32)
	Air Planes	1,320	574	574 (0)
	Ships	989	1,840	1,840 (0)
	Households	162	226	226 (0)
	Total	54,454	115,308	85,490 (26)
CO	Motor Vehicles	290,407	659,223	321,430 (51)
HC	Motor Vehicles	73,445	166,720	103,973 (38)

Figures in parentheses are amount of reduction in percentage

2.3.1 Oxides of Nitrogen

Oxides of nitrogen (NO_x) are the term given for the combustion product of nitrogen such as nitric oxide (NO), nitrogen dioxide (NO_2) and nitrous oxide (N_2O). NO_2 is the dominant form of NO_x in fuel lean burning but NO is the dominant form of NO_x from combustion processes. The major source of nitrogen in combustion processes is the air itself.

2.3.1.1 Nitric Oxide

Nitric oxide (NO) is the direct precursor of NO_2. The rate of oxidation from NO to NO_2 is too slow to give significant conversion during the short time of resident time in the combustion process. This reaction, however, has ample time to take place once released into the atmosphere. NO has some harmful effects on health but these effects are substantially less than those of an equivalent amount of NO_2. NO and NO_2 interact with the smog producing atmospheric photolytic cycle in different ways. Concentration of NO_2 are generally lower than those of NO but large concentration of NO_2 as a primary pollutant can reduce the induction time for photochemical smog since the relatively slow NO to NO_2 oxidation steps is bypassed. NO does not irritate the lungs but forms methemoglobin when absorbed. NO is an endogenous modulator of the vascular pressure (Al-Kabie, H.S., 1989).

An additional augmentation of NO formation is the temperature fluctuation. In turbulent flames instantaneous temperature levels will exceed the time average temperature level due to mixing imperfection and NO formation will be increased above the level predicted on the basis of the time average temperature (Kim, M.N., 1995). The fluctuation occurs due to variation in the mixture ratio and bulk movement of the flame.

NO can be produced by three different mechanism that is thermal NO, prompt NO and fuel NO.

Thermal NO is produced by oxidation of atmospheric nitrogen in the post flame gases and refers to NO formation in the combustion of lean and near stoichiometric fuel-air mixtures as suggested by the Zeldovich chain mechanism. The concentration of O_2 is low in fuel rich combustion therefore Reaction (1.3) is less important than in fuel lean combustion. Meanwhile, high activation energy is needed to break the N_2 triple bond in Reaction (1.2) therefore this reaction was concern in very high temperature combustion that is greater than $1500^{o}C$ (Escott, N.H., 1993).

$$\frac{1}{2}O_2 \rightleftharpoons O \qquad \ldots\ldots\ldots \qquad (2.1)$$

$$O + N_2 \rightleftharpoons NO + N \qquad \ldots\ldots\ldots \qquad (2.2)$$

$$N + O_2 \rightleftharpoons NO + O \qquad \ldots\ldots\ldots \qquad (2.3)$$

Prompt NO is produced by high speed reactions at the flame front for hydrocarbon fuels. Term prompt NO is used because the NO is formed in the flame front and not in the post flame gases like thermal NO. Flame temperature does not rely on the prompt NO. Kim (1995) suggested that prompt NO is the major source of NO emission in lean burning swirl stabilized flame. Meanwhile Fenimore (1970) observed that the amount of prompt NO increased markedly as the flame passes from fuel lean to fuel rich condition. The N atom produced in Reactions (1.4), (1.6) and (1.7) then react with O_2 in Reaction (1.3) to produce more NO (Escott, N.H., 1993).

$$CH + N_2 \rightleftharpoons HCN + N \qquad \ldots\ldots\ldots \qquad (2.4)$$

$$CH_2 + N_2 \rightleftharpoons HCN + NH \qquad \ldots\ldots\ldots \qquad (2.5)$$

$$CH_2 + N_2 \rightleftharpoons H_2CN + N \qquad \ldots\ldots\ldots \qquad (2.6)$$

$$C + N_2 \rightleftharpoons CN + N \qquad \ldots\ldots\ldots \qquad (2.7)$$
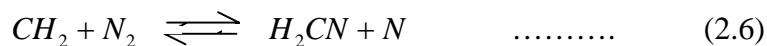
Fuel NO is produced by oxidation of nitrogen contained in the fuel. The fuel nitrogen is converted to HCN in the flame zone and depending on the degree of nitrogen conversion; the fuel NO represents a considerable portion of the total NO. For liquid fuel, kerosene does not contain fuel bound nitrogen, but gas oil contains significant amount of nitrogen. Fuels that contain sulphur and organically bound nitrogen produce complicated interactions that promote the formation of further NO.

2.3.1.2 Nitrogen Dioxide

Nitrogen dioxide (NO_2) has been known to have adverse effect on the human respiratory system. It has an affinity for haemoglobin, which carries oxygen to body tissues. It also forms acid in the lungs. Nitrogen dioxide is much more toxic than CO for the same concentrations. Besides that, it also forms smog from a series of photochemical reactions. Epidemiological studies of exposure to the nitrogen dioxide released during cooking with gas indicate an increase frequency of respiratory illness among children. NO_2 is formed by the oxidation of NO as shown below (Escott, N.H., 1993).

$$N_2 + O + M \rightleftharpoons NO_2 + M \qquad \text{..........} \qquad (2.8)$$

$$NO + NO + O_2 \rightleftharpoons NO_2 + NO_2 \qquad \text{..........} \qquad (2.9)$$

$$NO + HO_2 \rightleftharpoons NO_2 + OH \qquad \text{..........} \qquad (2.10)$$
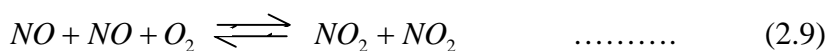
In hot regions of the flame the reverse of Reaction (1.9) occurs. The conversion of NO to NO_2 by Reaction (1.10) is generally slow because HO_2 concentration is low, however in fuel lean conditions HO_2 concentration increases (Flagan, R.C. and Seinfeld, J.H., 1988).

2.3.1.3 Nitrous Oxide

The increase of nitrous oxide (N_2O) concentration in the atmosphere contributes to the greenhouse effect and depletes the stratospheric ozone layer and this would increase ultraviolet radiation to the earth's surface and with it the occurrence of skin cancer in the population (Crutzen, P.J., 1970) and (Sothern, A., 1979). Nitrous oxide is formed mainly from biological activity of the soil. This gas is not a potential health problem, nor does having a damaging effect on vegetation. Only 20% of this gas is produced by fossil fuel combustion.

N_2O normally formed due to fuel NO where the fuel itself is nitrogen bounded. However, Escott (1993) suggested that N_2O could be formed through

prompt NO as well as in the fuel NO. The reaction of combustion product to form N_2O is as shown below (Escott, N.H., 1993).

.

$$HCN + OH \;\rightleftharpoons\; HNCO + H \qquad ……….\qquad (2.11)$$

$$HCN + O \;\rightleftharpoons\; NCO + H \qquad ……….\qquad (2.12)$$

$$HNCO + OH \;\rightleftharpoons\; NCO + H_2O \qquad ……….\qquad (2.13)$$
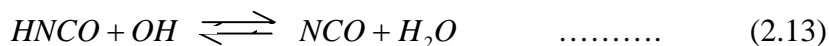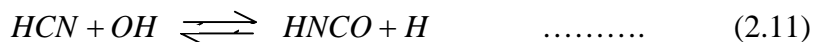
The NCO radical then reacts with NO to form:

$$NCO + NO \;\rightleftharpoons\; N_2O + CO \qquad ……….\qquad (2.14)$$

Studies have shown that temperature is a vital factor in the formation of N_2O with the maximum concentration of N_2O occurring around $750^{\circ}C$. At temperature lower than $750^{\circ}C$, Reaction (1.11) dominated thus N_2O prevented. As temperature increases above $750^{\circ}C$, N_2O is prevented by the reaction (Escott, N.H., 1993):

$$N_2O + H \;\rightleftharpoons\; N_2 + OH \qquad ……….\qquad (2.15)$$

$$N_2O + OH \;\rightleftharpoons\; N_2 + HO_2 \qquad ……….\qquad (2.16)$$

$$N_2O + M \;\rightleftharpoons\; N_2 + O + M \qquad ……….\qquad (2.17)$$

$$N_2O + O \;\rightleftharpoons\; N_2 + O_2 \qquad ……….\qquad (2.18)$$

$$N_2O + O \;\rightleftharpoons\; NO + NO \qquad ……….\qquad (2.19)$$
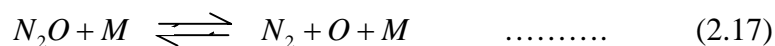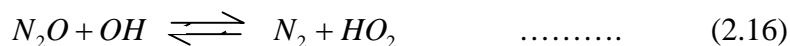
2.3.2   Carbon Monoxide

Carbon monoxide (CO) has a strong affinity to the haemoglobin of the bloodstream and is a dangerous asphyxiates. It produces carboxyhaemoglobin when it reacts with the proteins in the lungs. Carboxyhaemoglobin reduces the oxygen-carrying capacity of the blood and has the potential to starve the brain and other tissues of oxygen. At a low concentration, it has potential to cause headaches, slow reflexes, reduce manual dexterity, decrease exercise capability and cause drowsiness. At a high concentration, carbon monoxide can cause death.

Rapid reaction between hydrocarbons from the fuel and the air in the combustion process generates CO emission. This rapid reaction between hydrocarbon fuels and air will form CH_2O and CHO that will then further react with other radicals to form CO (Escott, N.H., 1993).

$$CH_2O + OH \rightleftharpoons CO + H + H_2O \qquad \ldots\ldots\ldots \qquad (2.20)$$

$$CHO + O_2 \rightleftharpoons CO + HO_2 \qquad \ldots\ldots\ldots \qquad (2.21)$$

$$CHO + M \rightleftharpoons CO + H + M \qquad \ldots\ldots\ldots \qquad (2.22)$$
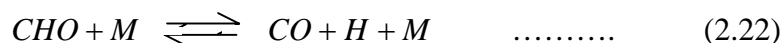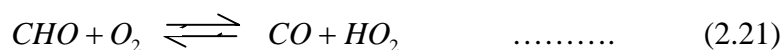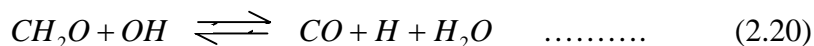
Emission level of CO can only be minimised by completing its oxidation to carbon dioxide (CO_2). Conditions favourable to the oxidation of CO are high temperature, oxygen availability, high pressure and long residence time. The predominant mechanism for CO oxidation is:

$$CO + OH \rightleftharpoons CO_2 + H \qquad \ldots\ldots\ldots \qquad (2.23)$$

2.3.3   Unburned Hydrocarbon

Unburned hydrocarbon (UHC) is also a product of incomplete combustion. A complete combustion does not produce hazardous emission, but it is impossible to produce complete combustion because the fuel-air mixing and ignition occur at a very rapid process. Unburned hydrocarbon is usually formed due to poor atomisation, inadequate burning rates and the chilling effects of burner walls or any combination of these. Some hydrocarbon species does not provide a serious health hazard. Other hydrocarbons could cause cancer when its deposition is above certain level. UHC also acts as a precursor to the formation of photochemical smog.

The inability to complete the combustion of the fuel affects the combustion efficiency. So maximising the combustion efficiency could reduce emission of hydrocarbons. Besides that, excess air also could reduce the combustion efficiency due to the lowering of temperatures and the increase in heat losses arising as mass

flow rate of exhaust gases increased. Residence time is also another factor to satisfy for good mixing in the combustor. Combustor should not be overloaded, that the heat extraction during the combustion is controlled, so that exhaust gases are not quenched before the combustion reactions can go to completion. This entire variable is interrelated.

2.3.4   Oxides of Sulphur

Sulphur dioxide (SO_2) presents in the combustion process when there are sulphur content in the fuel used in the combustion process. Normal persons who inhale sulphur dioxide for a brief period could exhibit shallower and more rapid breathing. The presence of aerosol may sweep the sulphur dioxide molecules deep into the respiratory system that may cause respiratory illnesses. Besides that, low concentration of sulphur dioxide, in association of other irritant gases and particles that are present, are sufficient to impair the function of the lungs (Crutzen, P.J., 1970). Oxides of sulphur also act as precursor to the formation of acid rain.

2.3.5   Carbon Dioxide

Carbon dioxide emission (CO_2) is stable and non-toxic but it is a greenhouse gas and can contribute to global climate change. There is no effective process to reduce this emission. The only way to reduce this emission is to burn less carbon. The only way of achieving this is by using lower carbon fuels (Kim, M.N., 1995).

2.4   Gas Turbine Combustor

Gas turbine engines are widely used in aircraft, marine, power generation and industrial application due to largely tremendous advantages in term of range, speed, fuel economy, passenger comfort, compactness and high power output.

Conventional gas turbine combustion chamber essentially consists of three main sections. These are primary, intermediate and dilution zones. The most vital section for the combustion chamber designer is the primary zone since combustion of fuel is initiated in this section (Al-Kabie, H.S., 1989). The achievement of complete combustion in the primary zone is the aim of the present work which reduces the need for other sections of the combustors fulfilling the requirement of small size and light weight of gas turbines.

2.4.1   Operation of a Gas Turbine Combustor
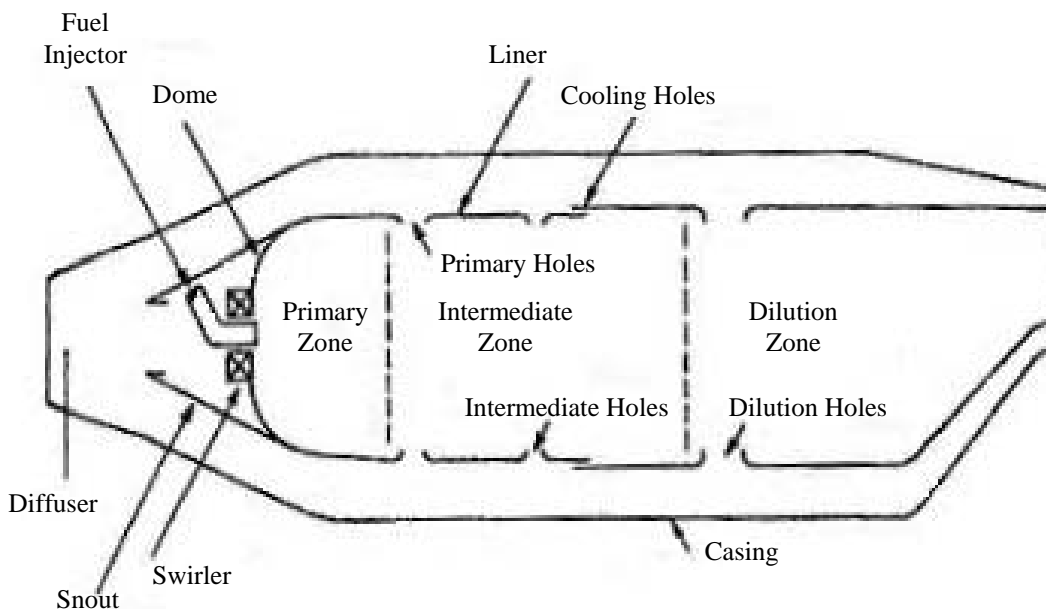
Figure 2.1: Typical Combustor Cross Section (Lefebvre, A.H., 1983)

The combustor is divided into three separate regions; those are primary zone, intermediate zone and dilution zone. If all the air and fuel supplied to the gas turbine

engine were supplied into the combustor directly, the resulting mixture would have a fuel-air ratio lower than the lean flammability limits. Thus the combustion is initiated and stabilized by the controlled mixing of fuel and air in the primary zone and the exact fuel-air ratio of the mixture will depend on the approach to emission reduction that is adopted, either lean, stoichiometric or rich. Stoichiometry refers to the amount of air required theoretically to combust completely a particular amount of fuel.

The role of the primary zone in the combustor is to ensure complete combustion of the fuel by providing sufficient time, temperature and turbulence. The intermediate zone serves as an extension to the primary zone providing an increased residence time at high temperature prior to cooling and virtual freezing of reaction in the dilution zone. Meanwhile, the role of the dilution zone is to admit the air remaining after the combustion and wall cooling requirement have been met, and to provide an outlet stream with a mean temperature and a temperature distribution that are acceptable to the turbine.

2.4.2   Combustor Arrangement

There are three common combustor arrangement; tubular, annular and tuboannular type combustors. Tubular combustor is also known as can-type combustor.

2.4.2.1 Tubular Combustor

Tubular combustor as shown in Figure 2.2 has one combustor on a central axis or several combustors arranged equidistant on the same pitched circle diameter. Each combustor consists of an inner flame tube or liner cylinder mounted on the same axis inside an outer casing cylinder. Tubular combustor is mainly used in industries, marine, vehicular and aircraft application. However modern aircraft applications are more concerned with the engines weight-thrust ratio and so

combustors that have a larger combustion volume, hence more thrust, are preferred. The advantages and disadvantages of tubular combustor were shown in Table 2.2.
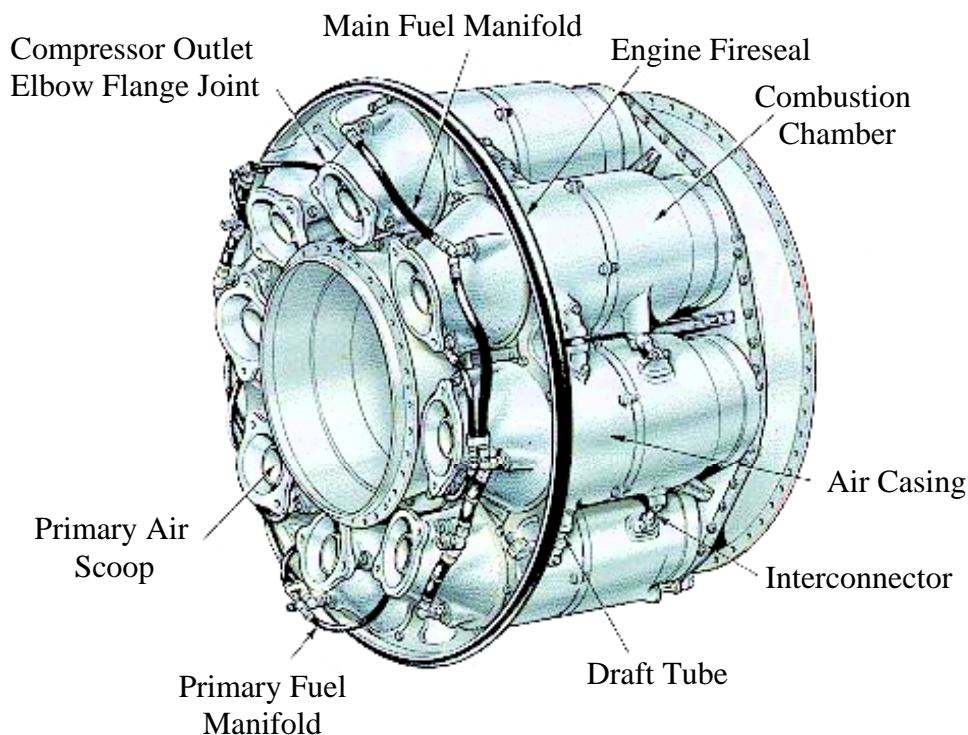
Figure 2.2: Tubular Combustor (Treager, I.E., 1995)

Table 2.2: Advantages and Disadvantages of Tubular Combustor (Treager, I.E., 1995)

Advantage	Disadvantage
1. Mechanically Robust	1. Bulk and weight
2. Small variation between individual combustor in combustion and aerodynamic performance	2. Ignitor for each combustor increases complexity of design except for single combustor
3. Rig testing can be performed with just one combustor using a fraction of the total engine air and fuel mass flow	3. Interconnection tubes between combustors for the air flow except for single combustor
	4. Problems associated with the initiation in combustion in all combustors except for single combustor
	5. High pressure loss

2.4.2.2 Annular Combustor

Annular combustor as shown in Figure 2.3 consists of an inner annulus mounted on the same axis inside an outer casing annulus. Annular combustor is widely used in modern aircraft application particularly in military aero engines. The advantages and disadvantages of annular combustor were shown in Table 2.3.
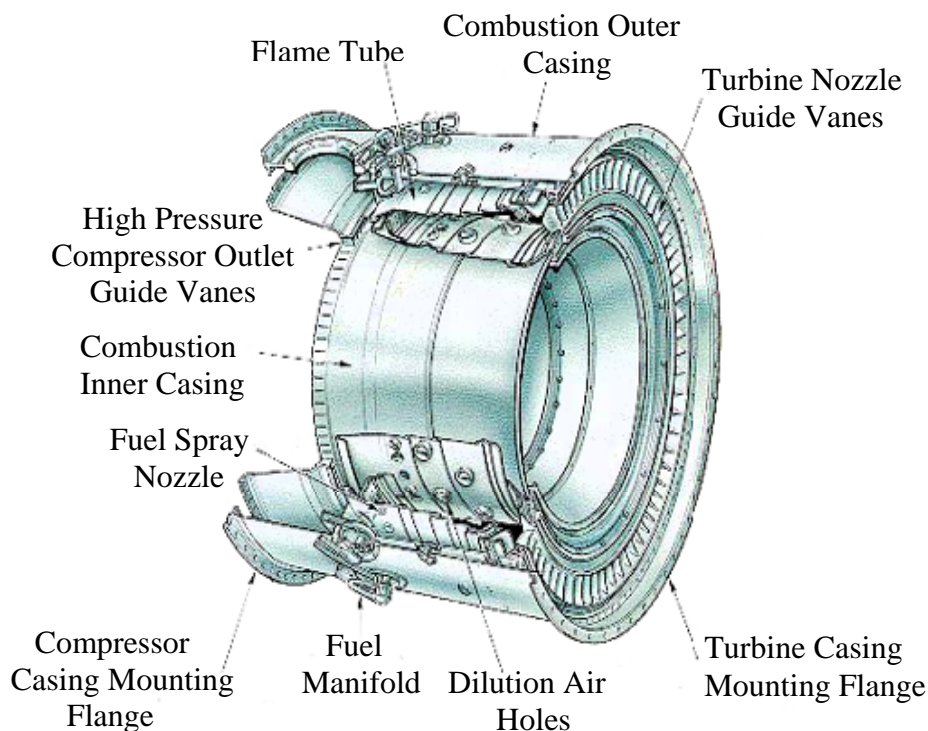
Figure 2.3: Annular Combustor (Treager, I.E., 1995)

Table 2.3: Advantages and Disadvantages of Annular Combustor (Treager, I.E., 1995)

Advantage	Disadvantage
1. Minimum Length and weight	1. Buckling problems on outer liner leading to disruption of cooling air flow and variation in outlet gas temperature creating possible thermal stresses in the turbine blades
2. Minimum pressure loss	2. Rig testing requires use of total engine air and fuel mass flow
3. Minimal problems with light around	3. Even distribution of fuel and air is difficult to achieve around the annular

2.4.2.3 Tuboannular Combustor

Tuboannular combustor as shown in Figure 2.4 is a hybrid of the previous two types of combustors. This combustor consist of several cylindrical liners arranged equidistant on the same pitched circle diameter are mounted inside a single outer casing annulus. The advantages and disadvantages of tuboannular combustor were shown in Table 2.4.
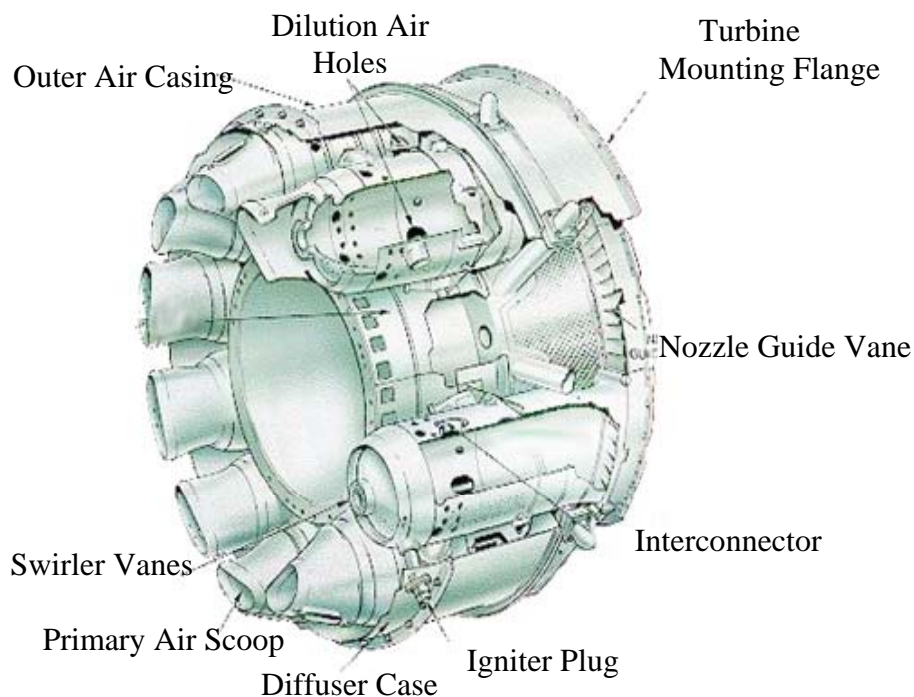
Figure 2.4: Tuboannular Combustor (Treager, I.E., 1995)

Table 2.4: Advantages and Disadvantages of Tuboannular Combustor (Treager, I.E., 1995)

Advantage	Disadvantage
1. Mechanically robust	1. Suffers from the problem of light around
2. Low pressure loss	2. Less compact than annular combustor
3. Shorter and lighter than tubular combustor	3. Even distribution of air is difficult to achieve around the annulus
4. Rig testing requires use of just one combustor, using fraction of total engine air and fuel flow	4. Ignitor for each combustor increases the complexity of design

2.4.3 Combustor Design Requirement

The basic function of a combustor is to convert admitted fuel and air mixture to a temperature rise for the turbine stage. However there are wide varieties of criteria that also need to be considered in order to achieve the best combustor design. The criteria are (Fricker,N. and Leuckel,W., 1976):

1. The combustor must be capable of reliable and smooth ignition over a wide range of ambient conditions.
2. After ignition, the flame must stay alight over wide range of inlet temperature, pressure and equivalent ratio.
3. The fuel should be completely burned so that all of its chemical energy is liberated as heat, typically modern combustors achieve combustion efficiencies of 99.9 percent over a wide range of equivalent ratios.
4. The pressure loss of the combustor should be low, between 2-7 percent of the combustor inlet pressure. Higher pressure loss would result in higher compressor pressures.
5. The temperature distribution at the exit of the combustor often needs to be altered in order to increase the life of turbine blades.
6. Low emissions of carbon monoxide, unburned hydrocarbons, oxides of nitrogen, oxides of sulphur and soot will be necessary to pass ever more stringent emission limits.
7. All combustor types must be designed to be durable and safe.
8. Aero engine requires short combustor length to keep the engine light weight.
9. Stationary and vehicular engines often require multifuel capability.

2.5   Flame Stabilizer

One of the main basic requirements of the combustor is to support combustion over a wide range of operating conditions. This could be achieved by an appropriately designed flame stabilizer. Flame stabilization could be achieved if a sheltered region is provided to entrain and recirculates some of the hot combustion

burnt gases with the fresh incoming fuel and air mixture. There are several types of flame stabilizer such as bluff bodies, opposed jets, jet mix and grid mix, axial swirler and radial swirler.

2.5.1 Bluff Body

The bluff body flame stabilizer causes a flow recirculation by creating a low pressure zone in its near wake region.
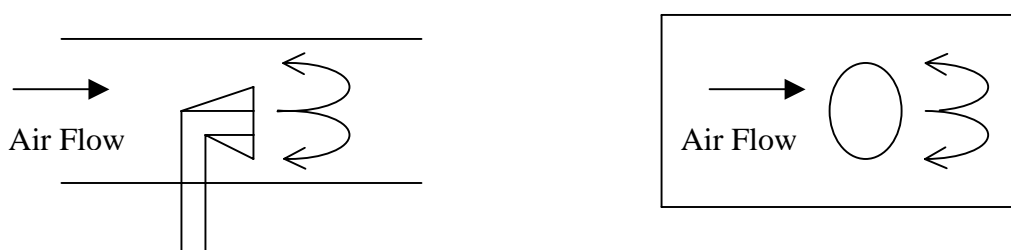
Figure 2.5: Bluff Body Flame Stabilizers

2.5.2 Opposed Jet

Opposed jet stabilizers cause a recirculation zone by the action of jets impinging either on one another or by the action of a jet being directed upstream into the oncoming main flow.
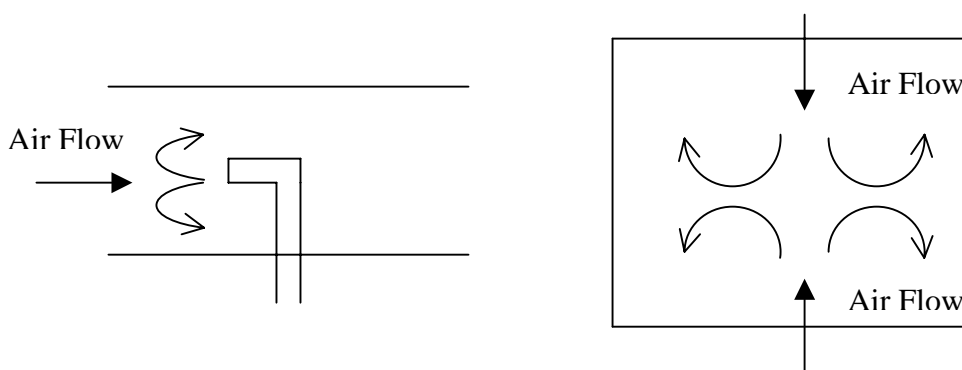
Figure 2.6: Opposed Jet Flame Stabilizers

2.5.3   Sudden Expansion

A sudden expansion in the diameter of the combustor also could generate recirculation zone hence stabilize the flame.
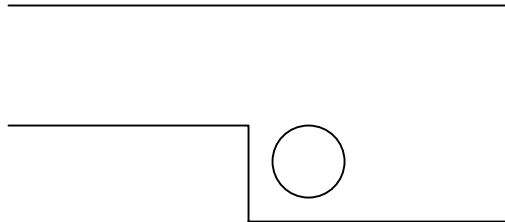
Figure 2.7: Sudden Expansion Flame Stabilization

2.5.4   Grid Mix and Jet Mix

Flame stabilization in the grid mix and jet mix is actually stabilized by injection of the fuel into the base of the fuel and air shear layer.
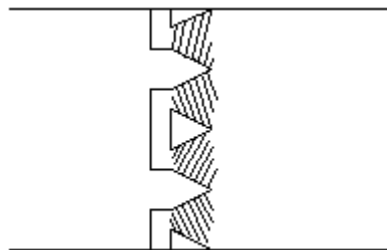
Figure 2.8: Grid Mix Flame Stabilizer

2.5.5   Axial and Radial Swirler

Axial and radial swirlers stabilize the flame through the generation of central recirculation zone that is formed when the vortex breakdown occur. Both of these swirlers attempt to inject the fuel into the base of the swirling shear layer to increase flame stability.
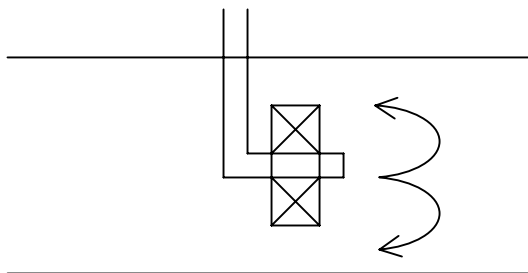
Figure 2.9: Axial or Radial Swirler

2.6 Injection System
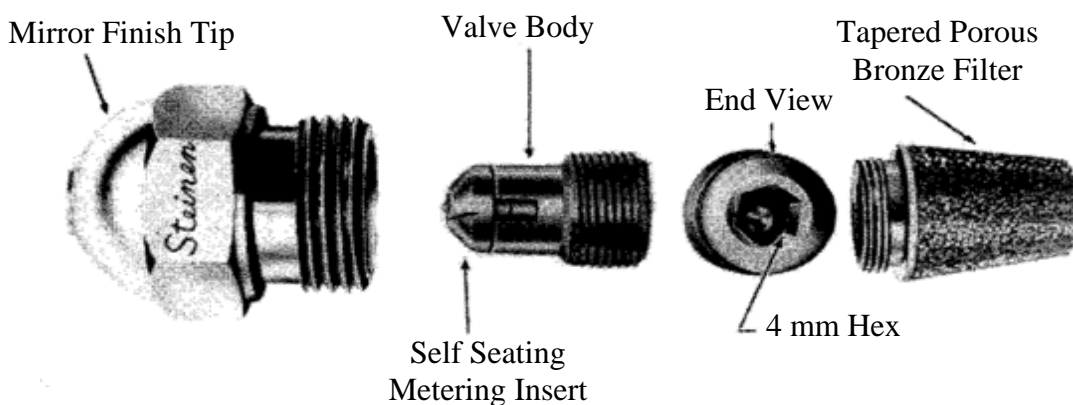
Figure 2.10: Injector (Mellor, A.M., 1990)

Fuel injection system also plays a major role in gas turbine combustion performance. Most combustion chambers employ high pressure fuel system in which the liquid fuel is forced through a small orifice to form a conical spray of fine droplets (atomization) in the primary zone. This is to produce a high ratio of surface to mass in the liquid phase, resulting in very high evaporation rates. The most obvious requirement in fuel injection is that the time required for burning of the spray (vaporize) must be kept short. The injector is also referred to as atomizer as its main function is to atomize the fuel.

2.6.1   Injectors Requirement

An ideal fuel injectors would posses all the following characteristics (Lefebvre, A.H., 1983) and (Bent, R.D. and Mckinlay, J.L., 1985) :

1.   Good atomization over the entire range of fuel flows.

2.   Rapid response to changes in throttle settings.

3.   Freedom from flow instabilities.

4.   Low susceptibility blockage by contamination and carbon deposition on the nozzle.

5.   Low susceptibility to gum formation by heat soakage.

6.   Capability for scaling, to provide design flexibility.

7.   Low cost, lightweight, ease of manufacture and ease of removal for servicing.

8.   Low susceptibility to damage during manufacture and installation.

9.   Freedom from vaporization icing, thus making it unnecessary to use carburettor heat except under the most severe atmospheric conditions.

10.   More uniform delivery of the fuel-air mixture.

11.   Improved control of the fuel-air ratio.

12.   Reduction of maintenance problems.

13.   Instant acceleration of the engine after idling, with no tendency to stall.

14.   Increase engine efficiency.

15.   An easy ignitable mixture.

16.   A ratio of maximum to minimum fuel flow that exceeds the ratio of maximum to minimum combustor airflow.

17.   Controlled dispersion of the fuel throughout the primary combustion zone.

18.   An exit gas temperature distribution that is insensitive to variations in fuel flow rate.

2.6.2   Atomization Process

In gas turbine combustion chambers, atomization is normally accomplished by spreading the fuel into a thin sheet to induce instability and promote disintegration of the sheet into drops. Thin sheets could be obtained by discharging the fuel through orifice with specially shaped approach passage by forcing it through narrow slots, by spreading it over a metal surface or by feeding it to the centre of a rotating disk. The function of the atomizer is to attenuate the fuel into a fine jet or thin sheet from which ligaments and ultimately drops will be produced and distribute the resulting drops throughout the combustion zone in a controlled pattern and direction.

2.6.2.1 Jet Break Up

Several modes of jet disintegration have been identified, but in all cases the final mechanism involves the break up of unstable threads of liquid into rows of drops conforming to the classical mechanism postulated by Rayleigh (Lefebvre, A.H., 1983).

According to Rayleigh's theory, liquid becomes unstable and breaks into drops when the amplitude of a small disturbance, symmetrical about the axis of the jet, grows to one half the diameter of the undisturbed liquid jet. This occurs when $\lambda / d_o = 4.5$, where λ is the wavelength of the disturbance and d_o is the initial jet diameter. For this value of 4.5, the average drop diameter of break up is $1.89\, d_o$, which is almost double of the diameter of initial jet diameter. In Rayleigh's theory, liquid viscosity is not considered. This theory later extended by Weber to include the effect of liquid viscosity effect on the break up (Lefebvre, A.H., 1983). According to Weber, the ratio of λ / d_o required to produce maximum instability for viscous jets is given by :

$$\frac{\lambda}{d_o} = \left[\pi\sqrt{2}T1 + \frac{3\mu_L}{\sqrt{\rho_L \sigma d_o}} \right]^{0.5} \tag{2.24}$$

When $\mu_1 = 0$, the value of $\lambda/d_o = 4.44$, which is almost the same as the value of Rayleigh's prediction. However, when a liquid with viscosity of 0.86 kg/ms is experimented, the ratio of λ/d_o for maximum instability ranged form 30 to 40. This clearly differs from Rayleigh's prediction.

In the case of liquid jet disintegration due to the influence of the surrounding air, the drop size obtained is governed by the ratio of disruptive aerodynamic force $\rho_A U^2{}_R$ to the consolidating surface tension force σ/d_o. This dimensionless ratio is also known as Weber number.

$$We = \frac{\rho_A U^2{}_R d_0}{\sigma}$$
(2.25)

In the case of liquid jet disintegration without the influence of the surrounding air, the atomization quality is dependent on jet diameter, liquid properties density, surface tension and viscosity. This break up mechanism is dependent to Z number.

$$Z = \frac{We^{0.5}}{\text{Re}} = \frac{\mu_L}{\sqrt{\sigma \rho_L d_o}}$$
(2.26)

2.6.2.2 Sheet Break Up

Fraser and Eisenklam, has identified three modes of sheet disintegration, described as rim, wave and perforated sheet disintegration (Bent, R.D. and Mckinlay, J.L., 1985).

In the rim disintegration mode, forces were created by surface tension causes the free edge of a liquid sheet to contract into a thick rim, which then breaks up by a mechanism corresponding to the disintegration of a free jet. When this occurs, the resulting drops continue to move in the original flow direction, but they remain attached to the receding surface by thin threads that also rapidly break up into rows of drops. This mode of disintegration is most prominent where the viscosity and

surface tension of the liquid are both high. It tends to produce large drops, together with numerous small satellite droplets.

In perforated sheet disintegration, holes appear in the sheet at a certain distance from the orifice. The holes are delineated by rims formed from the liquid that was initially included inside. These holes grow rapidly in size until the rims of adjacent holes coalesce to produce ligaments of irregular shape that finally break up into drops of varying size.

Atomizers that discharge the fuel in the form of sheet are usually capable of exhibiting all three modes of sheet disintegration. Sometimes two different modes occur simultaneously, and their relative importance can greatly influence both the mean drop size and the drop size distribution.

2.6.3   Spray Characteristic

Combustion performance is also dependence on spray characteristic such as mean drop size, drop size distribution, spray pattern, cone angle, dispersion and penetration. Mean drop size and drop size distribution are important in designing the atomizer meanwhile spray pattern, cone angle, dispersion and penetration are governed partly by atomizer design and partly by the aerodynamics influence to which the spray is subjected after atomization is completed.

2.6.3.1 Mean Drop Size

Mean diameter plays an important role in determining the evaporation rate and atomization qualities of various sprays. The general idea of the mean diameter is to replace the given spray with imaginary drops which have the same diameter while retaining certain criteria of the original spray. The sauter mean diameter (SMD) is the one which is most common and widely used. It is defined as the diameter of a

drop having the same volume/surface ratio as the entire spray (Hoe, Y.M., 2000).
Table 2.5 shows some mathematical definitions of mean drop size.

$$SMD = \frac{\sum nD^3}{\sum nD^2} \qquad (2.27)$$

Table 2.5: Some Mathematical Definitions of Mean Drop Size (Hoe, Y.M., 2000)

Parameter	Description	Symbol for Mean Diameter	Mathematical Definition of Mean Diameter
Diameter	Linear mean diameter of drops in spray	D or D_1	$\dfrac{\sum nD}{\sum n}$
Area Length	Diameter of a drop having the same surface/diameter ratio as the entire spray	D_o	$\dfrac{\sum nD^2}{\sum nD}$
Volume-Surface Diameter	Diameter of a drop having the same volume/surface ratio as the entire spray	SMD	$\dfrac{\sum nD^3}{\sum nD^2}$
Area Diameter	Diameter of a drop whose surface area is equal to the mean surface area of all the drops in the spray	D_2	$\left[\dfrac{\sum nD^2}{\sum n}\right]^{0.5}$
Volume (Mass) Diameter	Drop diameter below or above which lie 50% of the mass of the drops	MMD	$\left[\dfrac{\sum nD^3}{\sum n}\right]^{0.33}$

2.6.3.2 Drop Size Distribution

The drop size distribution is most difficult to predict theoretically and to determine experimentally. An instructive picture may be obtained by plotting a histogram of drop size, each ordinate representing the number of drops whose

dimensions fall between the limits $x \pm \Delta x / 2$. A typical histogram of drop size distribution is shown in Figure 2.11 in which $\Delta x = 17 \mu m$.
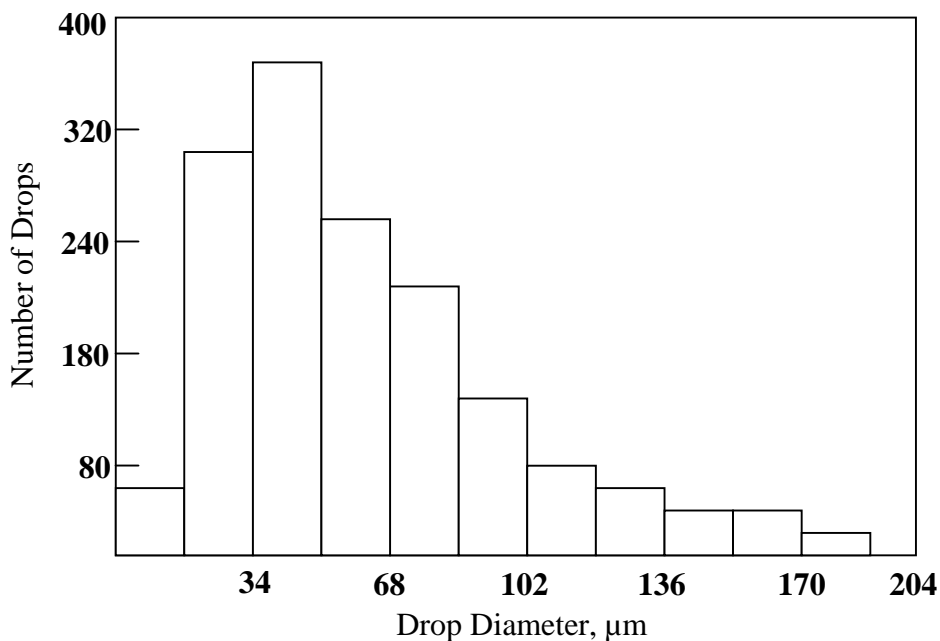
Figure 2.11: Typical drop-size histogram (Hoe, Y.M., 2000)

2.6.3.3 Spray Pattern and Cone Angle

The uniformity of the distribution of fuel in a conical spray is referred as spray pattern. Poor spray pattern adversely affects many important aspects such as combustion performance, pattern factor and pollutant emissions.

The spray cone has a strong influence on ignition, stability limits and exhausts emission. In plain orifice atomizer, the cone angle is narrow and fuel drops is fair evenly dispersed throughout the entire spray volume. It is possible to produce solid cones with swirl atomizers, but, for gas turbine applications, the spray is usually in the form of a hollow cone of wide angle with most of the drops at the periphery.

As plain orifice atomizers produce a narrow and compact spray in which only small proportion of the drops are subjected to the effects of air resistance, the

distribution of the spray as a whole is dictated mainly by the magnitude and direction of the velocity imparted to it on exiting from the atomizers orifice. With swirl atomizers however the hollow conical structure of the spray incurs appreciable exposure to the influence of the surrounding air. Normally, an increase in spray cone angle increases the extent of this exposure, leading to improve atomization and an increase in the proportion of drops whose distribution is dictated by the aerodynamics of the primary zone.

Figure 2.12: Spray Pattern (Hoe, Y.M., 2000)
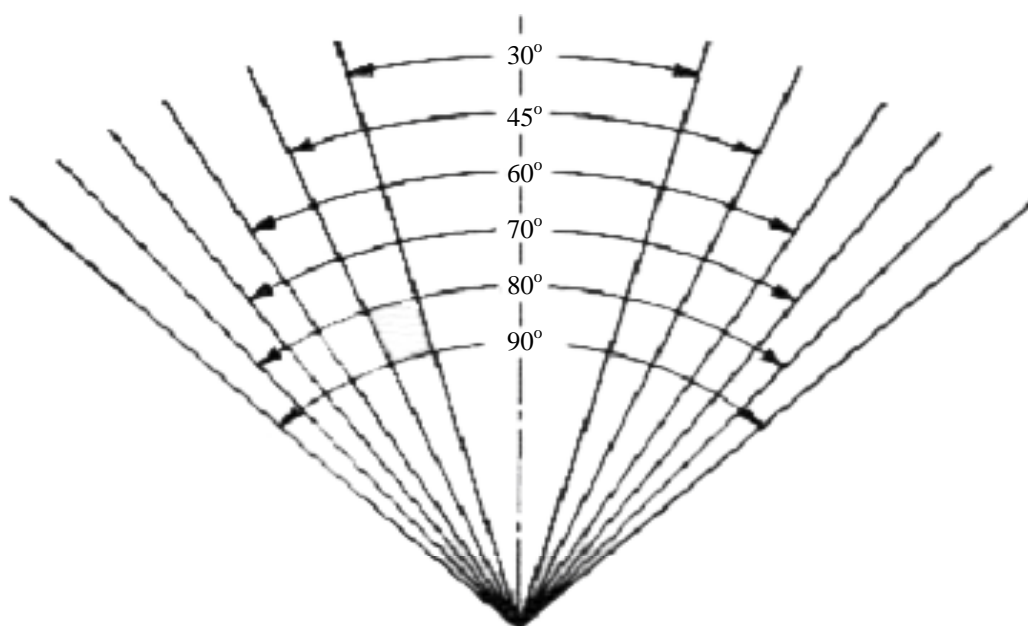
Figure 2.13: Cone Angle (Hoe, Y.M., 2000)

2.6.3.4 Dispersion and Penetration

Dispersion could be expressed as the ratio of the volume of the spray to the volume of the fuel contained within it. The advantage of a good dispersion is that the fuel mixes rapidly with the surrounding gas. This could increase the evaporation rate and heat release. Dispersion is small in narrow spray angle and high in wide spray angle (Hoe, Y.M., 2000). In swirl atomizers, dispersion are governed mainly by mean drop size, drop size distribution, cone angle, surrounding medium and fuel properties. However, those factors that increase the spray cone angle also tends to improve the spray dispersion.

Meanwhile, penetration of a spray may be defined as the maximum distance of fuel reaches when injected into stagnant air. It is governed by the relative magnitudes of two opposing forces: (1) the kinetic energy of the fuel jet and (2) the aerodynamic resistance of the surrounding gas. The initial jet velocity is high, but as atomization proceeds and the surface area of the spray increases, the kinetic energy of the fuel is gradually dissipated by frictional losses to the gas. When, the drops have finally exhausted their kinetic energy, mainly gravity and the movement of the surrounding gas dictate their trajectory (Hoe, Y.M., 2000). In general, a compact, narrow spray will have high penetration, while a well atomized spray of wide cone angle, incurring more air resistance, will tend to have low penetration. In all cases, the penetration of a spray is much greater than that of a single drop. The first drop to be formed impart their energy to the surrounding gas, which begins to move with the spray; the gas therefore offers less resistance to the following drops that consequently penetrate further.

2.6.4   Types of Atomizers

There are several atomizers that are used for combustion applications. Several types of atomizers are briefly described in this section. Relative merits of these atomizers were simplified and accessible in Appendix A.

2.6.4.1 Plain Orifice Atomizer

Plain orifice atomizer is widely used in afterburners, where the fuel injection system normally consists of one or more circular manifolds. The spray produced by plain orifice atomizer usually has a cone angle between 5° and 15°. The narrow spray angle exhibited by plain orifice atomizer makes it impractical for most application.
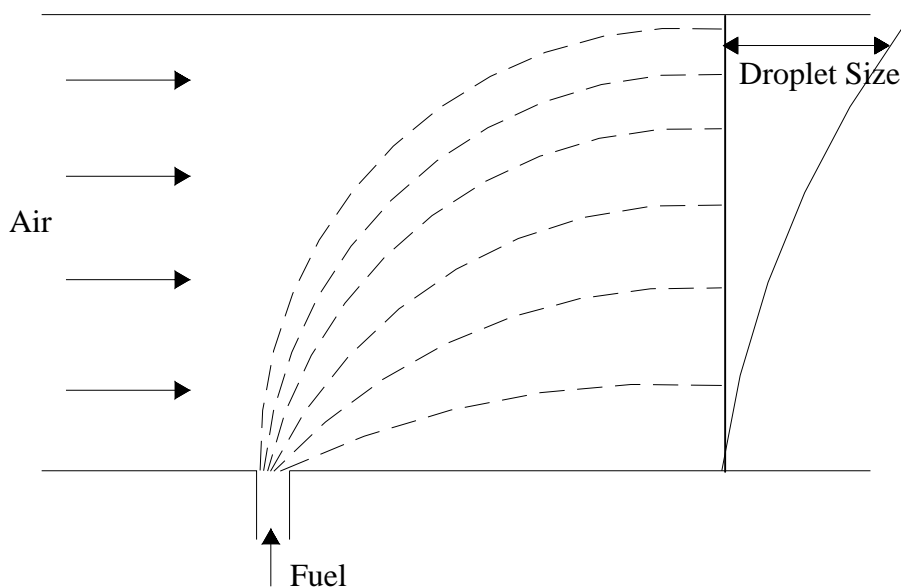
Figure 2.14: Plain Orifice Atomizer (Hoe, Y.M., 2000)

2.6.4.2 Simplex Atomizer

Simplex atomizer has a wider cone spray angle than plain orifice atomizer. Swirling motion is imparted to the fuel so that, under the action of centrifugal force, spread out in the form of hollow cone as soon as it leaves the orifice. Simplex atomizer is the simplest form of pressure swirl atomizer. A major drawback of the simplex atomizer is that its flow rate varies as the square root of the fuel injection pressure (Hoe, Y.M., 2000).

.
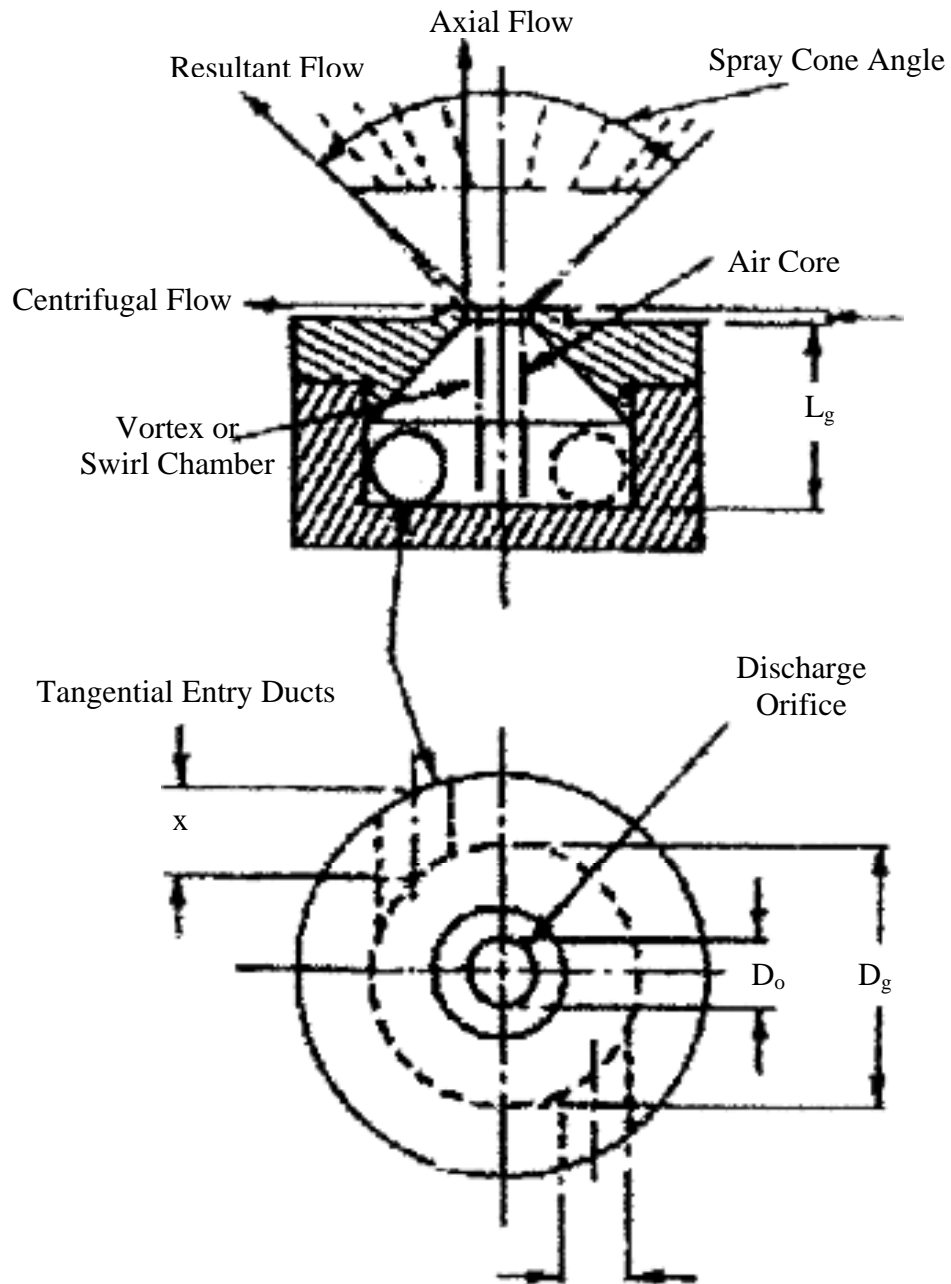
Figure 2.15: Simplex Atomizer (Hoe, Y.M., 2000)

2.6.4.3 Wide Range Atomizer

The major drawback in simplex atomizer has led to the development of wide range atomizer such as duplex, dual orifice and spill atomizer. These atomizers have ratio of maximum to minimum fuel output about 20 with fuel injection pressure not exceeding 7 MPa. There are two types of wide range atomizers that are duplex atomizer and dual orifice atomizer (Hoe, Y.M., 2000).

The different between duplex atomizer and simplex atomizer is that its swirl chamber employs two sets of tangential swirl port. One set is the pilot or primary ports for the low flows encountered when the engine is idling or at high altitudes and the other set comprises the main passage for the large flow required under normal operating condition. This atomizer is widely used in aircraft engine application.

Dual orifice atomizer is also known as duplex atomizer. It is comprised of two simplex atomizer that are fitted concentrically, one inside the other. At a low fuel flows all the fuel is supplied from pilot atomizer. When the fuel pressure reaches a predetermine value, the pressuring valve open and admits fuel to the main atomizer (Hoe, Y.M., 2000).
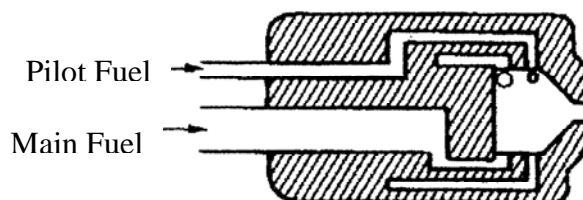
Figure 2.16: Duplex Orifice Atomizer (Hoe, Y.M., 2000)
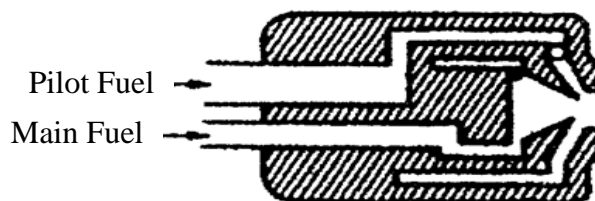
Figure 2.17: Dual Orifice Atomizer (Hoe, Y.M., 2000)

2.6.4.4 Spill Return Atomizer

Basically, spill return atomizer is almost similar to simplex atomizer. Spill return atomizer differs from simplex atomizer such that the rear wall of the swirl chamber instead of being solid, it contains an annular passage which fuel can be spilled away from the atomizer. Fuel is supplied to the swirl chamber at high pressure and high flow rate(Hoe, Y.M., 2000).
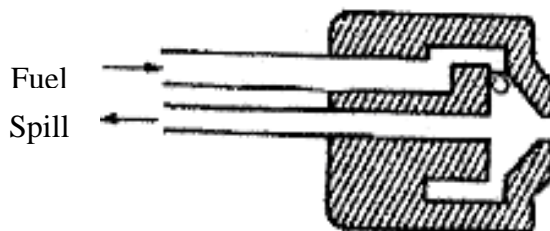
Figure 2.18: Spill Return Atomizer (Hoe, Y.M., 2000)

2.6.4.5 Fan Spray Atomizer

Fan spray atomizer is usually obtained by cutting slots into plane or cylindrical surfaces and arranging for the fuel into each slot from two opposite directions. In the single hole fan spray atomizer, there is only one single orifice; this orifice forces the liquid into two opposite streams within itself, so that a fan spray issues from the orifice and spreads out in the shape of a sector of a circle of about 75° angle. An air shroud is usually fitted around the atomizer tip, using the pressure differential across the linear wall (Hoe, Y.M., 2000).
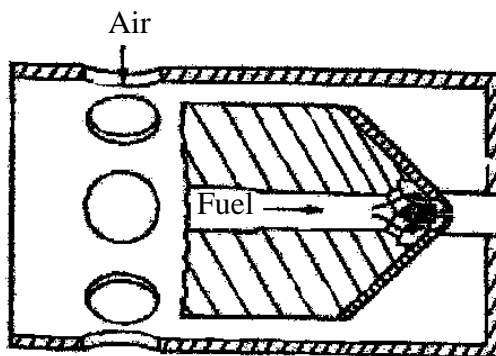
Figure 2.19: Fan Spray Atomizer (Hoe, Y.M., 2000)

2.6.4.6 Rotary Atomizer

In a rotary atomizer, liquid fuel is fed onto a rotating surface, where it spreads out quite uniformly under the action of centrifugal force. The rotating surface may take the form of a flat disk, vane disk, cup or slotted wheel. A coaxial air blast is used to assist atomization. This system has extreme versatility and has been shown to atomize successfully liquids that vary widely in viscosity (Hoe, Y.M., 2000).

2.6.4.7 Air Assist Atomizer

An example of this atomizer is the use of shroud air on fan spray and simplex atomizer. This atomizer's swirl port is sized to pass the maximum fuel flow at the maximum fuel injection pressure, then the fuel pressure differential is too low to give good atomization at the lowest fuel flow. Internal mixing air assist atomizer is very suitable for highly viscous fuels and good atomization can be obtained (Hoe, Y.M., 2000).

Fuel

Air
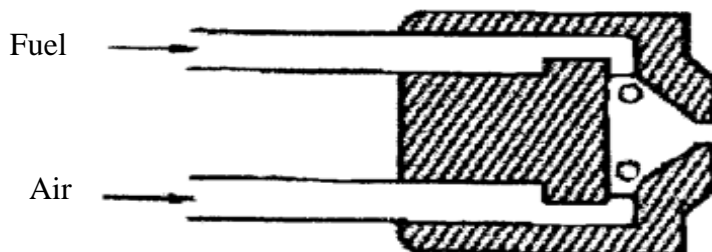
Figure 2.20: Air Assist Atomizer (Hoe, Y.M., 2000)

2.6.4.8 Air Blast Atomizer

In principle, the air blast atomizer functions in exactly the same manner as the air assist atomizer because both employ the kinetic energy of a flow airstreams to shatter the fuel jet or sheet into ligaments and then drops. The main difference

between these two systems lies in the quantity of air employed and its atomising velocity (Hoe, Y.M., 2000).

2.6.4.9 Slinger System

In slinger system, fuel is supplied at low pressure along the hollow main shaft and is discharged radially outwards through holes drilled in the shaft. These injection holes vary in number from 9 to 18 and in diameter from 2.0 to 3.2 mm. The holes may be drilled in the same plane as a single row but some installations feature a double row holes. The holes never run full; they have a capacity that is many times greater than the required flow rate. They are made large to obviate blockage. However, it is important that the holes be accurately machined and finished, since experience shown that uniformity of flow among injection holes depends on their dimensional accuracy and surface finish. If one injection holes supplies more fuel than others, a rotating hot spot will be formed in the exhaust gases, with disastrous consequence for the particular turbine blade on which the hot spot happens to impinge.

The advantage of the slinger system is that it is low in cost and simple. Only low pressure fuel pump is needed and atomization quality depends on engine speed. The influence of fuel viscosity is small, so the system has a potential multifuel capability. One drawback of the slinger system is its slow response to changes in fuel flow. A more serious problem is that of high altitude relighting performance. With the engine wind milling, the rotational speed is quite low and consequently the atomization quality is relatively poor. This system is suitable for small engines. The problems of wall cooling could arise if the system were applied to engines with high pressure ratios (Hoe, Y.M., 2000).

2.7   Air Fuel System

Stoichiometric combustion occurs when all the oxygen atoms in the oxidizer react chemically to appear in the products. The oxidizer in this case is the air mixing with the fuel in the combustion chamber. The chemical reaction is given by:

$$C_aH_bO_cN_d + a_1(O_2 + 3.76N_2) \Leftrightarrow b_1CO_2 + c_1H_2O + d_1N_2 \qquad (2.28)$$

where:

a_1, b_1, c_1, d_1 = molar coefficients

a, b, c, d = fuel components

The stoichiometric fuel to air ratio can be calculated with:

Fuel Air Ratio (FAR_s) = 1 mole of fuel / $a_1(O_2 + 3.76N_2)$ \qquad (2.29)

Table 2.6 below shows the stoichiometric air fuel ratios for various fuels. As the fuel used for the experimental testing was diesel, so stoichiometric air fuel ratio used was 14.5 which means that one unit of diesel needs 14.5 units of air to obtain stoichiometric level.

Table 2.6: Air Fuel Ratio for Various Fuels (Blas, Luis Javier Molero de, 1998)

Fuel	Chemical Formula	HHV [kJ/kg] [kg air/kg fuel]	Air/Fuel Ratio Stoichiometric	Fuel/Air Stoichiometric
Methane	CH_4	55,500	17.2	0.05814
Propane	C_3H_8	50,300	15.6	0.06410
Octane	C_8H_{18}	47,900	15.1	0.06623
Methanol	CH_3OH	22,700	6.5	0.15385
Ethanol	C_2H_5OH	29,700	8.99	0.11123
Hydrogen	H_2	141,600	27.2	0.03677
Gasoline	C_8H_{15}	47,300	14.6	0.06849
Diesel	$C_{12.5}H_{22.2}$	44,800	14.5	0.06897

Meanwhile, Table 2.7 shows the influence of various primary zone mixture strengths on the combustion process. The mixture strengths are essential to be determined before a combustor is operated.

Table 2.7: Influence of Various Primary Zone Mixture Strengths (Mellor, A.M., 1990).

Primary Zone Mixture Strength	Advantages	Disadvantages
Stoichiometric	1. Maximum heat release rate 2. Low luminosity flame 3. Little exhaust emission 4. No carbon deposits	1. High rate of heat release to liner walls 2. Requires intermediate zone 3. High nitric oxide emissions
Fuel Rich	1. Low recirculation velocity gives "weak extinction" point and easy ignition 2. High combustion efficiency at low power condition	1. Low Volumetric heat release rate 2. High luminosity flame 3. Copious exhaust smoke 4. Coke deposition on walls 5. Requires long intermediate zone
Fuel lean	1. Clean, blue flame 2. No exhaust smoke 3. No carbon deposits 4. Requires no intermediate zone 5. Good exit temperature deposit	1. High Recirculation velocity adversely affects stability and ignition performance

CHAPTER III

EMISSION CONTROL

3.1   Introduction

The main problem with the control of pollutants from the gas turbines is that the reduction of NO_x emissions can results in the increase in either CO or UHC emissions (Escott, N.H., 1993). This problem can be seen in Figure 3.1.
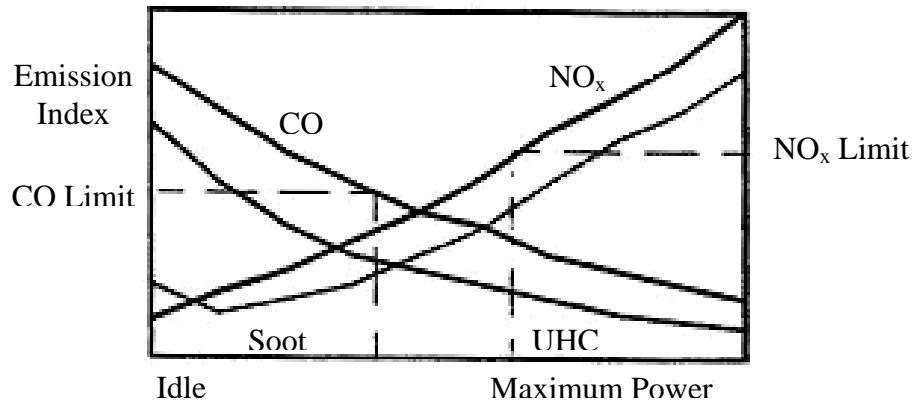
Figure 3.1: Emission Characteristic of a Gas Turbine (Escott, N.H., 1993)

The main approach to this problem is to ensure that CO emission is minimized by the homogeneous mixing of the fuel and air than to concentrate on the reduction of NO_x emissions (Mikus, T. and Heywood, S.B., 1971). In practical gas turbine combustors, this can be validated by achieving combustion efficiencies better than 99.5 percent at idle approaching 100 percent at full power. Homogeneous mixing can often achieved by premixing the fuel and air, but low NO_x system must

also ensure that flame stability is maintained over a wide range of operating conditions.

Most NO_x reduction techniques basically involve the reduction of the peak flame temperature to ensure that thermal NO is not formed. A reduction in the combustor inlet temperature would reduce the formation of thermal NO but this is not a practical solution because higher turbine inlet temperatures are required to increase the gas turbines thermal efficiency.

3.2 Factors Influencing NO_x Formation

Three main factors influences the formation of NO_x are flame temperature, flue gas residence time and the turbulence effect (Kim, M.N., 1995). The NO_x emission is proportional to the flame temperature. NO_x emission increases with the rise of flame temperature. Low flame temperature produces less NO_x emission. Flue gas residence time should be long enough to allow more time for combustion reaction. If the mixing rate between fuel and air is high, flue gas residence time could be reduced. Besides that, strong turbulence effect is needed to reduce NO_x emission. This could be achieved by creating pressure drop in the combustion zone that would generate turbulence energy in the shear layer region and increases mixing rate of fuel and air significantly (Kim, M.N., 1995).

3.3 NO_x Control Techniques

There are number of ways of combustion methods to reduce NO_x emission. Basically these methods could be categorised into two techniques; prevention of NO_x formation and destruction of NO_x.

3.3.1   Prevention of NO_x Formation

This category refers to measures that do not necessitate major process alteration or plant construction. This category generally required modifications to the conventional burner designs or operating condition. Capital expenditure and installation time are usually less than those needed for major retrofit work. This technique involves pre-combustion methods such as homogeneous mixing of fuel and oxidant and lean combustion.

Lean combustion is the main and earliest technology of low NO_x combustion. Lean combustion that works with low temperature is the easiest way of NO_x reduction as this technique eliminate thermal NO formation as suggested by Zeldovich chain mechanism.

Further studies show that low flame temperature together with homogeneous mixing could further reduce NO_x emission. This could be achieved with the use of swirler or premixed flame.

3.3.1.1 Premixed Combustor
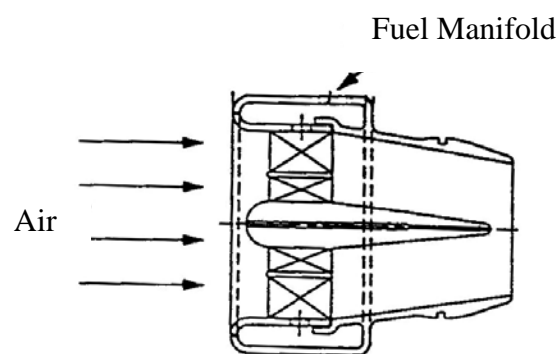
Figure 3.2: Premixed Combustor (Leonard, G. and Stegmaier, J., 1993)

In premixed combustor (Figure 3.2), the air and fuel are mixed before they are passed through a jet into the combustion zone and sufficient initial air is mixed to prevent soot formation. The velocity of the mixture through the combustor jet is

important. If the velocity is too low (below the burning velocity of the mixture) the flame can light back into the mixing region, whereas if the velocity is too high the flame can lift off from the combustor to the extent where it can be extinguished by entrainment of additional air around the burner. However, it has been noted that the fully premixed combustion system has several severe problems such as flame stability, auto ignition and combustion efficiency and stabilizer durability. Therefore, attention has been switched to rapid fuel and air mixing rather than premixing.

3.3.1.2 Rapid Mixing Combustor
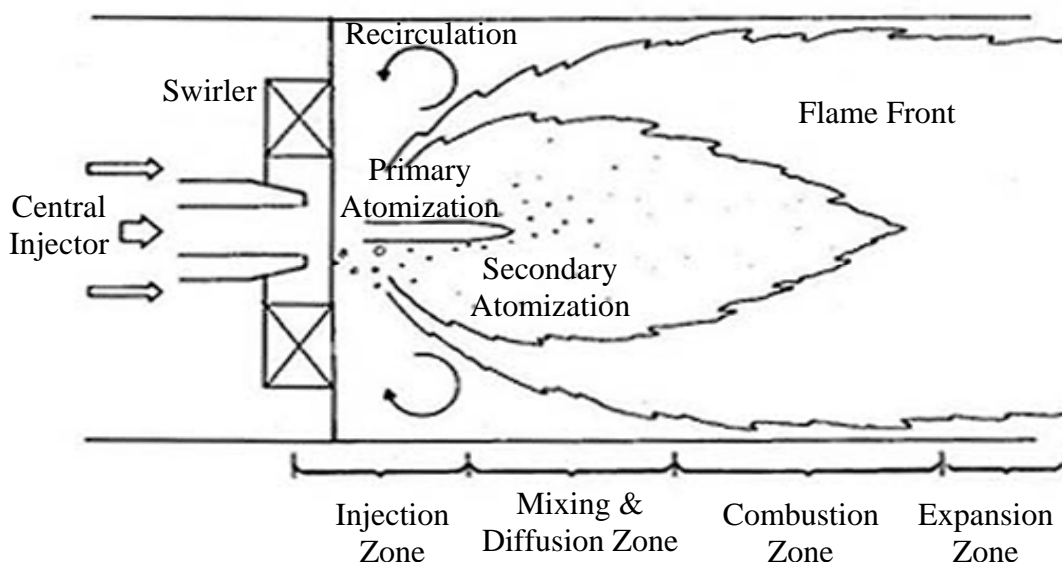
Figure 3.3: Rapid Mixing Combustor (Beer,J.M. and N.A. Chigier., 1972)

Rapid fuel and air mixing could be achieved using swirlers. Swirler could act as flame stabilizer that promotes the mixing by generating turbulence in the combustion chamber. Swirl flow forms central recirculation zone that could stabilize the flame resulting in better mixing and combustion. The recirculation zone is formed in both cold and combusting flows. The formation of such a flow pattern in the vicinity of the fuel injector results in stable combustion and rapid heat release. This is attributed to the enhanced mixing rates between the fuel and air and supply of energy required for ignition. Figure 3.3 is an example of a combustor applying swirler.

3.3.1.3 Variable Geometry Combustor
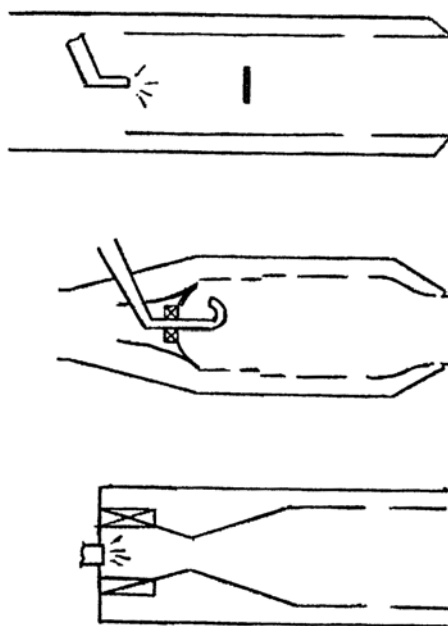
Figure 3.4: Variable Geometry Combustor (Escott, N.H., 1993)

A variable geometry combustor (Figure 3.4) seems to be the ideal solution to overcome both the high power and low power operating range of combustor. For minimum combustor emissions, if the thermal input is reduced from 50 kW to 5 kW at constant excess air then the airflow is reduced by a factor of 10. For a fixed flow blockage combustor this reduces the pressure loss by a factor of 100 that reduce the fuel and air mixing and the flow turbulence. If the combustor flow area is reduced so that it acts as a flow control valve then the combustor pressure loss is constant as the flow reduced. Mechanical complexities involved seem to repulse combustor designers from developing this technique. However, the considerable potential that variable geometry holds for emissions reduction has led to a renewal of interest in its application. In gas turbine combustor variable geometry is required to overcome flame stability problems in the lean low NO_x primary zones as the power is reduced by reducing the fuel flow at constant air flow (Mohammad Nazri, 1997).

3.3.1.4 Lean Premixed Prevapourized Combustor
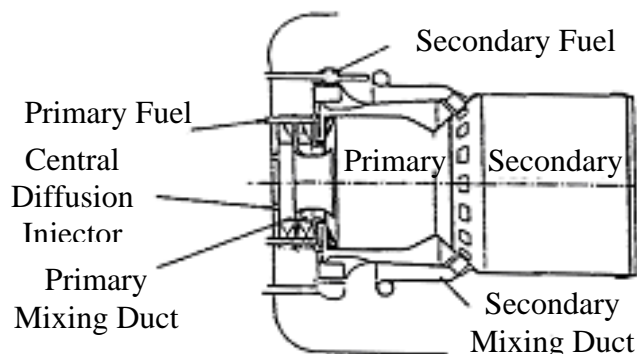
Figure 3.5: Lean Premixed Prevapourized Combustor (Willis, J.D. et al., 1993)

Another attractive technique for reducing nitric oxide emissions is the lean premixed prevapourized combustion for liquid fuel. The key factor is to attain complete evaporation of the fuel and complete mixing of fuel and air prior to combustion. By avoiding droplet combustion, operating the burner in fuel-lean with low reaction temperature and the elimination of hot spots in the combustion zone drastically reduced nitric oxide emissions (Lyon, R.K., 1975). However, there are some drawbacks for this technique. Risks of auto ignition and flashback in the premixing duct were perhaps the most severe problems. Other problems involved ensuring flame stability, stabilizer stability and combustion efficiency. The use of flame stabilizers removes the need for a premixing duct. Good fuel and air mixing is achieved by swirl stabilizers (Jeffs,E., 1992). Lean premixed prevapourized combustor is shown in Figure 3.5.

3.3.2 Destruction of NO_x

These processes generally involve the treatment of the flue gases after the combustion has occurred in the chamber and before exiting to the stack. Very high reduction of NO_x is possible (up to 90 percent) using selective reduction technique. However, these methods need more capital intensively and required more frequent maintenance procedures.

3.3.2.1 Staged Combustor
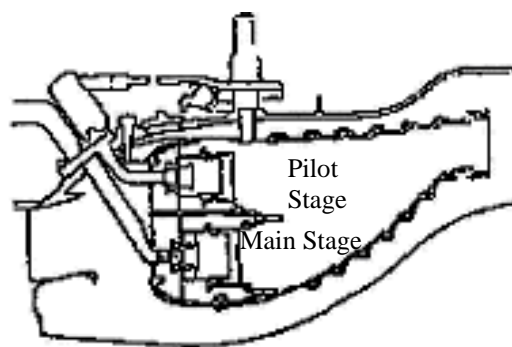
Figure 3.6: Fuel Staging Combustor (Jamieson, J.B., 1990)
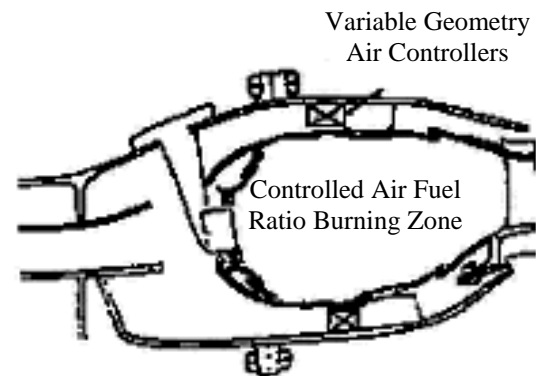
Figure 3.7: Air Staging Combustor (Jamieson, J.B., 1990)

Staged combustion is divided into two sections that are fuel staged combustor and air staged combustor. In fuel staged combustor, as shown in Figure 3.6, at low power conditions the fuel is supplied to the first stage only for flame stability. However, as the required power increases to a certain critical point the fuel is supplied to both stages. As well as fuel, the air is also introduced in the second stage to ensure lean burn operation is achieved over the entire power range.

Air staging in a burner is often called two-stage combustion and is an exaggerated form of low excess air combustion whereby the primary combustion zone air is reduced to such an extent that a sub-stoichiometric region exists in the lower chamber. The additional air is necessary to complete combustion is added, progressively at points further downstream. NO_x formation does not take place at lower temperatures and where levels of oxygen present in the combustion zone are low. Fuel-bound nitrogen volatised in the fuel rich region has more opportunity to form molecular nitrogen than NO_x. Generally, between 10 percent and 30 percent of the total combustion air is used for staging. Figure 3.7 is an example of air staging combustor.

3.3.2.2 Flue Gas Recirculation Combustor
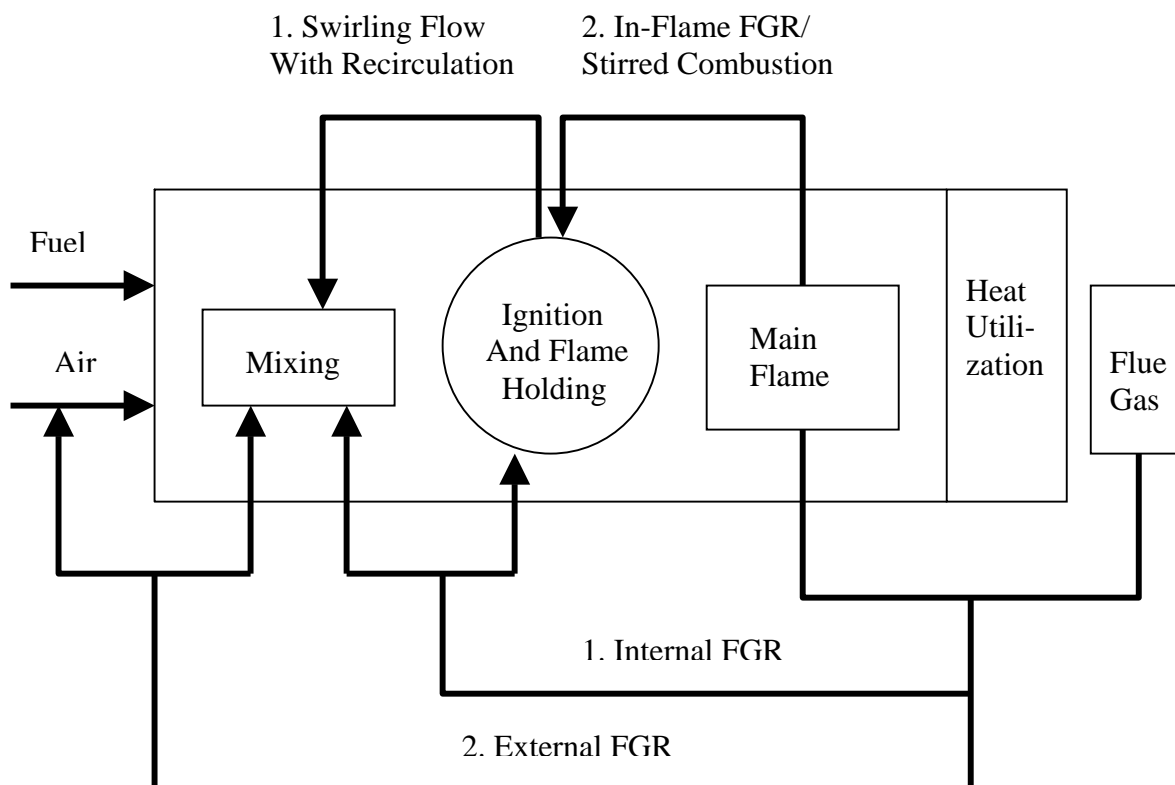
Figure 3.8: Schemes of flue gas recirculation (Masataka A., 2000)

From the viewpoint of low oxygen and lean combustion, flue gas recirculation (FGR) that was commonly used as exhaust gas recirculation (EGR) in internal combustion engine was considered as an effective way to reduce NO_x emission. The flue gas was recirculated into the chamber that acts as an inert gas to decrease the flame temperature hence reduces the NO_x emission. This method is not so popular but its system is partially employed in many combustion systems (Masataka A., 2000). There are many types of flue gas recirculation that could be applied such as swirling flow with recirculation, in-flame FGR, internal FGR and external FGR. Figure 3.8 shows schemes of flue gas recirculation.

3.3.2.3 Rich-Burn Quench Lean-Burn Staged Combustor
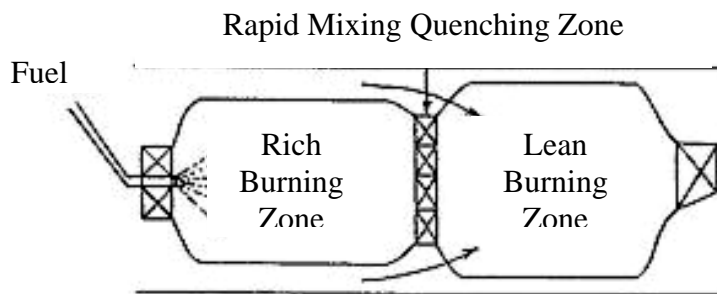
Figure 3.9: Rich-Burn Quench Lean-Burn Staged Combustor (Jamieson, J.B. 1990)

Rich-burn quench lean-burn staged combustor (RQL) achieves low NO_x emissions by having a rich-burn first stage, reduces NO_x, followed by a lean-burn second stage, which completes CO and UHC oxidation. In order to ensure that temperatures in the main reaction zone are lowered before entering second stage, a rapid quenching zone is required. Completion of combustion products of CO and UHC is then achieved at leaner equivalence ratios where NO_x formation reaction is at a minimum. One of the main problems associated with simple two stage and RQL combustion systems is that the reactions involving the oxidation of CO and UHC could well quenched by the addition of the secondary quenching air, but if the addition of the secondary quenching air is too slow local high temperature NO_x products region could arise. Figure 3.9 shows scheme of RQL combustor.

3.3.2.4 Selective Catalytic Reduction Combustor (SCR)
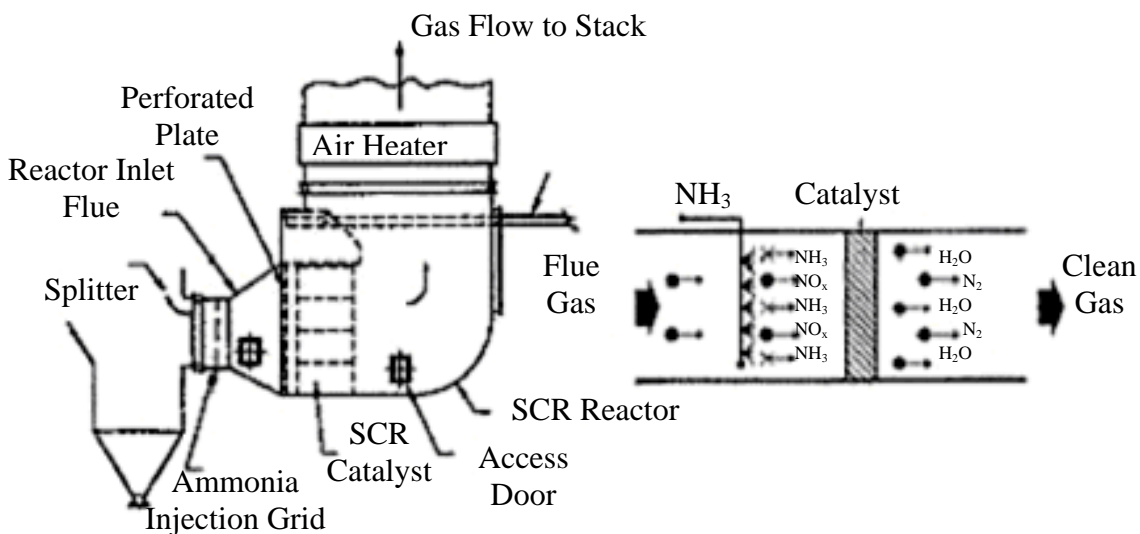
Figure 3.10: Selective Catalytic Reduction Combustor (McLaughlin, B.R. et al., 1997)

This process involves the treatment of the flue gases after combustion has occurred in the chamber and before exiting to the stack. NO_x in the flue gases are reduced by injecting ammonia in the presence of a catalyst to form nitrogen and water. As the reaction is selective, ammonia should not be oxidized at the correct operating temperature. A number of catalyst materials can be employed. They are chosen according to prevailing criteria such as available flue gas temperature, permissible ammonia slip and NO_x reduction required. SCR systems as shown in Figure 3.10 are becoming more widespread, however problems associated with catalyst degradation and poisoning and storage ammonia emission through various channels are restricting and delaying further implementation due to financial and safety concerns.

3.3.2.5 Selective Non-Catalytic Reduction Combustor (SNCR)
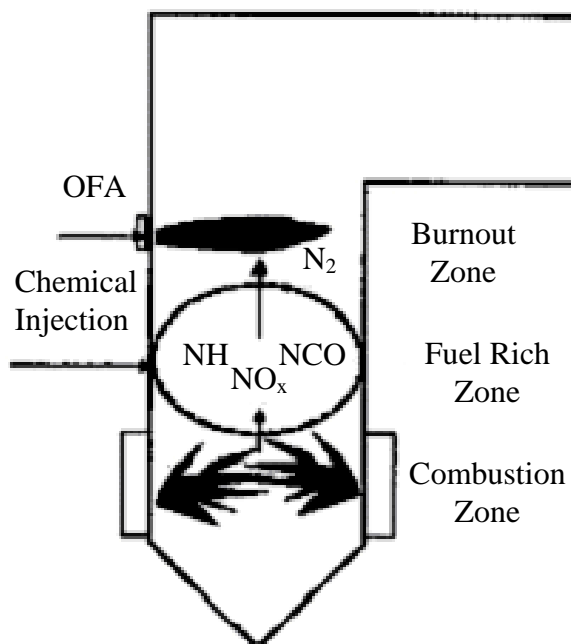
Figure 3.11: Selective Non-Catalytic Reduction Combustor (Cremer, M.A. et al., 2002)

This method of NO_x control use chemicals in controlled thermal reaction to reduce NO selectively. A higher efficiency of NO_x reduction can be achieved without a catalyst although chemical consumption levels are high. A number of different chemical compounds can be used although the majority comprise of ammonia and its derivatives such as urea and cyanuric acid. The reduction reactions occur within a limited temperature range between $800^{o}C$ to $1150^{o}C$ for most common additives although the use of enhancing agents or an alteration of the combustion conditions can lower or widen this window of operation. Mixing of the injected chemicals with the flue gas is paramount to achieve good NO_x reduction rates. Problems encountered here include the high viscosity of the flue gas, the positioning of the type of injectors, availability of chemicals and the extent of allowable ammonia slip. Selective non-catalytic combustor diagram is shown in Figure 3.11.

3.4   Practical Low NO_x Combustor

It has been discussed previously that CO and UHC emissions are minimized when the fuel and air mixing of the combustion chamber system is thorough. It is assumed that any NO_x combustion system will automatically ensure that the CO and UHC emissions kept at a minimum by good fuel and air mixing. However, this does depends on the emission technique employed. There are two main approaches to NO_x reduction techniques. One approach is to make minor changes to the existing combustor such as to provide better fuel atomisation and distribution that will promote homogeneous mixing of fuel and air. This approach has seen a modest reduction in average NO_x emission level from aero engines over the past 25 years. The second approach involves major combustor design modification such as staged, premixed, variable geometry and catalytic approaches. NO_x emission can be highly dependent on the flame temperature within the combustor and the flame temperature itself is dependent on combustor inlet temperature and the air-fuel ratio.

There are two ways of reducing NO_x emission by altering the operating range of equivalence ratio (EQR). One is to operate at fuel rich EQR and the other is fuel lean EQR. The justification for this approach is shown by the variation of NO_x formation with EQR in Figure 3.12. Flame temperature is higher near stoichiometric combustion.
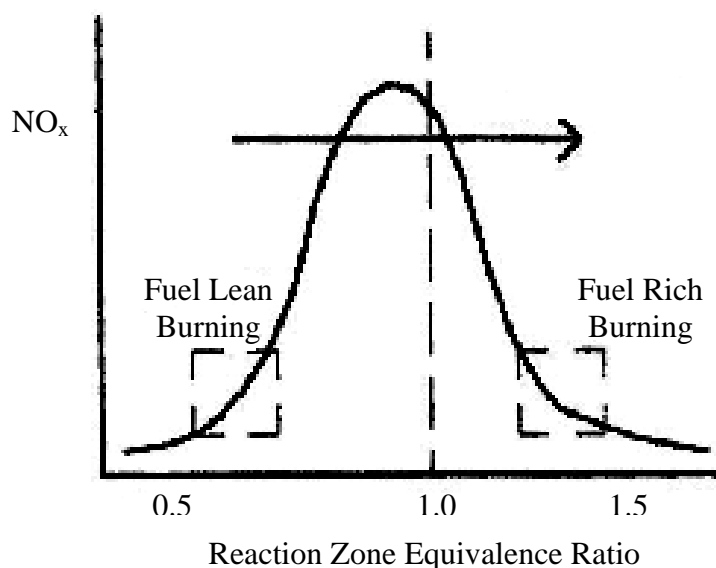
Figure 3.12: Effect of Reaction Zone Equivalence Ratio on NO_x Emission (Escott, N.H., 1993)

Burning in the fuel rich region of EQR could present problems with soot formation and the necessary addition of air after the reaction zone could lead to stoichiometric conditions and thus increase NO_x emission. Burning in fuel lean region of EQR avoids these problems but is susceptible to lean flammability and flame blow off problems. Designing a combustor with low NO_x emission approaches present problems because the combustor has to operate over a wide range of overall EQR, thus the air and/or the fuel is normally staged.

CHAPTER IV

BURNER DESIGN CONCEPT

4.1   Introduction

This chapter provides the complete description of the laboratory scale experimental set up designed for testing the emission characteristic of a liquid fuel burner. The designs are extensively dependent to the employed operating parameters such as fuel flow rate, injection air flow rate, fuel pressure and injection air pressure.

Ideal gas turbine combustor should provide low NO_x formation and negligible CO and UHC combined with good flame stability. The success of this ideal combustor will depend upon the thorough mixing of the fuel and air in the primary zone. Information about the fuel and air mixing can only be adequately retrieved by measuring local gas composition within the combustor. Mellor et al. (1972) reported the measurements of species and temperature in an Allison J-33 combustor and the results indicated that for a well atomized fuel spray, due to turbulence, the mixing controls the local equivalence ratios and hence reduce the pollution formation.

4.2 Combustion Chamber Design

The specification of combustion chamber should be determined in order to build a chamber that operates in the desired performance. There are many factors affecting the combustion chamber size, such as length to diameter ratio, pressure loss parameter and mass flow parameter. The combustion chamber used was a modified standard of existing combustion chamber.

4.2.1 Length and Diameter

Combustion chamber length and diameter are the most important parameter in designing the combustor. An appropriate length and diameter of combustion chamber would allow more time for complete combustion with high combustion efficiency hence reduce emissions. The length to diameter ratio (L_c / D_c) should be in the range of 1.5 to 5.

Table 4.1: Researcher's suggestion on Length to Diameter Ratio (Mellor, 1990)

Researcher	Suggestion on L_c / D_c
Boyce, M.P. (theory)	2 - 5
Boyce, M.P. (Practical)	
Small Combustor	2
Large Combustor	3 - 4
Hawthorne H.R. & Olson W.T.	1.5
Lefebvre A.H. & Norster E.R.	1.5

The suggested ratio of L_c / D_c for the combustion chamber is 2. This is because practically for small combustor the ratio of length to diameter for combustion chamber should be small as shown in the Table 4.1. Besides that, shorter combustor could reduce the formation of NO_x emission and reduces the weight of the combustor.

4.2.2 Pressure Loss Parameter

Two dimensional pressure loss parameters are of importance in combustor design. One is the ratio of the total pressure drop across the combustor to the inlet total pressure ($\Delta P_{3-4} / P_3$), and the other is the ratio of the total pressure drop across the combustor across the combustor to the reference dynamic pressure ($\Delta P_{3-4} / q_{ref}$). The term ($\Delta P_{3-4} / q_{ref}$) is also called pressure loss factor. The two parameters are related by the equation (Escott, N.H., 1993):

$$\frac{\Delta P_{3-4}}{P_3} = \frac{\Delta P_{3-4}}{q_{ref}} \frac{R}{2} \left(\frac{\dot{m}_3 T_3^{0.5}}{A_{ref} P_3} \right)^2 \tag{4.1}$$

Both of the parameters are of prime importance in combustion engineering, since it denotes the flow resistance introduced into the air stream between the compressor outlet and the turbine inlet. Aerodynamically, it may be regarded as equivalent to a drag coefficient. Meanwhile the quantity $(R/2)(\dot{m}_3 T_3^{0.5} / A_{ref} P_3)^2$ in Equation (4.1) is effectively a measure of combustor reference velocity.

For low fuel consumption, the overall pressure loss of the chamber, $\Delta P_{3-4} / P_3$, must be low. However, if the chamber is small and has adequate mixing, both pressure loss factor and combustor reference velocity must be large.

Table 4.2 shows some typical values of pressure loss in practical chambers. From the table, the annular chamber has the lowest pressure loss factor.

Type of Chamber	$\dfrac{\Delta P_{3-4}}{P_3}$	$\dfrac{\Delta P_{3-4}}{q_{ref}}$	$\dfrac{\dot{m}_3 T_3^{0.5}}{A_{ref} P_3}$
Tubular	0.07	37	0.0036
Tuboannular	0.06	28	0.0039
Annular	0.06	20	0.0046

Table 4.2: Pressure Losses in Combustion Chambers (Mellor, 1990)

The relationship between size and pressure loss for the optimal cross sectional area of the casing, A_{ref} for straight combustors in most industrial combustors and some aircraft combustors are (Mellor, 1990):

$$A_{ref} = \left[\frac{R}{2} \frac{\dot{m}_3 T_3^{0.5}}{P_3} \frac{\Delta P_{3-4}}{q_{ref}} \left(\frac{\Delta P_{3-4}}{P_3} \right)^{-1} \right]^{0.5}$$

(4.2)

4.3   Swirler Design

Swirling jets were used for stabilization and control of flame and to achieve a high intensity combustion. The common method of generating swirl is by using angled vanes in the passages of air.

Most conventional combustors employ the axial flow type swirlers. The swirler vanes were usually flat for ease of manufacture, but curved vane was sometimes used for their better aerodynamics properties (Lefebvre, 1983). Ahmad, et al. (1986) found problems in the achievement of adequate combustion efficiency and stability with lean primary zones using large air flow axial swirler with central fuel injection (Kim, 1995). Alkabie, et al. (1988) showed that these problems could be overcome by the use of radial swirler followed by a dump expansion with their quite different near swirler aerodynamic. For large air flow, the axial swirler has disadvantages for accommodating more air because the expansion from the swirler is reduced by the requirement to increase the swirler diameter. Increasing the air flow would reduce the flow expansion to the combustor diameter. The expansion ratio should be more than 1.5 to create a corner recirculation zone. However, this problem is not encountered with radial swirlers since the radial swirler outlet can be maintained constant and the vane depth increased to accommodate more air to achieve the pressure loss required. Alkabie (1989) found the noticeable improvement in performance and NO_x emission of the radial swirler over the axial swirler due to the immediate contact of fuel with the turbulent swirled air as it leaves the central

fuel injector. As proven, radial swirler provides better advantages over the axial swirler. So, in this research, the radial swirlers would be used.

4.3.1   Rapid Mixing System

There are number of ways of producing better mixing between air and fuel. One of the ways is by creating rapid mixing combustion system. Rapid fuel and air mixing are best produced by using swirlers.

To achieve rapid fuel and air mixing, turbulence must be generated to promote the mixing. Turbulence energy is created from pressure energy dissipated downstream of the stabilizer. In swirlers, increasing the blockage or pressure drop of the swirler can generate turbulence. Swirler pressure drop could be done in number of ways:

(a)   Increasing the swirler vane angle

(b)   Decreasing the swirler outlet diameter (d/D) or increasing the swirler hub diameter, both of which increase the swirler flow blockage

(c)   Increasing the number of vanes

Besides the effect of rapid fuel and air mixing, all of these factors also increase the size of the recirculation zone. An increase in the size of the recirculation zone together with the turbulence generated in the shear layer region can increase fuel and air mixing significantly.

4.3.2   Swirl Flow

Swirl flow is a main flow produced by air swirled in burner system. Such flow is the combination of swirling motion and vortex breakdown. Swirling flow is widely used to stabilize the flame in combustion chamber. Swirling flow induces a

highly turbulent recirculation zone that stabilizes the flame resulting in better mixing and combustion. An advantage of swirling flow is the fact that a centrifugal force field, present in swirling, tends to accelerate the mixing of two flows having different densities and thus increase the reaction rate in the combustion process (Fricker, N. and Leuckel, W., 1976).

The primary function of this flow is to achieve a mixture that can sustain continuous, and to maintain or stabilize combustion over a wide range of operating conditions. Air is introduced tangentially into the combustion chamber and forced to change its path, which contributes to the formation of swirling flow. The strength of the flow is dependent on the swirler vane angle and the air pressure supplied.

Swirl is widely used in industrial application ranging from gas turbine combustors to diesel engines. It is often dictates that the supported flame must be short and intense in continuous combustion system such as gas turbine combustor in order to achieve the maximum heat release quickly. Long flames are generally less well mixed, this can be gauged by the apparent of yellow flame and contribute more to pollutant formation as the residence time is higher. Additionally yellow flames, as there are more rich regions, the temperature is less uniform across the flame and fluctuations in temperature can have a profound increasing effect on the NO_x emissions (Escott, N.H., 1993).

4.3.3   Effect of Swirl

The introduction of swirl has been applied extensively in industrial furnace and combustion chambers in order to improve flame stabilization (Wu, H. L. and Fricker, N., 1976). Swirl also has been used as a mean of controlling flame shape and combustion intensity in furnace flames. The effect of swirl is to decrease the velocity gradient at the exit of burner thus causing a faster decay of the velocities in the flow field with increase of swirl flow (Chervinskey, A. and Manheimertiment, Y., 1968). One of the main effects of the application of swirl into a flow is the central reverse flow zone that is formed and a highly complex turbulent flow field created.
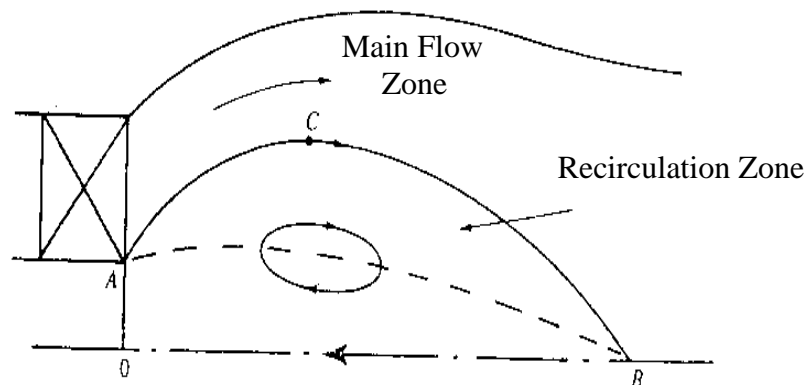
Figure 4.1: Recirculation Zone (Kim, M.N., 1995)

The reverse flow zone or recirculation zone, as shown in Figure 4.1, has traditionally been regarded as a reservoir or store of heat and active chemical species. It cyclically transports hot combustion products from downstream regions into the flame region. The high temperature products, despite the dilution effect, serve as an energy source for preheating and ignition assistance. Between the forward flow and the reverse flow zone boundary is a region of steep velocity gradients and high intensity turbulence, which promotes high entrainment rates and rapid mixing between the fuel and air. As a result of the high entrainment and homogeneous mixing, swirl reduces both flame lengths and flame attachment lengths and consequently shortens the combustion chamber length necessary for complete combustion (Kim, M.N., 1995). Swirl also promotes high combustion efficiency, easy ignition, reactant recirculation zone residence time, pollutant optimisation potential, widened stability and blow off limits.

Geometry of the combustor also affects the reverse flow zone. The precise effect of swirl on a flow field is found to be depending on many factors as well as on the swirl number. For example:-

Nozzle Geometry – The presence of a central hub encourages a larger recirculation zone.

Size of Enclosure – Central recirculation zone can be more pronounced in enclosures than those of comparable free jets.

Exit Velocity Profile – Recirculation zones tend to be longer when the flow is produced via swirl vanes as opposed to an axial and tangential entry swirl generators.

The location and the shape of the recirculation zone are a function of the various inlets and swirl generator configurations, enclosure size, extent of reaction and any other factor that manipulates the imposed pressure gradient. Syred and Dahman (1965) suggest that smaller chamber diameters reduce the interference between the flow field and furnace enclosure, thus providing a recirculation zone that is longer and more advantageous for flame stabilization.

4.3.4　Swirl Stabilized Flame

The primary zone airflow pattern of gas turbine combustors is of major importance of flame stability. Various types of airflow pattern are employed, but one feature common to all is the creation of a torroidal reverse flow. This torroidal vortex system plays an important role in flame stabilization since it entrains and recirculates a portion of the hot combustion product to mix with the incoming air and fuel.

One of the most effective ways to induce recirculation flow in the primary zone is by fitting a swirler around the fuel injector. This type of recirculation zone may provide better mixing than that obtained by other means such as bluff body. This is because of the strong shear regions, high turbulence and rapid mixing rates produced by the swirling action. Besides that, the presence of a solid surface exposed to the high temperature is reduced and the deposition of coke such as occur on bluff bodies in heterogeneous combustion is also reduced.

Swirl increases the production of turbulence above that generated by non-swirling flows because the presence of the tangential velocity component provides additional velocity gradient. Swirling also increases the turbulence burning velocity to ensure blow off does not occur. Besides that, recirculation vortex produced by swirl acts as a heat source forcing combustion product to move upstream and mix with the partially premixed reactant. This increases the amount of contact between fuel, air and hot combustion products (Syred, N. and Beer, J.M., 1974). An additional factor that explains why swirl has a stabilizing effect is that stagnation points are found at upstream and / or downstream positions of central recirculation zone. This

stagnation point would act as a bluff body with the flame attaching in the sheltered downstream near wake region.

4.3.5   Swirler Pressure Drop

Swirler pressure drop is equal to the different in pressure between the plenum chamber and the combustor. The swirler pressure drop was calculated as follows (Escott, N.H., 1993):
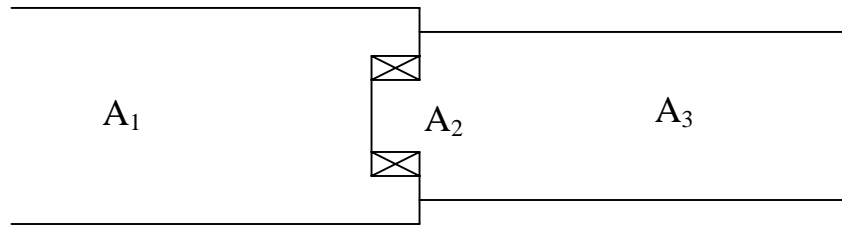
$$\Delta P = P_{1T} - P_{3T} = (h_{1T} - h_{3T})\rho_w g \tag{4.3}$$

where $\qquad P_{1T} = P_{1S} + P_{1D} + \rho_1 . g . \Delta h_1 + P_a \tag{4.4}$

and $\qquad P_{3T} = P_{3S} + P_{3D} + \rho_3 . g . \Delta h_3 + P_a \tag{4.5}$

P_{nS} and P_{nD} are the static and dynamic pressure in the n region. P_a is the atmospheric pressure. As the combustor is placed horizontally, it was assumed that $\Delta h_1 \approx \Delta h_3 \approx 0$ and $\rho_1 = \rho_3$. Thus, the equations (4.4) and (4.5) can be combined to yield:

$$\Delta P = (P_{1S} + P_{1D}) - (P_{3S} + P_{3D}) \tag{4.6}$$

Values of pressure loss in a typical gas turbine combustor lie between 2 percent to 7 percent at reference Mach number of 0.047 (Clements, T.R., 1976). The pressure loss can be calculated by using the following equation:

$$\Delta P / P = \gamma / 2 \left(M / C_D \ x \ A_1 / A_2 \right)^2 \tag{4.7}$$

where,

$$\Delta P/P = \text{Swirler Pressure loss} \qquad C_D = \text{Swirler discharge coefficiency}$$

$$\gamma = \text{Ratio of specific heat} \qquad A_1 , \ A_2 = \text{Combustor and swirler open area}$$

$$M = \text{Airflow Mach number}$$

4.3.6   Swirl Number

Experimental studies have shown that the flame size, shape, stability and combustion intensity are affected by the degree of swirl imposed on the flow. This degree of swirl is denoted by the swirl number S, which is a non-dimensional number characterizing the amount of rotation imposed to the flow. An advantage of swirling flow combustion is the fact that a centrifugal force field, present in swirling or vortex flow, tends to accelerate the mixing of two flows having different densities and thus increase the reaction rate in the combustion process.

The common method of generating swirl is by using angled vanes in the passages of air. The characteristic of the swirling flow depends on the swirler vane angle. Basically there are two types of swirler design; axial swirler and radial swirler. Most conventional combustor employs the axial flow type of swirler. The swirler vane is usually flat for ease of manufacture, but curved vane is sometimes performed for their better aerodynamic properties.

Alkabie, et al (1988) found problems in the achievement of adequate combustion efficiency and stability with lean primary zones using large air flow axial swirler with central fuel injection. Alkabie, et al (1988) showed that these problems could be overcome by the use of radial swirler followed by dump expansion with their quite different near swirler aerodynamic. Flat vane swirler is inefficient because they run under stalled condition.

Swirl number represents the axial flux of swirl momentum divided by the axial flux of axial momentum and is widely used for characterizing the intensity of swirl in enclosed and fully separated flow. That is (Kim, M.N., 1995)

$$S = \frac{G_\theta}{G_x \times D/2} \tag{4.8}$$

Where:

G_θ = Axial flux of angular momentum

G_x = Axial flux of axial momentum

$D/2$ = Nozzle radius

This is a very basic calculation of a swirl number. There is better suggestion on the calculation for the swirl number. Claypole and Syred (1981) proposed a geometrical swirl number, S_g which was taken as non-dimensional measure of the tangential momentum supplied to the flow and if perfect mixing and conservation of momentum is assumed, then the swirl number can be defined in terms of the geometry of the combustor.

$$S_g = r_o \pi r_e / A_t \quad \text{(tangential flow / total flow)}^2 \tag{4.9}$$

where:

A_t = Area of tangential inlets r_e = Radius of the exit of the combustor

r_o = Radius of the tangential inlets from the centre of the combustor

In the present work, swirl number calculation based on Leuckel method would be employed. This method would not much represent the real situation. However, Leuckel method was a basic method used to simulate the effectiveness of fuel and air mixture for a particular swirler vane angle. Past researchers agree that there is an optimum value of swirl number, where above that value, the emissions will begin to increase. Kim (1995) proposed that swirl number higher that 3.25 would raise the emissions. From, the Leuckel method swirl number calculation, swirl vane angle of 70° and above were not recommended. Swirl number, σ calculation based on Leuckel method was as follow (Appendix B):

$$\psi = \frac{n.s}{2\pi r_1 . \cos \alpha} \qquad (4.10)$$

$$\sigma = \frac{Tan\,\alpha}{1-\psi} \qquad (4.11)$$

Where,

$n =$ number of Vanes $\qquad\qquad s =$ Thickness of Vanes

$r_1 =$ Swirler Outlet Area $\qquad\quad \alpha =$ Swirler Vane Angle

4.4 Fuel Injector Design

Fuel injection could be provided by three distinct injection methods: central fuel injection, vane passage fuel injection and wall fuel injection. The common method of fuel injection in swirl stabilized flows is injection axially through the centre of the swirler. However, another variation from conventional central axial fuel injection is to inject the fuel radially from the central axis across the entering air jet. The present work is involved with the former method of fuel injection. In this research, fuel injector would not be emphasized much as the rationality of having injector in this research is to serve its purpose of injecting fuel into the combustion chamber. However, for the intention of optimizing emissions reduction, injector could be one of a major contributor.

CHAPTER V

EXPERIMENTAL SET UP

5.1   Introduction

In this chapter, the experimental rig set up and procedures used for the assessment of various radial swirler angle performances were described. Combustion rig description, fuel injection and exhaust gas sampling shall also be described.

5.2   Experimental Set Up

The general rig set-up for the liquid fuel burner test is shown in Appendix C. The rig was placed horizontally on a movable trolley. The combustion zone consists of 4 chambers that are plenum chamber, combustion chamber, extension chamber and safety chamber.

The air is introduced through the inlet pipe and flows axially into the plenum chamber before entering the combustion chamber through the radial swirler of 40 mm outlet diameter that is installed at exit plane of plenum chamber. The amount of air entering the combustor is controlled by the air swirler's minimum area.

The rig is equipped with a central fuel injector. The inside diameter of the combustor is 163 mm and the total length is 852 mm. The combustor was cooled by convection from the ambient air. The length of the combustion chamber is representative of the minimum used in aero engines but is generally shorter than the combustors used in gas turbines. Diesel fuel was used for the testing, which was supplied by Universiti Teknologi Malaysia, obtained from Petronas fuel station.

An extension chamber was introduced because the test is conducted in both fuel lean and fuel rich regions where the flames in the fuel rich region are generally long. An additional chamber was also introduced for the safety of gas sampling probe and gas measurement purpose. The gas analyzer will be placed at the exit plane of safety chamber.

Tests on exhaust emission were carried out using 4 different swirler vane angles of 30°, 40°, 50° and 60°. Central fuel injector was placed in dual situations, upstream (Figure 5.3) and downstream (Figure 5.4) of the swirler exit plane. Besides the swirler vane angles, orifice plates with different orifice sizes also will be varied. Orifice sizes of 20mm, 25mm and 30mm will be used.

The exhaust gas sampling probe was placed at the end pipe of combustion chamber. The gas analyzer used in these tests was the portable Kane May gas analyzer that could measures oxides of nitrogen, sulphur dioxide and carbon monoxide emission.

5.2.1   Liquid Fuel Burner

A liquid fuel burner has been developed after considering on its design concepts. Burner consists of three main components that are combustion chamber, swirler and fuel injector. Modification on the existing combustion chamber and injector were performed to produce desired output of stable combustion over wide range of equivalence ratio with combustion temperature of less than 1200^oC. The temperature shall be less than 1200^oC because it is difficult to work under very hot

environment. Furthermore, the allowable temperature to reach gas analyzer sensors is 40°C. Temperature of less than 1000°C was hardly achievable as the desired output was to hold combustion over wide range of equivalence ratio that is from 0.55 to 1.1.

5.2.1.1 Combustion Chamber

The entire burner system consists of four chambers; plenum chamber, combustion chamber, extension chamber and safety chamber. The plenum chamber was built at L_c / D_c of 1.5. Air and fuel were delivered to plenum chamber before there were introduced into the combustion chamber. Fuel injector was located in the plenum chamber. Combustion chamber was built at L_c / D_c ratio of 2. Combustion chamber was built at diameter of 163mm with length of 338mm. An extension chamber is designed at L_c / D_c ratio of 1.5 for a fuel rich region experimental purpose, as the flame obtained in this region is generally long. An additional safety chamber is mounted at the end of extension chamber for a safety and measurement purpose. This will allow lower temperature of combustion product to be measured by gas analyzer, as the gas analyser should not be exposed to high temperature of combustion product. The detail of plenum chamber, combustion chamber, extension chamber and safety chamber were as shown in Appendix D, Appendix E, Appendix F and Appendix G respectively.

5.2.1.2 Swirler and Orifice Plate

The experiment was conducted using four existing radial swirlers with swirler vane angle of 30°, 40°, 50° and 60°. The swirlers were prepared by previous researcher using CNC machine in Kolej Universiti Tun Hussein Onn, Batu Pahat, Johor. Orifice plate of 25mm and 30mm were also been in place when this research was conducted. An additional 20mm orifice plate was fabricated to investigate performance of smaller orifice plate size. All swirlers and orifice plates were

fabricated using mild steel. The detail of swirler design and orifice plate design were in the appendix H and Appendix I respectively.

5.2.1.3 Injector Design

Injector consists of two components; nozzle connector and the nozzle. The nozzle was made using a recyclable hollow pin with an opening of 1mm as shown in Appendix J. This injector upholds the principle of an air assisted plain orifice atomizer, combination of plain atomizer and air assist atomizer. An air assist injector was used in the present work as this injector is very suitable for highly viscous fuels and good atomisation could be obtained. Besides that, it could provide good atomisation at low fuel flow rate. Meanwhile, the nozzle connector was fabricated to deliver fuel and atomizing air to the nozzle. The nozzle connector allows the atomizing air pumped to nozzle evenly all around. The nozzle connector design was shown in Appendix K.

Other components designs such as fuel air nozzle flange, downstream injection extension, swirler-orifice plate attachment flange were as shown in Appendix L, Appendix M and Appendix N respectively. The overall burner assembly drawing was also attached in Appendix O.

5.2.2   Fuel System

Fuel transportation system consists of fuel tank and a compressed air supply. Fuel was drawn vertically into the nozzle connector with the assist of compressed air. This is to increase the fuel pressure. The fuel should be pressurized to improve its atomizing properties while injected into the combustion chamber. The air and fuel should be properly delivered into the combustion chamber to get good mixing of fuel and air in order to produce low emission combustion. Diesel fuel was also introduced

into the combustion chamber through the nozzle connector. The fuel was delivered with constant air pressure of 2 bar and fuel flow rate of 50 mℓ/min.

5.2.2.1 Fuel Tank

The fuel tank was prepared using cylindrical recyclable tank that could uphold compressed air until 10 bar. A safety pressure valve was placed on the left top of the tank for safety reason. The tank was pressurized by compressed air at 2 bar. The fuel was drawn from bottom of the tank so that the fuel could flow smoothly and pressurized by the compressed air. The tank capacity is 15 litres.

5.2.2.2 Air Compressor

An air compressor with 0.373 kW output power and pressurizing capacity of 10 bar was used to serve a purpose of assisting the fuel to be delivered into the combustion chamber.

5.2.3   Air Supply System

Besides the fuel system, air supply system was another system which requires attention. Air is an equally important as a fuel to be in the combustion chamber as it is needed to promote mixing of fuel and air. The air was introduced into the plenum chamber in two different ways. Swirling air was introduced in the plenum chamber with constant pressure of 2 bar while the air flow rate was varied. This air was forced to change its path by swirler's vane angle that contributes to the formation of swirling flow. Meanwhile, the atomizing air that was used to assist the fuel was introduced in the combustion chamber through a nozzle connector with constant pressure of 2 bar.

5.2.3.1 Air Compressor

An air compressor with 1.865 kW output power and pressurizing capacity of 10 bar was used for air atomizing purpose. Bigger compressor was essential for this process as to provide sufficient air for atomizing purpose. Smaller tank capacity air compressor unable to deliver high flow rate of air.

5.2.3.2 Blower

A 0.249 kW blower was used in this experimental testing. This blower could provide air capacity of 0.707925 m^3/min (25 CFM). The blower was used to provide air for swirling option. For the point of swirling motion, air flow rate was the main concern rather than the air pressure. The volume of air should be sufficient enough to generate desired equivalence ratio.

5.2.4   Instrumentation

Filter, Lubricator and Regulator gauges, flow meters, pressure gauges, gas sampling probe, thermocouples and gas analyzer were additional instruments needed in this experimental testing. Flow meters, thermocouples and gas analyzer were calibrated due to experimental testing. The flow meter, on the other hand, was calibrated for the desired medium prior to experimental testing. The water flow meter was calibrated for diesel as the fuel used was diesel. The calibration chart was as shown in Appendix P. Meanwhile, thermocouples were calibrated for its sensitivity and accuracy using ice cubes and boiled water. The calibration results were attached in Appendix Q.

5.2.4.1 Filter, Lubricator and Regulator Gauge

Three Filter, Lubricator and Regulator (FLR) were used in this experimental testing. The FLR was mounted one each for both compressors and another one for the blower. The purpose of the FLR is to filter out water from compress air, lubricate the joints and regulate the pressure for stable pressure supply.

5.2.4.2 Flow Meters

Two air flow meters and a water flow meter that was calibrated for diesel was used for experimental testing. The air flow meters are used to measure airflow rate supplied for swirling and fuel atomizing. Meanwhile the fuel flow meter is used to measure the flow rate of the fuel.

5.2.4.3 Pressure Gauge

Pressure gauge was used to measure and control the pressure supplied to the tank and combustor. Three pressure gauges were used in this experimental testing. One pressure gauge was used for air swirling pressure control and the others for fuel pressurizing and fuel atomizing control.

5.2.4.4 Gas Sampling Probe

An '8' configuration gas sampling probe was used for mean exit sampling. The flue gas sample will be drawn to the gas analyser through the '8' configuration gas sampling probe to measure oxides of nitrogen, carbon monoxide and sulphur dioxide. It consisted of a '8' configuration bended stainless steel tube and welded at the end. The gas sampling probe is shown in Figure 5.1
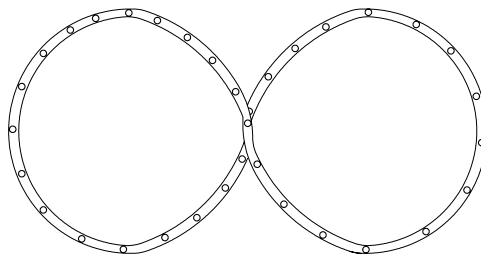
Figure 5.1: Gas Sampling Probe

5.2.4.5 Gas Analyzer

Kane May 9106 gas analyzer was used in this research. This device was used to measure gaseous such as oxides of nitrogen, carbon monoxides and sulphur dioxide. The analyzer has a single emission probe, which could be inserted directly into the flue gas. The analyzer has a suction pump, which sucks the hot flue gas through the probe. The analyzer also has a series of filters, long tube and different gas sensors. The flue gas has to flow through different gas sensors before exhausting to the air. When the flue gas enters into the sensors, its temperature should not exceed 40°C and free of water particles, chemical and dust. These were achieved by using long tube to radiate the heat, water filter, dust filter and chemical filter. The analyzer was purged frequently, to draw fresh air into the sensors for accurate functions of the sensors. The sensors detect the presence of the toxic gases and display the results directly on the screen.

5.3 General Test Procedure

1. A swirler vane angle of 30° and 30mm orifice plate with upstream injection configuration is mounted at the exit plane of plenum chamber.

2. The gas analyzer system is switched on 10 minutes prior to experimental testing to stabilize the analyzer's electronics. The thermocouple recorder, compressors and blower should also be switched on.

3. The air blower valve is turned on. Once the compressor reaches its upper pressure limit, the compressor valve should be turned on. All pressure gauges and flow meter is checked to be in the operating conditions.

4. The air blower is set at 24 CFM to provide equivalence ratio of 0.562.

5. Fuel valve is turned on and the fuel is ignited to start the combustion using a torch. Pressure gauges and flow meters are rechecked to be in the operating conditions.

6. Once the flame is stabilized, the emissions are measured using the gas analyzer. The temperatures obtained from the thermocouple are recorded.

7. The air blower capacity is lessen to designate the flow rate. All 8 reading at each fuel setting is repeated to determine the emissions and temperatures.

8. Steps one to seven are repeated for swirler vane angle of 40°, 50° and 60° with orifice plate sizes of 30mm, 25mm and 20mm with upstream injection configuration.

9. Steps two to seven are once again repeated with swirler vane angle 30°, 40°, 50° and 60° swirler vane angle for orifice plate sizes of 30mm, 25mm and 20mm with downstream injection configuration.
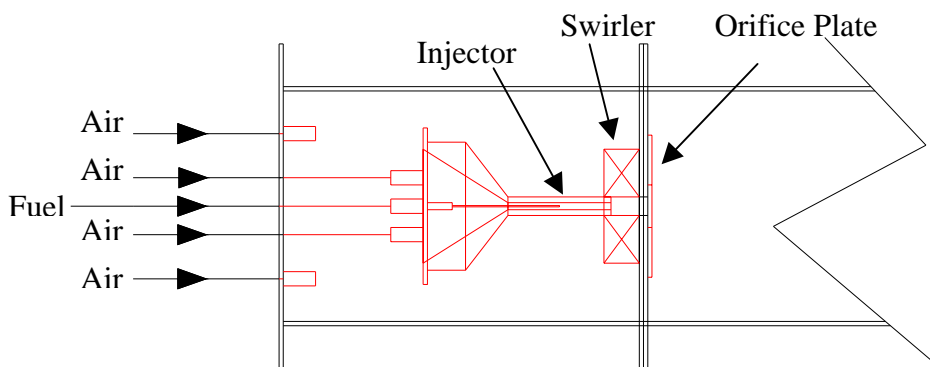
Figure 5.2: Experimental Set up for Upstream Injection
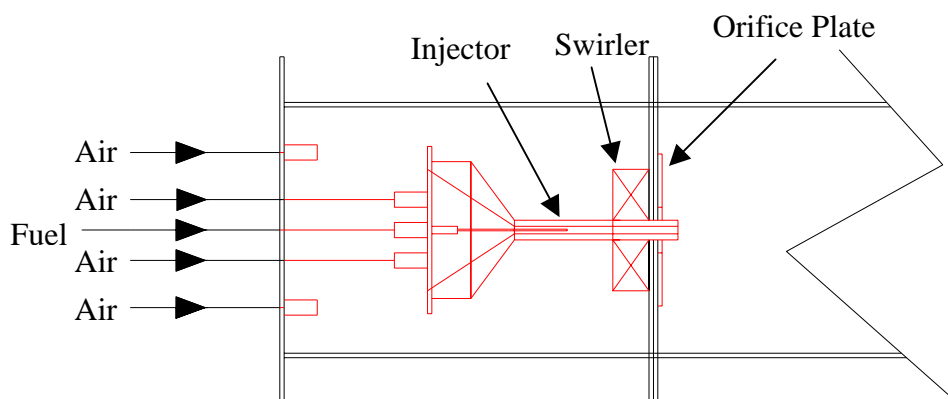
Figure 5.3: Experimental Set up for Downstream Injection

5.4   Experimental Testing Parameters

Table 5.1, Table 5.2 and Table 5.3 below clearly illustrates the parameters used for current experimental testing. The parameters were divided into three main categories of constant parameters, manipulated parameters and measured parameters. The calculation of combustion equivalence ratio was shown in Appendix R. Meanwhile an example of detail calculations of equivalence ratio was shown in Appendix S.

Table 5.1: Experimental Testing Constant Parameters

	CONSTANT PARAMETERS	
1	Fuel	**Diesel**
2	Fuel Pressure, P_f (bar)	**2**
3	Fuel Flow rate, V_f (mℓ/min)	**50**
4	Injection Air Pressure, P_a (bar)	**2**

Table 5.2: Experimental Testing Manipulated Parameters

	MANIPULATED PARAMETERS	
1	Swirling Air Flow Rate, V_{as} (LPM)	**24, 22, 20, 18, 15, 13, 11, 9**
2	Swirler Vane Angle	**30°, 40°, 50°, 60°**
3	Injection Position	**Upstream, Downstream**
4	Orifice Plate Size (mm)	**20, 25, 30**

Table 5.3: Experimental Testing Measured Parameters

	MEASURED PARAMETERS	
1	Combustion Temperature (^{o}C)	**450 to 1100**
2	Emission (ppm)	**NO_x, CO, SO_2**

5.5   Temperature Measurement

Wall fixed thermocouples were located at nine different axial positions along the whole length of the 168 outer diameter combustor. The measurement was taken from the end of upstream flange of combustion chamber as shown in Figure 5.4. The positions are given in Table 5.1. The K-type thermocouple is used in this experimental testing which measures temperature range from $0^{o}C$ to $1300^{o}C$.

Table 5.4: Combustor Wall Thermocouple Position

Position	A	B	C	D	E	F	G	H	I
Thermocouple Position (mm)	10	40	110	170	230	290	345	395	625

CHAPTER VI

EXPERIMENTAL RESULTS AND DISCUSSION ON COMBUSTION PERFORMANCE

6.1   Introduction

A single radial air swirler with swirler vane angles of 30°, 40°, 50° and 60° using orifice plates of 20mm, 25mm and 30mm has been investigated for combusting flow condition using experimental techniques for both downstream and upstream injection.

The curved vane angle swirler was designed to avoid flow separation in the chamber with the added advantages of lower pressure loss. Four different swirler vane angles of radial swirler were designed to study the effect of vane angles on both swirl number and strength of swirl. Three different orifice plates were designed to investigate the consequence of orifice plate insertion on the air and fuel mixing improvement. Meanwhile two injection position of upstream and downstream were designed to examine the effect of these positions on the emissions results. All these variables do help in improving the combustion stability and emissions reduction in various ways.

6.2 Upstream Injection

As discussed in the previous chapter, upstream injection is that the central fuel injector was placed upstream of the swirler exit plane. Investigation has been carried out using 3 different orifice plates of 20mm, 25mm and 30mm for 4 different swirler vane angles of 30°, 40°, 50° and 60°.

6.2.1 Temperature Profile in Accordance to Equivalence Ratio along the Combustion Chamber Using Orifice Plate of 30mm with Upstream Injection
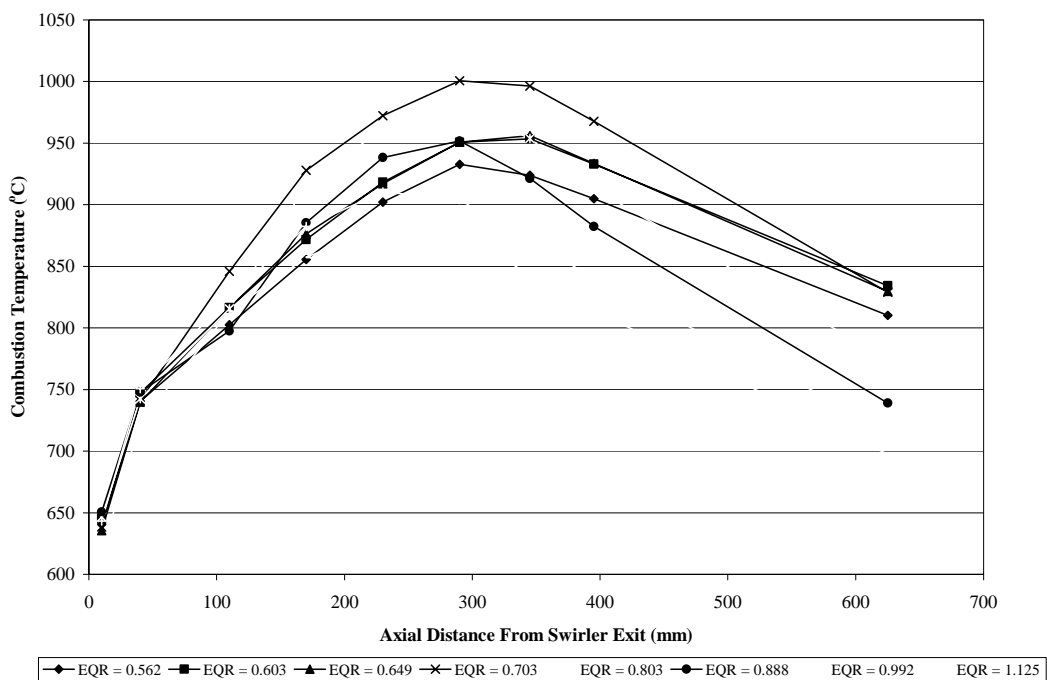
Figure 6.1: Combustion Temperature vs. Axial Distance from Swirler Exit for flames at Different Equivalence Ratios Using Swirler Vane Angle of 30° and Orifice Plate of 30mm with Upstream Injection

The combustion temperature as a function of the axial distance from swirler exit for swirler vane angle of 30° is shown in Figure 6.1. The highest temperature was produced at the equivalence ratio of 0.703 for this setting. This was apparently highest along the chamber. Theoretically highest NO_x emission and lowest CO

emission should occur at this equivalence ratio. Myers and Lefebvre (1986) noted that the flame speed increase with the fuel/air ratio and attain their maximum value at mixture strength close to stoichiometric. This might be because of the flame spread was slow where incoming fuel from the swirler is blocked in that region for the reason of slow outgoing fuel towards the end of combustor. So, more fuel needs to be burned in this region which then increases the temperature. Ahmad et. al. (1985) suggested that larger expansion ratio from the swirler was necessary to ensure rapid flame spread. Since equivalence ratio of 0.703 produces highest temperature, so the highest flame speed occurs at this equivalence ratio. Higher equivalence ratios also seem to enhance the flame towards the wall region. This was due to the more effective penetration of the fuel jet to the jet boundary of the incoming flow from the swirler that give rise to the higher NO_x emission and lower CO emission (Al-Kabie H.S., 1989). At about the first 100mm from the swirler exit, there was no significant variation of temperatures between all equivalence ratios. The starting flame temperature for all equivalence ratios was about 650^oC. Flame temperature in fuel rich region was lower than the temperature in fuel lean region. This is because there is still some fuel left unburned in fuel rich region resulting in lower temperature and bad air and fuel mixing.
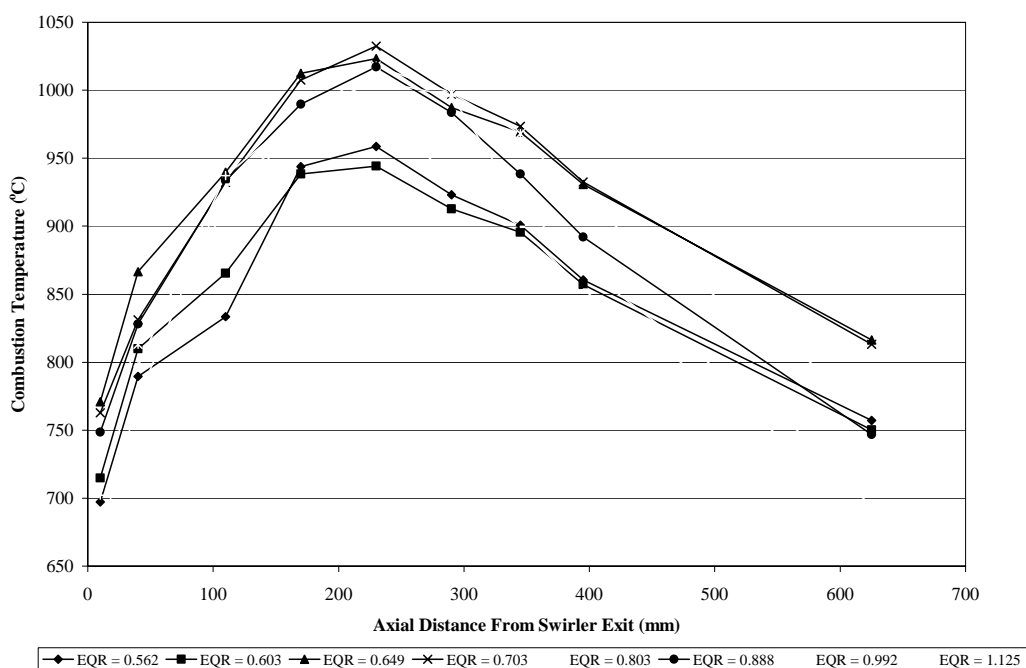
Figure 6.2: Combustion Temperature vs. Axial Distance from Swirler Exit for flames at Different Equivalence Ratios Using Swirler Vane Angle of 40° and Orifice Plate of 30mm with Upstream Injection

Figure 6.2 shows the combustion temperature in accordance to equivalence ratio along the combustion chamber for swirler vane angle of 40° using orifice plate of 30mm with upstream injection. Apparently for all flame, the highest temperature was shown at the distance of 230mm. At this distance, flame at equivalence ratio of 0.703 shows the highest temperature. This once again shows that highest flame speed occurs at equivalence ratio of 0.703. The temperatures rise along the chamber, and reach its peak at distance of 230mm before the temperature reduces back towards the end of combustor. It is noted by Al-Kabie (1989) that highest temperature occurs at lean equivalence ratio near to the core of the flame. In this experimental testing, the flame reaches its peak at the distance of 230mm from the swirler exit which also means that highest flame speed occurs at the distance of 230mm from the swirler exit. So the highest flame speed occurs at equivalence ratio of 0.703 at the distance of 230mm from the swirler exit for this setting. This also could be concluded that the flame length is about 230mm for this setting as fundamental of flame temperature suggested that the highest flame temperature occurs near to the flame tail.

Figure 6.3: Combustion Temperature vs. Axial Distance from Swirler Exit for flames at Different Equivalence Ratios Using Swirler Vane Angle of 50° and Orifice Plate of 30mm with Upstream Injection
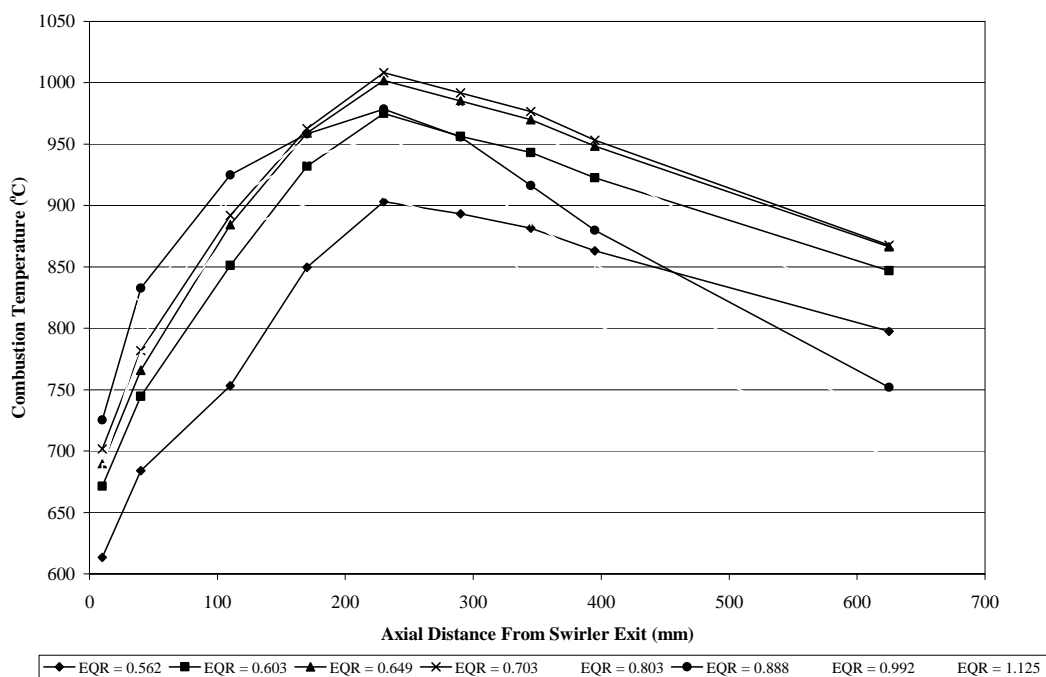
Figure 6.3 shows the combustion temperature in accordance to equivalence ratio along the combustion chamber for swirler vane angle of 50° using orifice plate

of 30mm with upstream injection. The temperature at equivalence ratio of 0.562 shows very low temperature compared to other equivalence ratios at the flame front. The lowest temperature was shown by equivalence ratio of 1.125 that is 694.7^{o}C at the combustor exit. At the flame front, flame with equivalence ratio of 0.888 produces highest temperature, meanwhile flame with equivalence ratio of 0.703 produces highest temperature at the flame tail. This shows that higher flame speed was shown by equivalence ratio of 0.888 at the flame front while equivalence ratio of 0.703 produce higher flame speed in the flame tail. Once again, the maximum temperature was shown by flame with equivalence ratio of 0.703 at the distance of 230mm from the swirler exit. From the results, it could be concluded that for different setting of swirler vane angles, the variance on the highest and lowest temperature at the flame front and flame tail occur with different equivalence ratios. This was mainly because of different swirler vane angles produce different profile of turbulence structure which changing the flame profile and temperature along the combustion chamber.

Figure 6.4: Combustion Temperature vs. Axial Distance from Swirler Exit for flames at Different Equivalence Ratios Using Swirler Vane Angle of 60° and Orifice Plate of 30mm with Upstream Injection
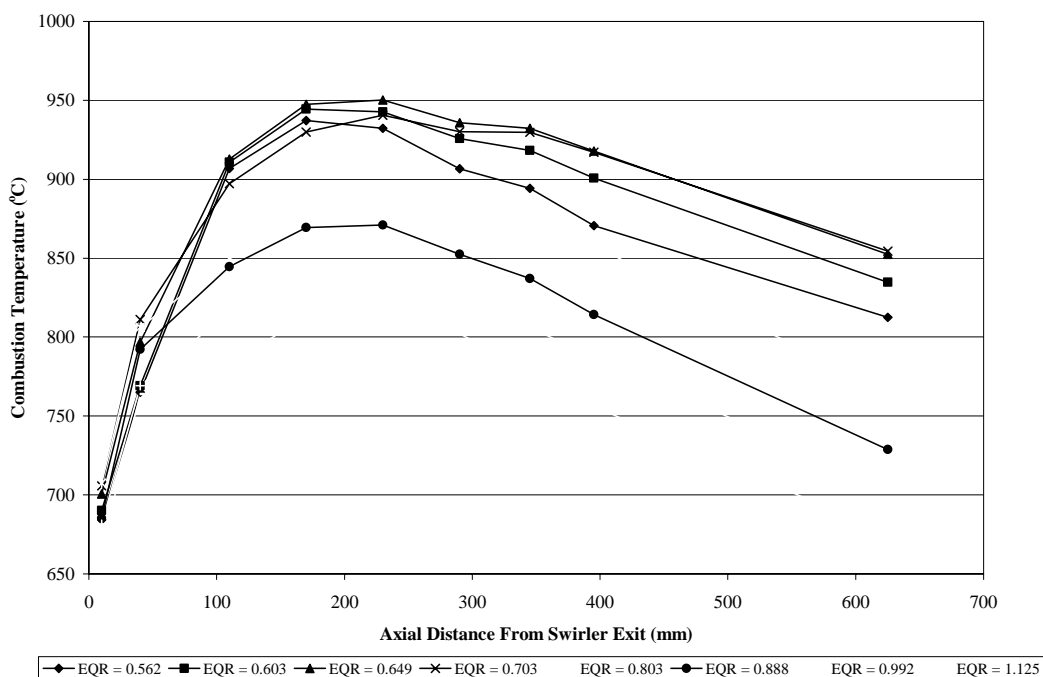
Figure 6.4 on the other hand, shows the combustion temperature in accordance to equivalence ratio along the combustion chamber for swirler vane angle

of 60° using orifice plate of 30mm with upstream injection. The highest temperature of less than 950^oC was obtained along the combustion chamber. Besides that, the highest temperature at the flame tail was also less than the swirler vane angles of 30°, 40° and 50°. The maximum temperature at distance of 230mm from the swirler exit was shown by the flame with equivalence ratio of 0.649. However, flame with equivalence ratio of 0.703 shows highest temperature at the flame tail. It was noticed that the flame length in this setting was about the same with the 50° swirler vane angle configuration. Highest flame speed occur at equivalence ratio of 0.649 which means that the changing of swirler vane angles does vary the turbulence structure and swirling profile in the combustion chamber which in turn produce dissimilar temperature contour that create various highest and lowest temperature point with different equivalence ratios.

6.2.2 Emission Investigation Using Orifice Plate of 30mm with Upstream Injection
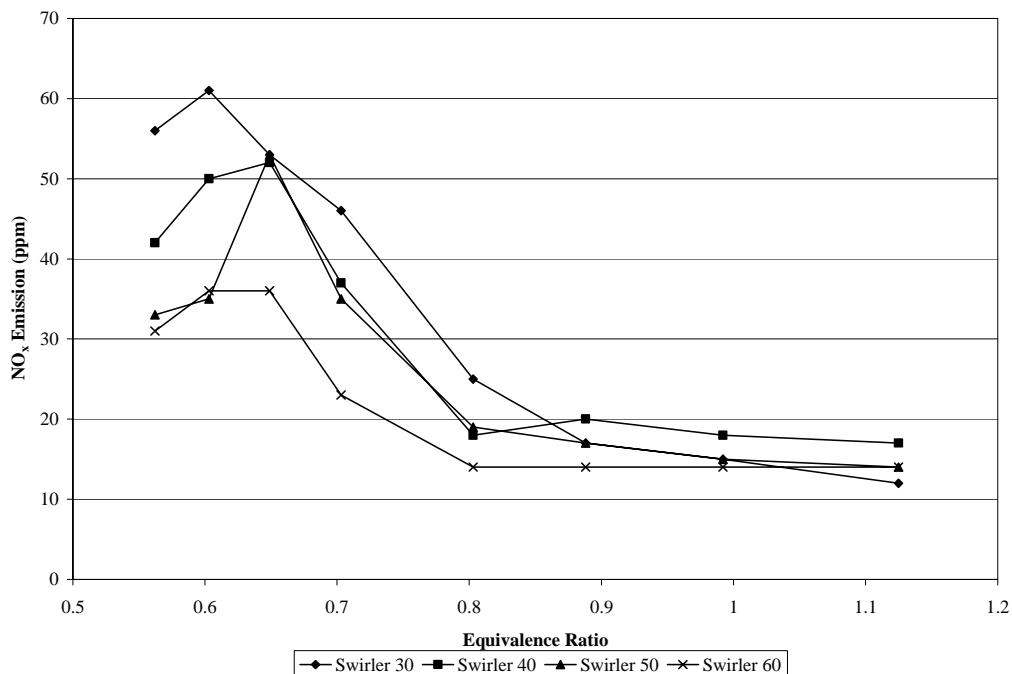
Figure 6.5: NO_x Emission vs. Equivalence Ratio for Various Swirlers Using Orifice Plate of 30mm with Upstream Injection

Figure 6.5 shows NO_x emission versus equivalence ratio for 4 different swirler vane angles of 30°, 40°, 50° and 60° using orifice plate of 30mm with upstream injection. Even though swirler vane angle of 60° produces better results compared to other swirler vane angles, the results pattern are not convincing as the emission results were not stable. Swirler vane angle of 30° produce highest NO_x emission compared to all other swirler vane angles. Swirler vane angle of 40° produced NO_x emission less than swirler vane angle of 30° but higher than swirler vane angle of 50°. At equivalence ratio of 0.803, NO_x emission was reduced about 44 percent, 24 percent and 28 percent for swirler vane angle of 60°, 50° and 40° compared to swirler vane angle of 30°, respectively.
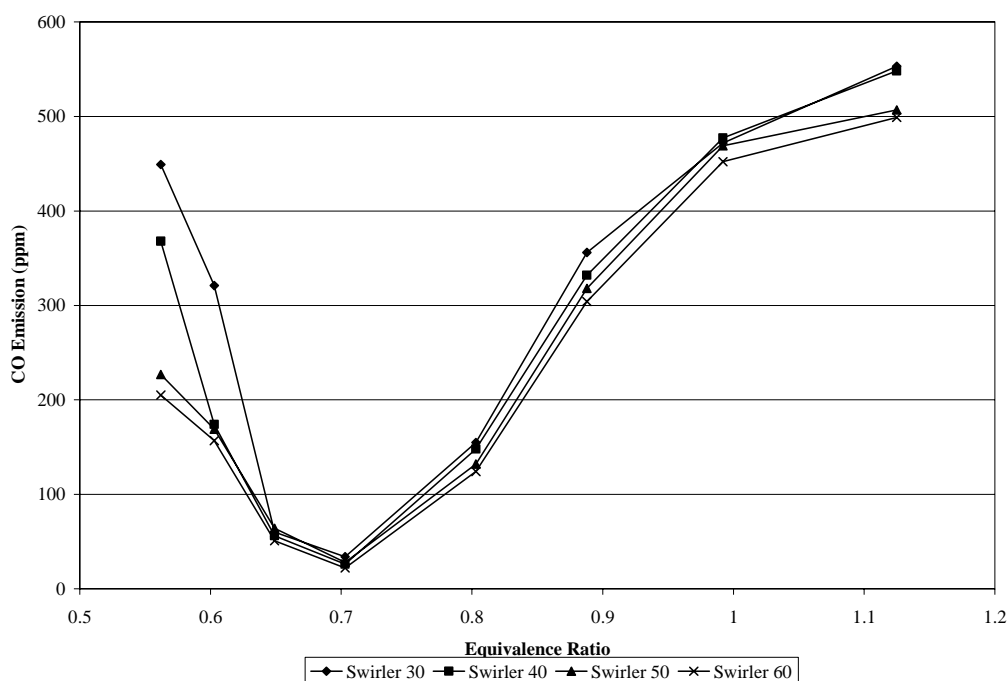
Figure 6.6: CO Emission vs. Equivalence Ratio for Various Swirlers Using Orifice Plate of 30mm with Upstream Injection

Figure 6.6 shows CO emission versus equivalence ratio for 4 different swirler vane angles of 30°, 40°, 50° and 60° using orifice plate of 30mm with upstream injection. High CO emission was produced at equivalence ratio of 0.562 that was about 450 ppm for swirler vane angle of 30° and about 200 ppm for swirler vane angle of 60°. CO emission decreases with respect to equivalence ratio until equivalence ratio of 0.7 and increases back with respect to equivalence ratio through the fuel rich region. There was no significant different in CO emission between all

swirler vane angles except in very fuel lean region. However, swirler vane angle of 60° produced better emission results compared to others. The CO emission reduction was about 20 percent for swirler vane angle of 60° compared to swirler vane angle of 30° at equivalence ratio of 0.803. CO emission reduction was about 4 percent for swirler vane angle of 40° compared to swirler vane angle of 30°. Meanwhile the CO emission reduction was about 6 percent for swirler vane angle of 60° compared to swirler vane angle of 50°. All comparison was taken at equivalence ratio of 0.803.

Figure 6.7: SO$_2$ Emission vs. Equivalence Ratio for Various Swirlers Using Orifice Plate of 30mm with Upstream Injection

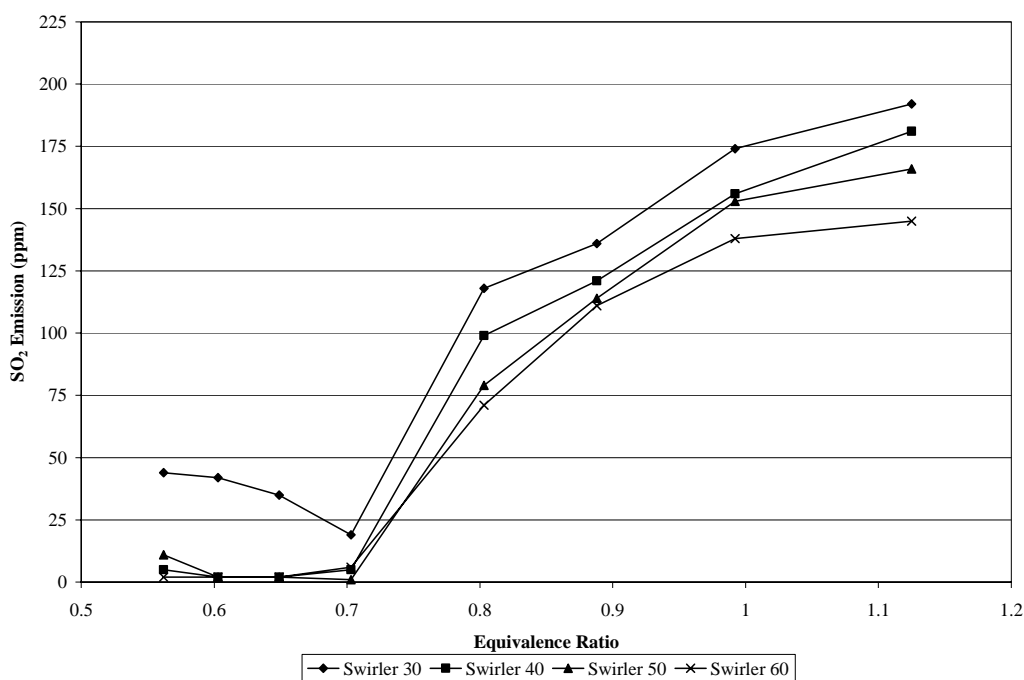Figure 6.7 shows SO$_2$ emission versus equivalence ratio for 4 different swirler vane angles of 30°, 40°, 50° and 60° using orifice plate of 30mm with upstream injection. SO$_2$ emission decreases with respect to equivalence ratio in low fuel lean region. The emission increases with respect to equivalence ratio from the equivalence ratio of 0.7 through the fuel rich region. But, SO$_2$ emission was almost in level for swirler vane angle of 40°, 50° and 60° at very fuel lean region that is at equivalence ratio of 0.55 to 0.7. For swirler vane angle of 40°, SO$_2$ emission was reduced about 19 ppm compared to swirler vane angle of 30° at equivalence ratio of 0.803. Emission reduction of about 20 percent was achieved for swirler vane angle of 50° compared to swirler vane angle of 40° at equivalence ratio of 0.803. Meanwhile

SO_2 emission reduced about 10 percent for swirler vane angle 60° as compared to swirler vane angle of 50° at equivalence ratio of 0.803.

6.2.3 Temperature Profile in Accordance to Equivalence Ratio along the Combustion Chamber Using Orifice Plate of 25mm with Upstream Injection

The temperature profile in accordance to equivalence ratio along the combustion chamber using orifice plate of 25mm with upstream injection for four different swirler vane angles of 30°, 40°, 50° and 60° was shown in Figure 6.8, 6.9, 6.10 and 6.11, respectively.
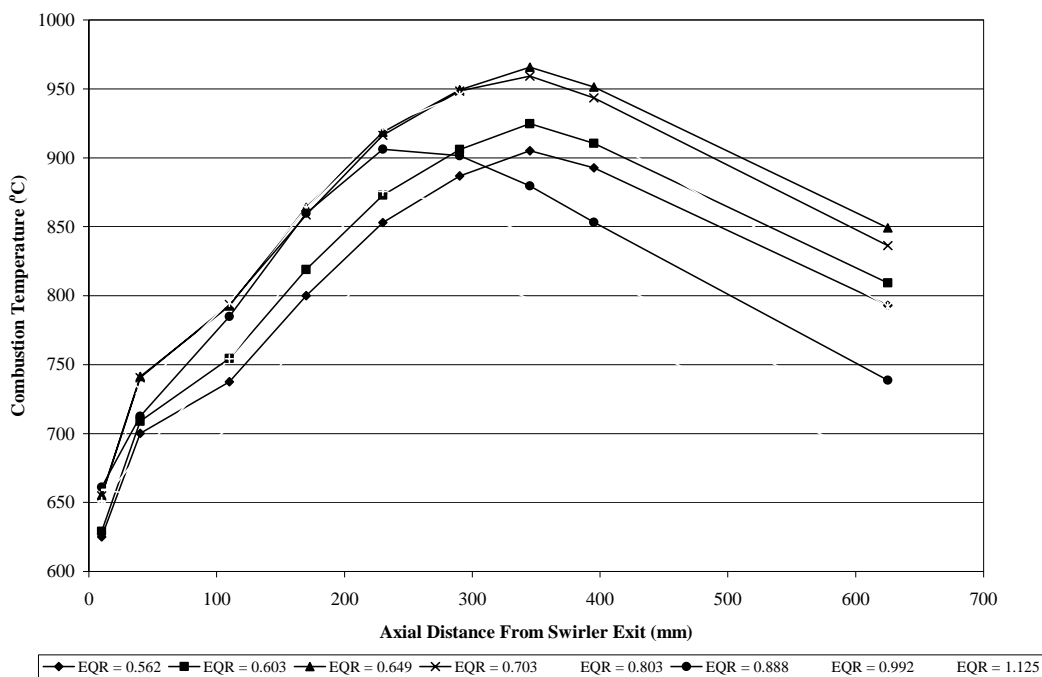
Figure 6.8: Combustion Temperature vs. Axial Distance from Swirler Exit for flames at Different Equivalence Ratios Using Swirler Vane Angle of 30° and Orifice Plate of 25mm with Upstream Injection

Referring to Figure 6.8, the highest temperature for swirler vane angle of 30° was shifted to the distance of 345mm from the swirler exit except for the equivalence ratio of 0.888, 0.992 and fuel rich region. Flame with these equivalence ratios shows

highest temperature at the distance of 230mm from the swirler exit. Once again, the highest temperature at distance of 345mm from the swirler exit was produced by flame with equivalence ratio of 0.649. The highest temperature at flame tail was produced by flame with equivalence ratio of 0.649. The lowest flame tail temperature is 675.9^{o}C shown by fuel rich flame. Generally, this setting with orifice plate of 25mm shows that the flame was a bit longer compared to the configuration with orifice plate of 30mm. This was proved by the detection of highest temperature spot at the distance more downstream compared to the configuration with orifice plate of 30mm. This situation occurs might be because of smaller opening of orifice plate limited the flame to be spread widely which in turn become more longer to complete the combustion further downstream of the combustion chamber. This limitation also creates shear boundary layer turbulences to improve the upstream mixing of fuel and air.
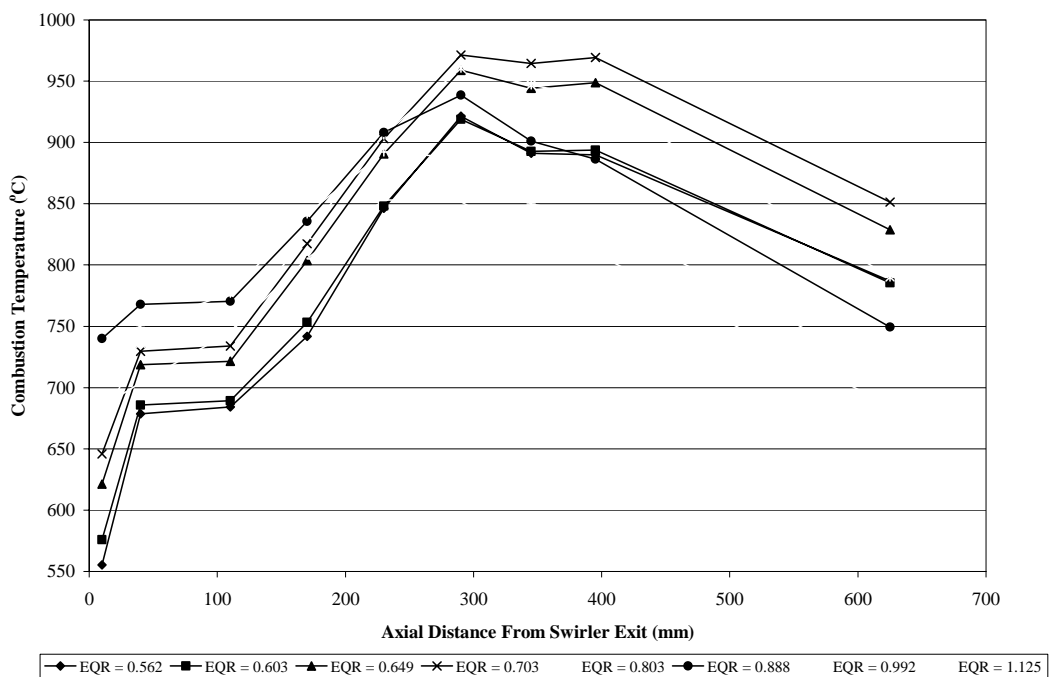
Figure 6.9: Combustion Temperature vs. Axial Distance from Swirler Exit for flames at Different Equivalence Ratios Using Swirler Vane Angle of 40° and Orifice Plate of 25mm with Upstream Injection

As shown in Figure 6.9, the highest temperature was produced at the distance of 295mm from the swirler exit except for the last two equivalence ratios where the highest temperature was at 230mm from the swirler exit. The flame length was shorter with swirler vane angle of 40° compared to swirler vane angle of 30°. This is

because of bigger swirler vane angle creates larger swirler pressure drop that generates greater turbulence effect which makes the flame wider. At fuel lean region with equivalence ratio of 0.55 to 0.65, the temperature of less than $600^{o}C$ was exhibited. The highest temperature near the swirler exit was shown by flame with equivalence ratio of 0.888. The lowest temperature at the end was exhibited by fuel rich equivalence ratio.
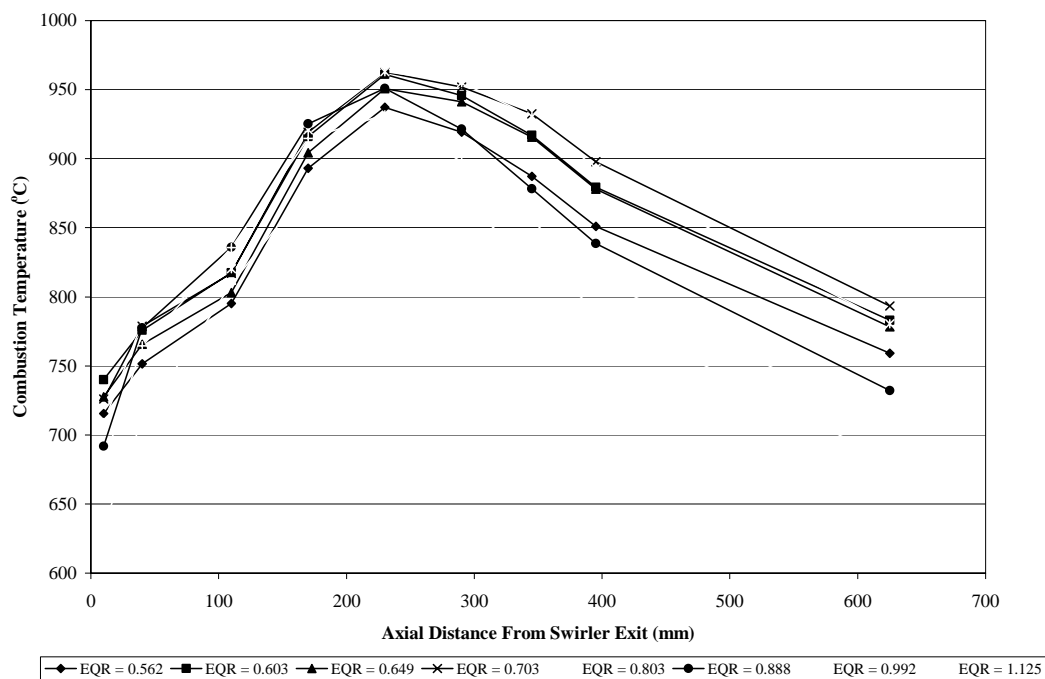
Figure 6.10: Combustion Temperature vs. Axial Distance from Swirler Exit for flames at Different Equivalence Ratios Using Swirler Vane Angle of 50° and Orifice Plate of 25mm with Upstream Injection

Meanwhile, the lowest temperature near the swirler exit and at the end of the combustor for swirler vane angle of 50° using orifice plate of 25mm with upstream injection was the flame with equivalence ratio of 1.125 as shown in Figure 6.10. For this configuration, the highest temperatures for all equivalence ratios were at the distance of 230mm from the swirler exit. The highest temperature at the end is $793.4^{o}C$ which was shown by flame at equivalence ratio of 0.703. The temperature different between the highest temperature and the lowest temperature at distance of 230mm from the swirler exit was $67.3^{o}C$ where the highest temperature was shown by flame at equivalence ratio of 0.803, meanwhile the lowest temperature was shown by flame at equivalence ratio of 1.125. From these results, it could be concluded that bigger swirler vane angles produce shorter flame length compared to smaller swirler

vane angles as for swirler vane angle of 50°, the highest temperature point was further shifted more upstream compared to both swirler vane angles of 30° and 40°.
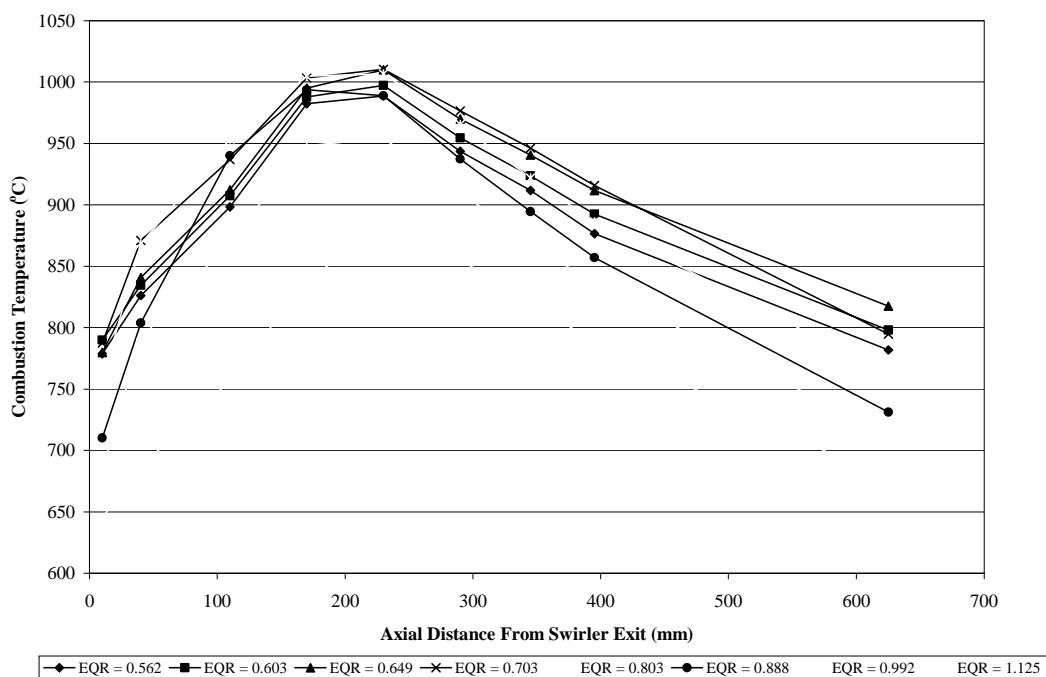
Figure 6.11: Combustion Temperature vs. Axial Distance from Swirler Exit for flames at Different Equivalence Ratios Using Swirler Vane Angle of 60° and Orifice Plate of 25mm with Upstream Injection

From Figure 6.11, we could clearly see that flame at equivalence ratio of 1.125, shows overall lower temperature compared to other flames. The highest temperature at this equivalence ratio is 881.3^oC. The highest temperature was shown by flame with equivalence ratio of 0.703, which was 1010.5^oC at distance of 230mm from the swirler exit. This temperature exceeds 1000^oC, which was not shown by previous settings. There was not much temperature different at this distance between the flame with equivalence ratios of 0.649, 0.703 and 0.803. The different between one another was less than 3^oC. The highest temperature at the combustor end was shown by the flame with equivalence ratio of 0.649.

6.2.4   Emission Investigation Using Orifice Plate of 25mm with Upstream Injection

Figures 6.12, 6.13 and 6.14 shows NO_x, CO and SO_2 emission investigation using orifice plate of 25mm with upstream injection for 4 different swirler vane angles of 30°, 40°, 50° and 60°.
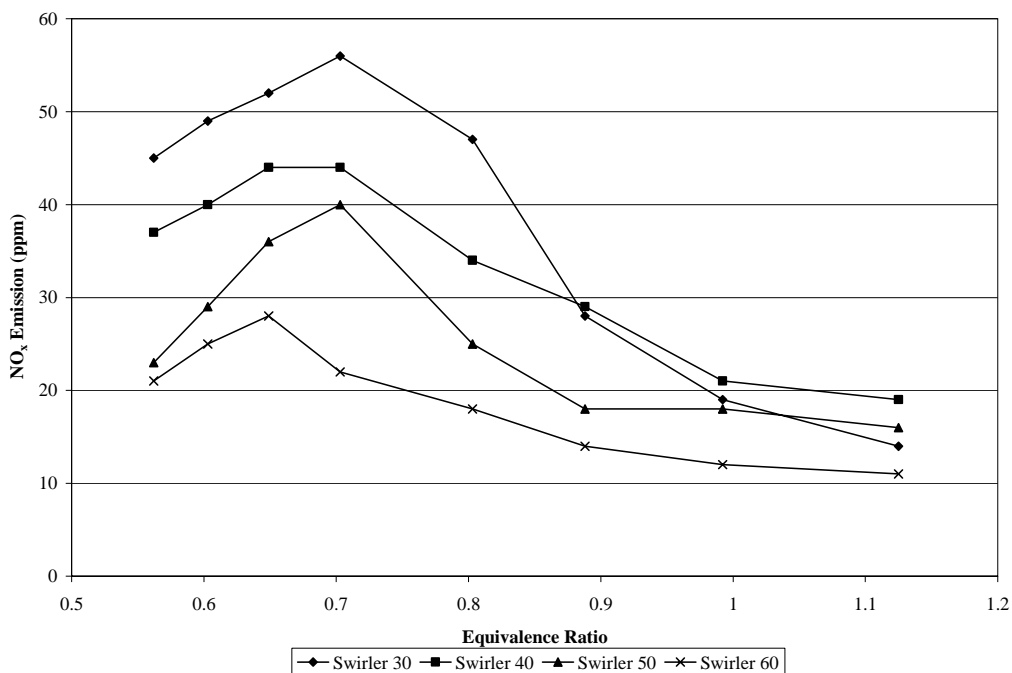
Figure 6.12: NO_x Emission vs. Equivalence Ratio for Various Swirlers Using Orifice Plate of 25mm with Upstream Injection

The results show that NO_x emission increases with respect to equivalence ratio until the equivalence ratio of 0.7 and decreases with respect to equivalence ratio after that value as shown in Figure 6.12. The turning point occurs at the equivalent ratio from 0.7 to 0.8, where at this point NO_x emission was highest for a particular setting. The graph also shows that NO_x emission decreases when the swirler vane angle was increased from 30° to 60°. Higher swirler vane angle produced better emission reduction because it could produce stronger swirling effect and better turbulence flow which further increase the pressure drop in the combustion chamber (Escott, N.H., 1993). The NO_x emission was reduced about 28 percent for swirler vane angle of 40° compared to swirler vane angle of 30° at equivalence ratio of 0.803. The emission was further reduced about 26 percent when the swirler vane

angle was increased to 50° at the same equivalence ratio. The NO_x emission was again reduced to 18 ppm that is about 28 percent reduction for swirler vane angle of 60° compared to swirler vane angle of 50° at equivalence ratio of 0.803.
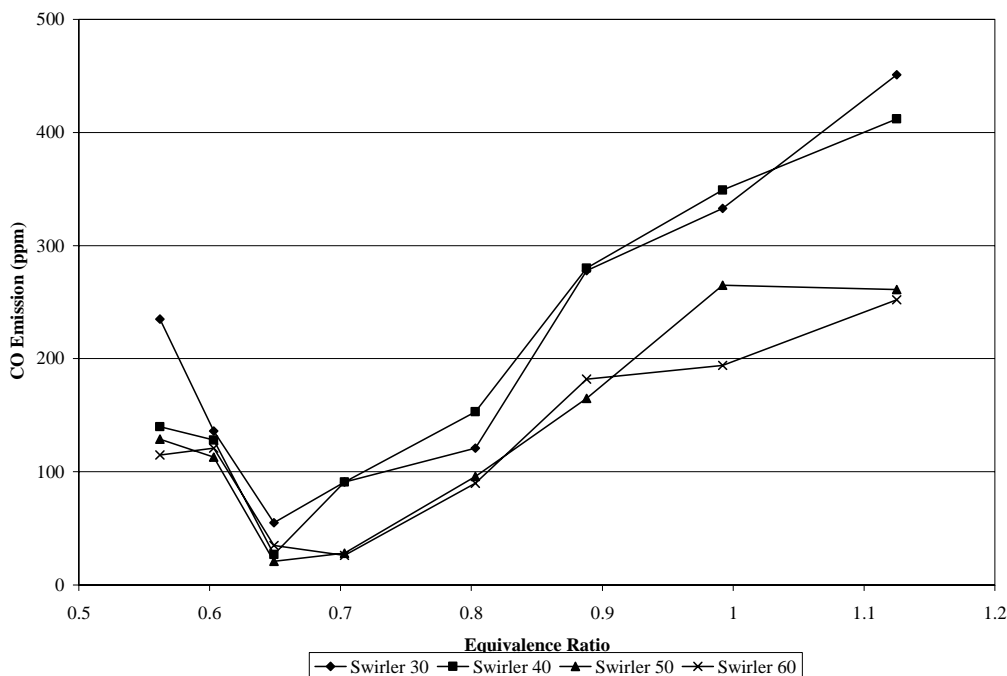
Figure 6.13: CO Emission vs. Equivalence Ratio for Various Swirlers Using Orifice Plate of 25mm with Upstream Injection

Figure 6.13 shows CO emission results for 4 different swirler vane angles using orifice plate of 25mm with upstream injection. Until the equivalence ratio of 0.7, CO emission does not show significant reduction for all swirler vane angles except for swirler vane angle of 30° at equivalence ratio of 0.562. CO emission decreases about 100 ppm for swirler vane angle of 40° compared to swirler vane angle of 30° at equivalence ratio of 0.562. CO emission increases significantly after the equivalence ratio of 0.7 for all swirler vane angles. There are great difference of emission reduction between swirler vane angles of 30° and 40° with swirler vane angles of 50° and 60° at fuel rich region. Swirler vane angle of 50° and 60° generate small amount of emission in fuel rich region. However, this emission is still higher than the emission generated in fuel lean region. The different of CO emission between highest swirler vane angle and lowest swirler vane angle is 31 ppm. Meanwhile, emission reduction of about 37 percent was achieved between swirler vane angle of 50° and 30°. Comparison was taken at equivalence ratio of 0.803.
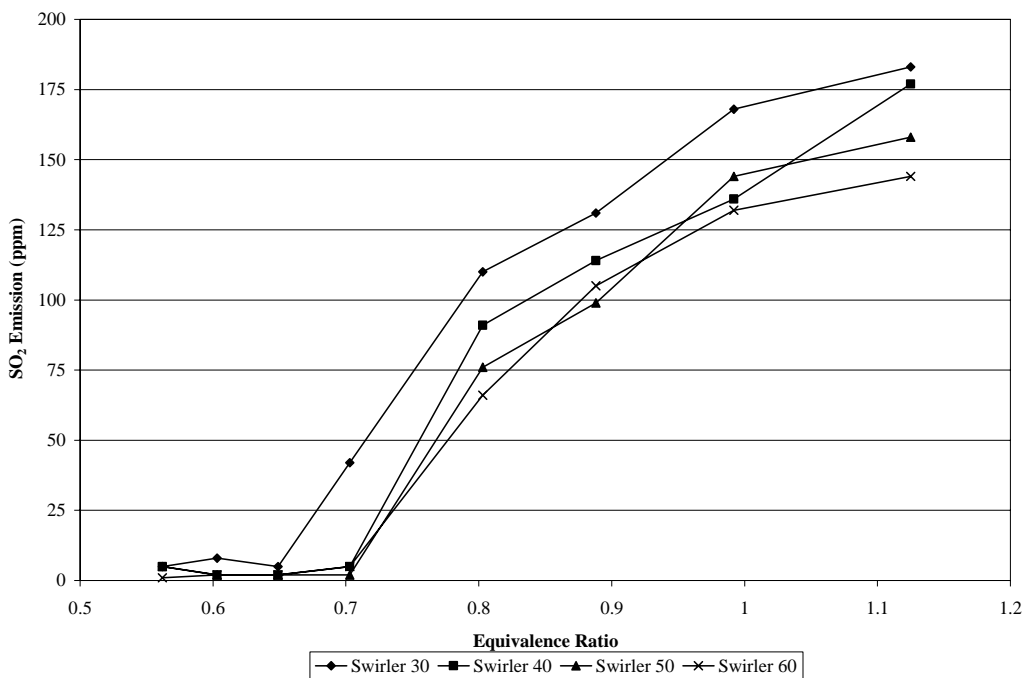
Figure 6.14: SO$_2$ Emission vs. Equivalence Ratio for Various Swirlers Using Orifice Plate of 25mm with Upstream Injection

Figure 6.14 shows SO$_2$ emission versus equivalence ratio for 4 different swirler vane angles using orifice plate of 25mm with upstream injection. Between the equivalence ratios of 0.55 and 0.7, the SO$_2$ emission is almost constant where the emission increases very slowly. After the equivalence ratio of 0.7, the SO$_2$ emission increases rapidly for all swirler vane angles. Although, the emission increases rapidly for all swirler vane angles, swirler vane angle of 30° shows highest emission that is 183 ppm at equivalence ratio of 1.125. Swirler vane angle of 60° shows better emission result compared to all other swirler vane angles. At equivalence ratio of 0.803, the SO$_2$ emission was reduced about 40 percent for swirler vane angle of 60° compared to swirler vane angle of 30°.

6.2.5   Temperature Profile in Accordance to Equivalence Ratio along the Combustion Chamber Using Orifice Plate of 20mm with Upstream Injection

Besides experimental testing for temperature profile using orifice plate of 30mm and 25mm, another orifice plate configuration is orifice plate of 20mm. 4 graphs of temperature profile in accordance to equivalence ratio along the combustion chamber with upstream injection were plotted. The same swirler vane angles were used.
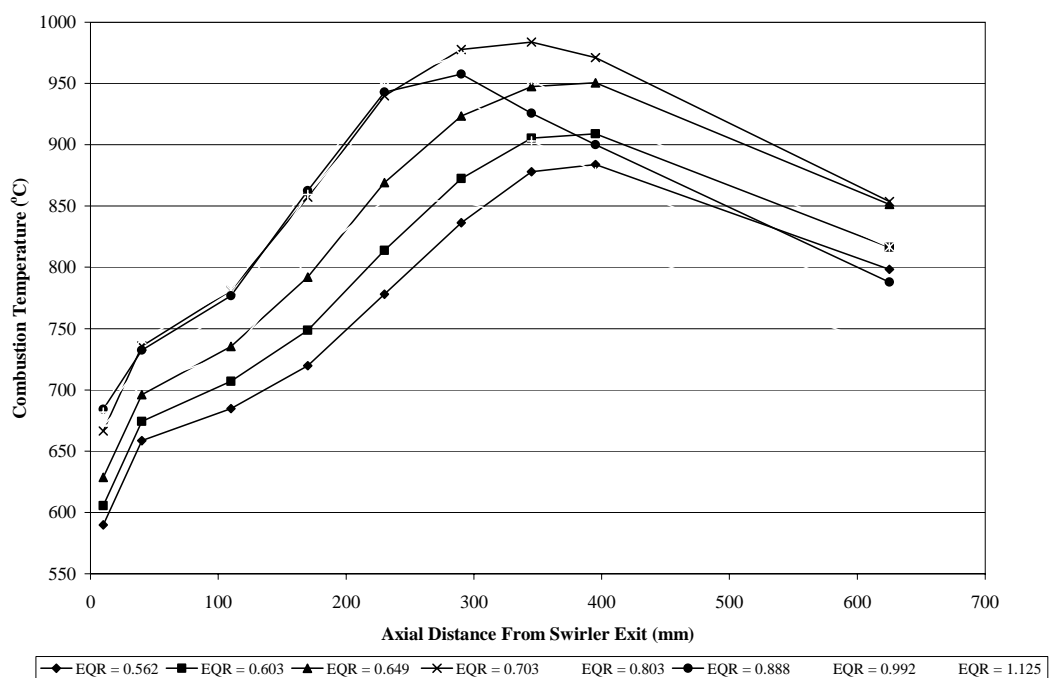
Figure 6.15: Combustion Temperature vs. Axial Distance from Swirler Exit for flames at Different Equivalence Ratios Using Swirler Vane Angle of 30° and Orifice Plate of 20mm with Upstream Injection

The temperature profile provided by swirler vane angle of 30° shows that temperature increases along the chamber and reaches its peak before decreasing back towards the exit of combustion chamber as shown in Figure 6.15. Flame with fuel rich equivalence ratio produces lowest temperature from the distance of 300mm towards the end of combustion chamber. The rapid decrease of temperature for this equivalence ratio was due to some fuel left unburned as less air is provided for combusting the flame. The highest temperature of less than 1000°C was exhibited in

this setting. Flame at equivalence ratio of 0.703; produced highest temperature at the end of combustion chamber.
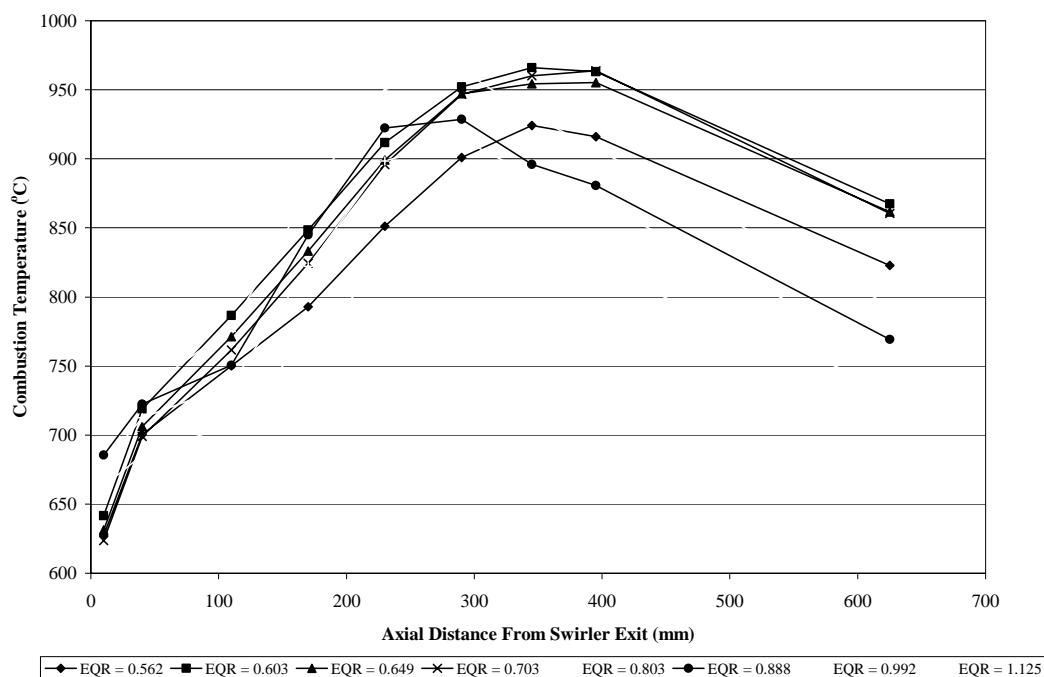
Figure 6.16: Combustion Temperature vs. Axial Distance from Swirler Exit for flames at Different Equivalence Ratios Using Swirler Vane Angle of 40° and Orifice Plate of 20mm with Upstream Injection

Based on Figure 6.16, overall temperature of less than 1000°C was obtained for swirler vane angle of 40°. The temperature profiles were about the same, where temperature increases along the chamber and reaches its peak before decreasing back towards the end of combustion chamber. Flames with equivalence ratio of less than 0.703, shows peak temperature further downstream compared to the flames with equivalence ratio of more than 0.703. Lowest temperature at the exit of combustion chamber was shown by the flame at equivalence ratio of 1.125, while highest temperature at the same spot was shown by flame at equivalence ratio of 0.603. The highest peak temperature was shown by flame at equivalence ratio of 0.803.
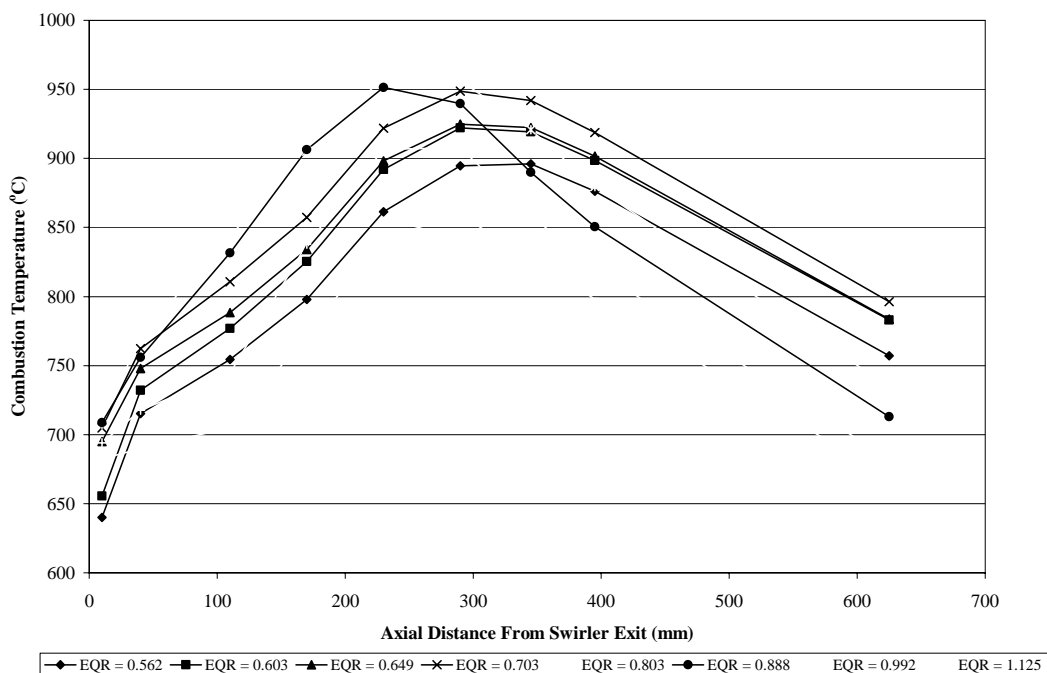
Figure 6.17: Combustion Temperature vs. Axial Distance from Swirler Exit for flames at Different Equivalence Ratios Using Swirler Vane Angle of 50° and Orifice Plate of 20mm with Upstream Injection

Figure 6.17 shows the temperature profile in accordance to equivalence ratio along the combustion chamber using orifice plate of 20mm with upstream injection. Generally, highest temperatures for all equivalence ratio fall at distance of 290mm from the swirler exit except for equivalence ratio of 0.803 and 0.888 which fall at the distance of 230mm from the swirler exit while for equivalence ratio of 0.562 falls at the distance of 345mm from the swirler exit. For orifice plate of 20mm, leanest equivalence ratio of 0.562 produces longest flame length meanwhile richer equivalence ratio produces shorter flame length. This might be because of too much excess air present in the mixture with equivalence ratio of 0.562 which unable to maximize the shear layer boundary turbulence to spread the flame wider. The flame length increases to complete the combustion further downstream of the combustion chamber. Near the swirler exit, flame at equivalence ratio of 0.562 produces lowest temperature while highest temperature was shown by the flame at equivalence ratio of 0.888. Flame at equivalence ratio of 1.125, exhibits overall lowest temperature except near the swirler exit.

Figure 6.18: Combustion Temperature vs. Axial Distance from Swirler Exit for flames at Different Equivalence Ratios Using Swirler Vane Angle of 60° and Orifice Plate of 20mm with Upstream Injection
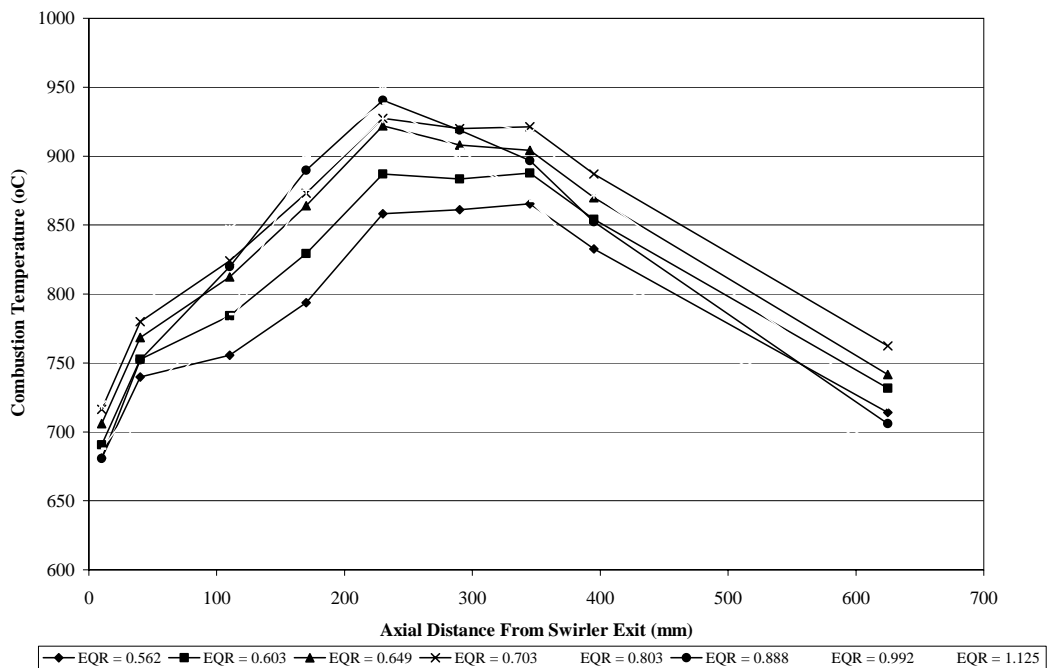
Figure 6.18 shows similar pattern to Figure 6.20, where flames with equivalence ratio of less than 0.703, produce peak temperature further downstream compared to flames with equivalence ratio more than 0.703 except for flame at equivalence ratio of 0.649, which produces peak at the distance of 230mm. The lowest temperature near to swirler exit and at the exit of combustion chamber was shown by flame at equivalence ratio of 0.992. This is quite different compared to the other results which mostly show lowest temperature at the exit was flame with equivalence ratio of 1.125. Meanwhile the lowest peak temperature is 793.7^{o}C produced by the flame at equivalence ratio of 0.562. The highest peak temperature was exhibited by flame at equivalence ratio of 0.803.

6.2.6   Emission Investigation Using Orifice Plate of 20mm with Upstream Injection

The measured NO_x, CO and SO_2 emissions as a function of the gas analysis metered equivalence ratio using orifice plate of 20mm with upstream injection are shown in Figures 6.19, 6.20 and 6.21, respectively. The emission pattern for all three emissions is almost the same as the emission investigation results using orifice plate of 25mm. However, the emission values are much lesser for orifice plate of 20mm compared to the results in orifice plate of 25mm. NO_x emission below 50 ppm was obtained for all swirler vane angles. Meanwhile, SO_2 emission below 200 ppm was obtained for all swirler vane angles.
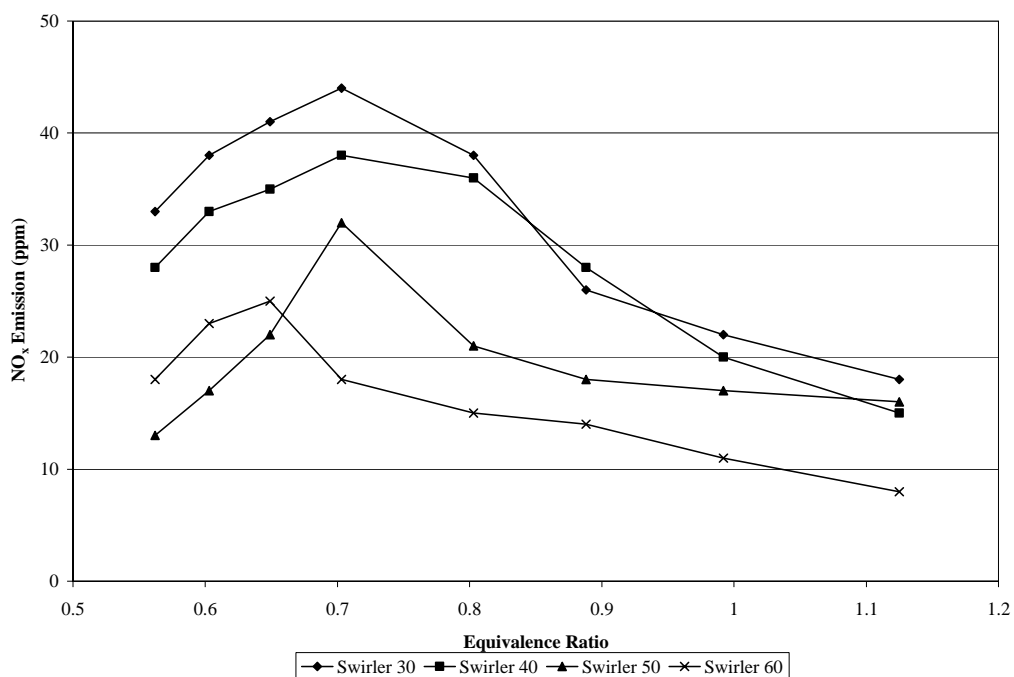
Figure 6.19: NO_x Emission vs. Equivalence Ratio for Various Swirlers Using Orifice Plate of 20mm with Upstream Injection

Referring to Figure 6.19, swirler vane angle of 30° generates highest NO_x emission. Meanwhile, swirler vane angle of 60°, generates lowest NO_x emission. However, swirler vane angle of 50° produced better emission results compared to swirler vane angle of 60° below the equivalence ratio of 0.7. This order disagree with the theory which indicates that swirler vane angle of 60° should provide better emission results compared to swirler vane angle of 50°. The emission decreased

about 29 percent for swirler vane angle of 60° compared to swirler vane angle of 50° at equivalence ratio of 0.803. At the same equivalence ratio, NO_x emission was reduced about 58 percent for swirler vane angle of 60° compared to swirler vane angle of 40°. Meanwhile, the emission reduction was about 60 percent for swirler vane angle of 60° compared to swirler vane angle of 30° at equivalence ratio of 0.803. The emission reduction between swirler vane angle of 40° and 30° was only 2 ppm.
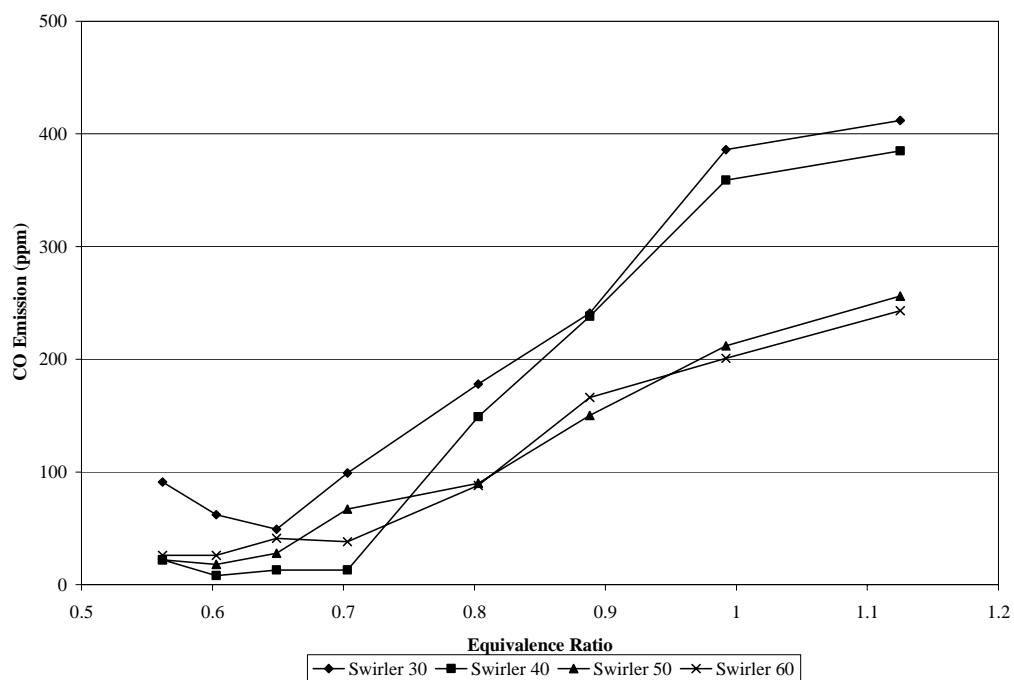
Figure 6.20: CO Emission vs. Equivalence Ratio for Various Swirlers Using Orifice Plate of 20mm with Upstream Injection

CO emission also shows poor results where the emission results disagree with the theory. In fuel lean region below the equivalence ratio of 0.7, swirler vane angle of 40° produces better emission results while in high fuel lean region which is at equivalence ratio from 0.7 to 0.9, swirler vane angle of 50° generates lowest emission results. Meanwhile, in fuel rich region, the lowest emission results were shown by swirler vane angle of 60°. However at equivalence ratio of 0.803, the emission reduction was similar to the theory where swirler vane angle of 60° produces lowest emission followed by swirler vane angle of 50°, 40° and 30°.
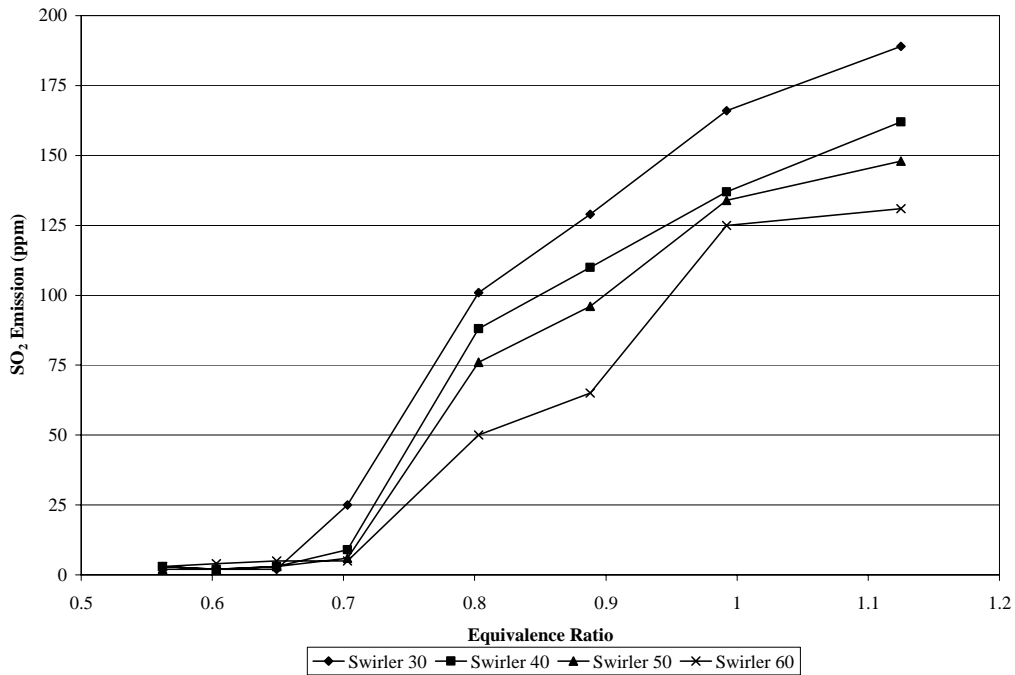
Figure 6.21: SO_2 Emission vs. Equivalence Ratio for Various Swirlers Using Orifice Plate of 20mm with Upstream Injection

Referring to Figure 6.21, SO_2 emission is almost constant in fuel lean region below the equivalence ratio of 0.7 and increases rapidly since then through the fuel rich region. Swirler vane angle of 60° shows lowest emission result that is about 130 ppm at equivalence ratio of 1.125. SO_2 emission of less than 200 ppm was generated for all swirler vane angles using orifice plate of 20mm with upstream injection.

6.3   Downstream Injection

Besides the investigation on upstream injection, downstream injection was another method carried out in this study. Fuel injector was placed further downstream into the combustion chamber. Results were compared between these two methods. Investigation has been carried out using 3 different orifice plates of 20mm, 25mm and 30mm for 4 different swirler vane angles of 30°, 40°, 50° and 60°.

6.3.1 Temperature Profile in Accordance to Equivalence Ratio along the Combustion Chamber Using Orifice Plate of 30mm with Downstream Injection
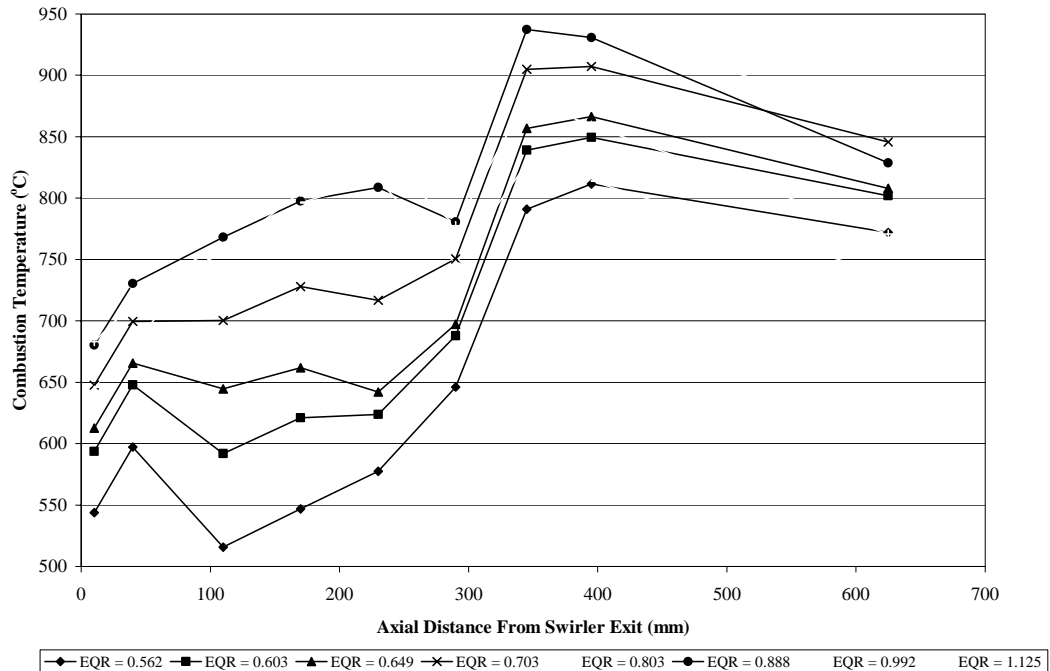
Figure 6.22: Combustion Temperature vs. Axial Distance from Swirler Exit for flames at Different Equivalence Ratios Using Swirler Vane Angle of 30° and Orifice Plate of 30mm with Downstream Injection

Figure 6.22 shows combustion temperature in accordance to equivalence ratio along the axial length of the combustion chamber for swirler vane angle of 30° using orifice plate of 30mm with downstream injection. The temperature profile scattered along the combustion chamber. The lowest temperature was 515.7°C shown by flame with equivalence ratio of 0.562 at the distance of 110mm from the swirler exit. Mainly in the flame front, the temperature does not increase steadily along the combustion chamber. The temperature increases and then decreases along the chamber. Steep increase of temperature was found at distance of 290mm to 345mm from the swirler exit. Highest temperature was shown at the distance of 345mm from the swirler exit. Flame at equivalence ratio of 0.562 produces lowest temperature along the combustion chamber except at the end where flame with equivalence ratio of 1.125 shows lowest temperature. Meanwhile, highest temperature was shown by flame with equivalence ratio of 0.803 at the combustion chamber exit.
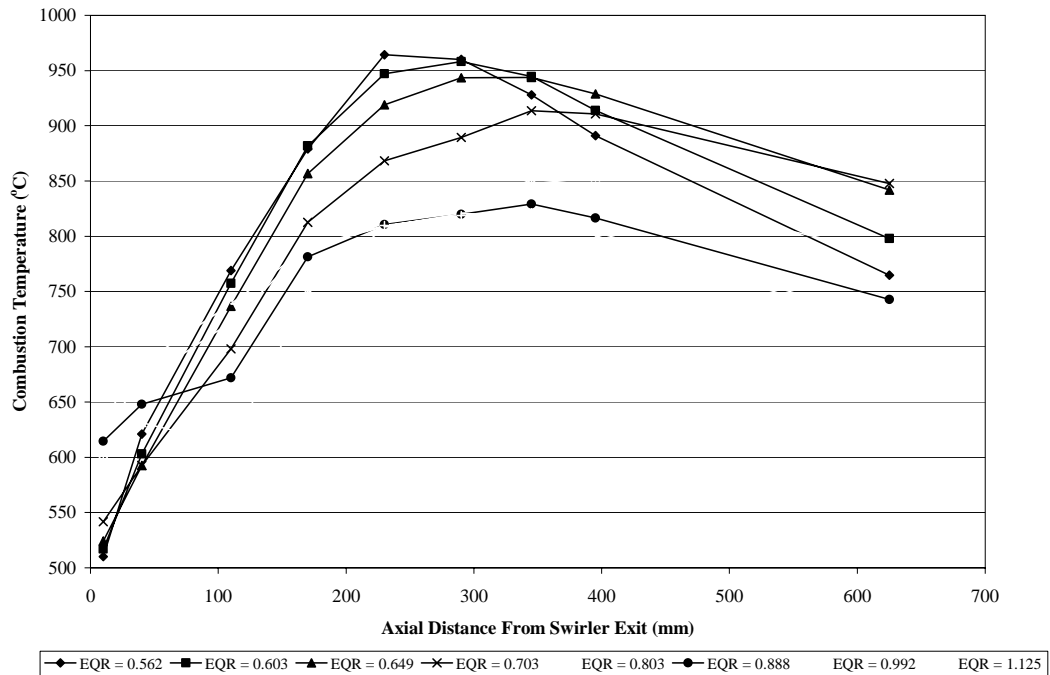
Figure 6.23: Combustion Temperature vs. Axial Distance from Swirler Exit for flames at Different Equivalence Ratios Using Swirler Vane Angle of 40° and Orifice Plate of 30mm with Downstream Injection

Figure 6.23 shows temperature profile for swirler vane angle of 40° in accordance to equivalence ratio using orifice plate of 30mm with downstream injection. Flames for the low equivalence ratios produce lower temperature compared to flames with higher equivalence ratios near to the swirler exit. However, lowest temperature was exhibited by flame with equivalence ratio of 0.803 at the distance of 110mm from the swirler exit. Looking at the graph, it is noticed that equivalence ratio of 0.803 provides with lower temperature for equivalence ratios below 0.7. This shows that for this setting with swirler vane angle of 30° and orifice plate of 30mm using downstream injection, probably the best pressure drop and turbulence structure occurs at equivalence ratio of 0.803. This could be because of the even temperature distribution throughout the chamber as fuel spreads widely to occupy the entire combustion chamber. Meanwhile, highest temperature was exhibited at the distance of 230mm from the swirler exit by flame at equivalence ratio of 0.562. The major factor of this circumstance was because of narrow flame and higher flame speed at the distance of 230mm from the swirler exit. At the chamber exit, the lowest temperature was shown by equivalence ratio of 1.125 while highest temperature was produced by flame at equivalence ratio of 0.703.
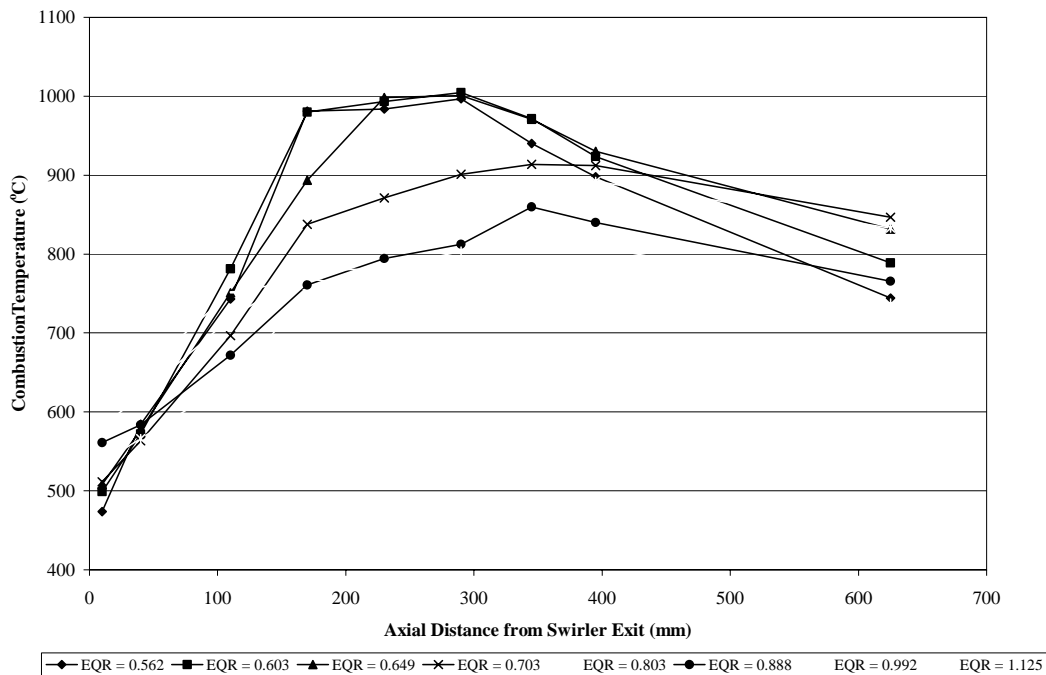
Figure 6.24: Combustion Temperature vs. Axial Distance from Swirler Exit for flames at Different Equivalence Ratios Using Swirler Vane Angle of 50° and Orifice Plate of 30mm with Downstream Injection

Referring to Figure 6.24, the temperature gradient for higher equivalence ratio was low where they show temperature of less than 900°C. Steeper temperature gradient was shown by lower equivalence ratios along the combustion chamber. Highest temperature was exhibited by flame with equivalence ratio of 0.603 at the distance of 290mm from the swirler exit. Flame with equivalence ratio of 1.125; produce highest temperature near to the swirler exit and lowest temperature at the combustion chamber exit. Highest temperature at the exit was shown by flame with equivalence ratio of 0.703.
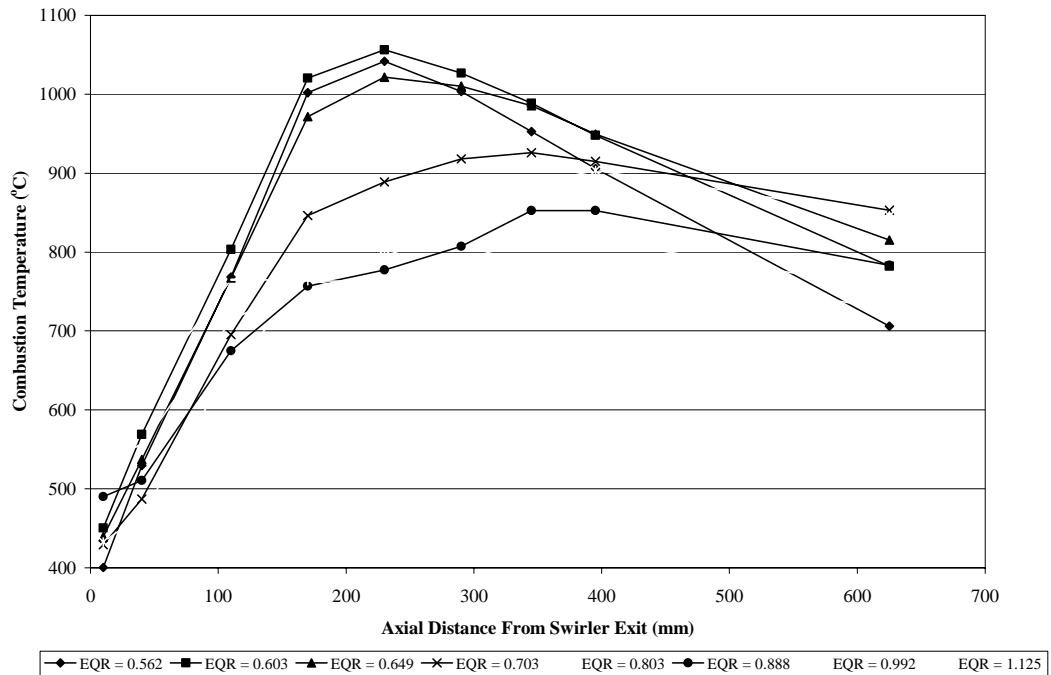
Figure 6.25: Combustion Temperature vs. Axial Distance from Swirler Exit for flames at Different Equivalence Ratios Using Swirler Vane Angle of 60° and Orifice Plate of 30mm with Downstream Injection

Temperature profile of about the same pattern with Figure 6.27 was observed in Figure 6.25, where temperature gradients for higher equivalence ratio were lower than those with lower equivalence ratios. The first three equivalence ratios exceed the temperature of $1000^{o}C$ at the peak area at distance of 230mm from the swirler exit. Peak area for higher equivalence ratios flame was produced further downstream in the combustion chamber compared to those lower equivalence ratios flame. The highest temperature near the swirler exit was exhibited by fuel rich flame. Meanwhile, lowest temperature at the combustion chamber exit was shown by flame with equivalence ratio of 0.562. Highest temperature at the exit was produced by flame with equivalence ratio of 0.703.

6.3.2 Emission Investigation Using Orifice Plate of 30mm with Downstream Injection
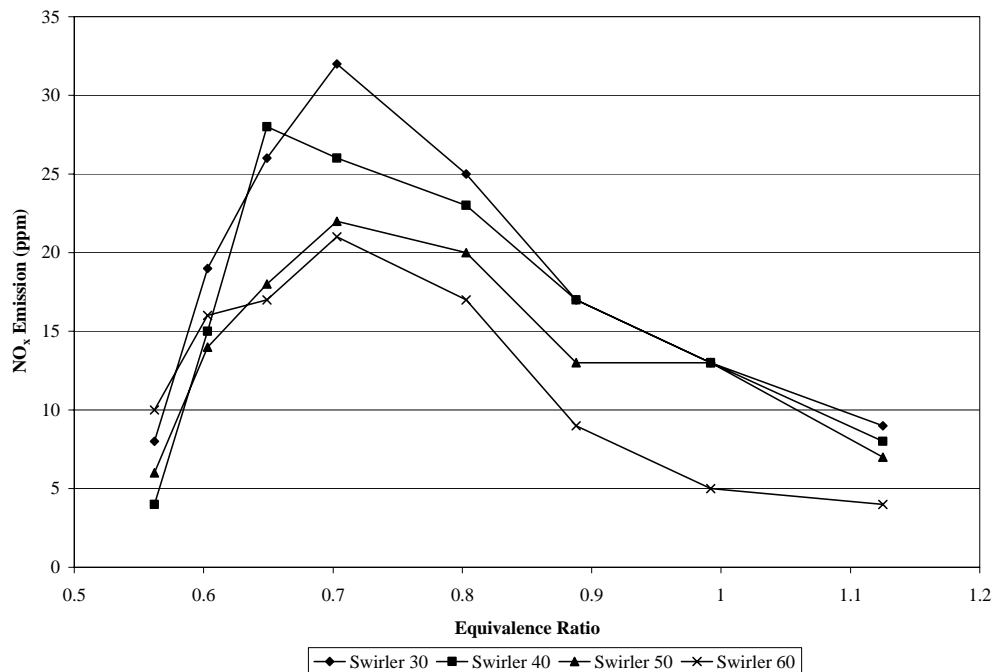
Figure 6.26: NO_x Emission vs. Equivalence Ratio for Various Swirlers Using Orifice Plate of 30mm with Downstream Injection

Figure 6.26 shows NO_x emission versus equivalence ratio for 4 different swirler vane angles of 30°, 40°, 50° and 60° using orifice plate of 30mm with downstream injection. For swirler vane angle of 30°, NO_x emission produced by the downstream injection was almost twice lower than the NO_x emission produced by the upstream injection for all swirler vane angles. However, the flame was not stable, produces less convincing NO_x emission results. High NO_x emission was shown by this setting. Once again, the results show that swirler vane angle of 60° produces better results compared to other swirler vane angles. Swirler vane angle of 30° produces highest NO_x emission results for the entire swirler vane angles. This match the theory, which states that stronger swirling flow helps in mixing of fuel and air, thus reduces the emissions. At equivalence ratio of 0.803, the emission reduction was not significant where it reduced only about 8 ppm for swirler vane angle of 60° compared to swirler vane angle of 30°. This value contributes about 32 percent of reduction between these two swirlers. Meanwhile, NO_x emission decreased about 13 percent for swirler vane angle of 50° compared to swirler vane angle of 40°.
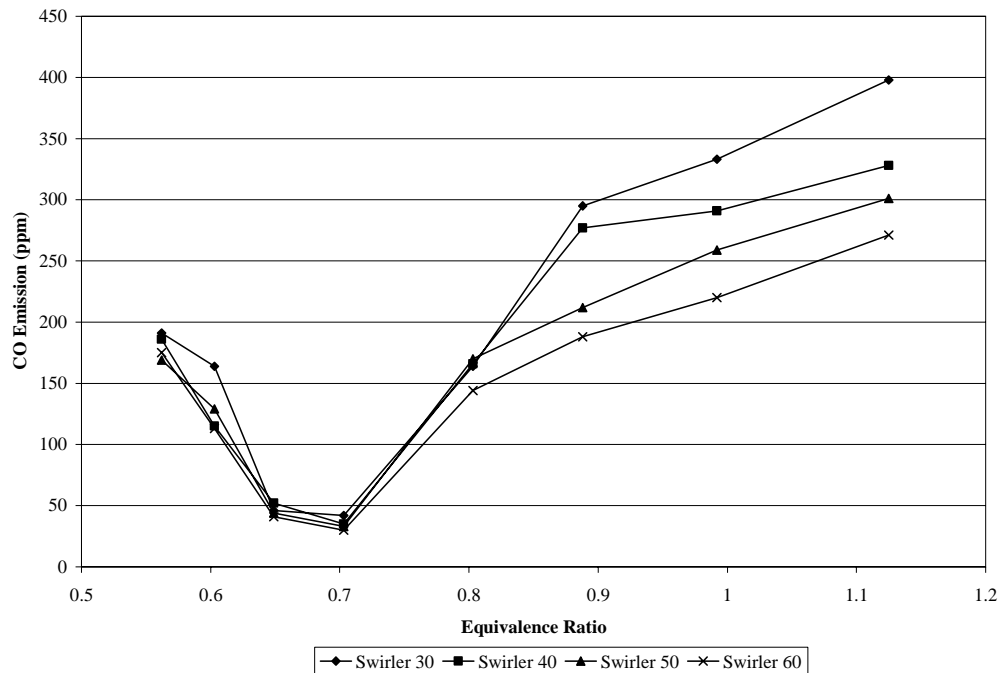
Figure 6.27: CO Emission vs. Equivalence Ratio for Various Swirlers Using Orifice Plate of 30mm with Downstream Injection

Figure 6.27 shows CO emission versus equivalence ratio for 4 different swirler vane angles of 30°, 40°, 50° and 60° using orifice plate of 30mm with downstream injection. CO emission decreases with respect to equivalence ratio in fuel lean region below equivalence ratio of 0.7 and increases with respect to equivalence ratio at equivalence ratio of 0.7 through the fuel rich region. There is no significant different of CO emission between all the swirler until equivalence ratio of 0.8. Swirler vane angle of 60° produces lowest CO emission. Meanwhile, swirler vane angle of 30° produces highest CO emission. However, these emissions results are much lesser compared to the emissions produced by upstream injection. The CO emission reduction for Swirler vane angle of 60° with downstream injection and upstream injection is about 230 ppm. This might be because of better mixing of fuel and air was enhanced in the downstream injection as the fuel, which enters the combustor, were in turbulence flow. Meanwhile in upstream injection, the fuel goes through a laminar flow before changing to turbulence flow. Turbulence profile of the mixture produces thorough and proper air fuel mixing. This generates good combustion and low pollution formation. The two structure of mixture profile in upstream injection causes poor combustion performances and generates higher pollution. At equivalence ratio of 0.803, CO emission increases slowly from swirler

vane angle of 30° to swirler vane angle of 50° and dropped for swirler vane angle of 60°. The slow increase was about 3 percent that was 6 ppm for swirler vane angle of 50° compared to swirler vane angle of 30°. The emission then dropped about 18 percent for swirler vane angle of 60°.

Figure 6.28: SO$_2$ Emission vs. Equivalence Ratio for Various Swirlers Using Orifice Plate of 30mm with Downstream Injection
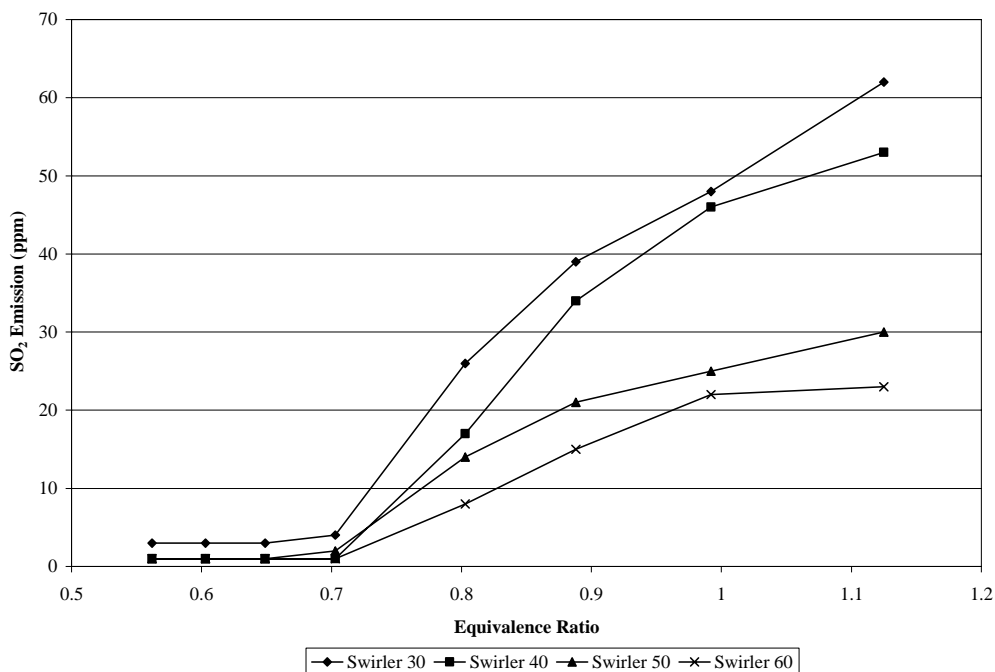
Figure 6.28 shows SO$_2$ emission versus equivalence ratio for 4 different swirler vane angles of 30°, 40°, 50° and 60° using orifice plate of 30mm with downstream injection. SO$_2$ emission increases with respect to equivalence ratio. Until the equivalence ratio of 0.7, SO$_2$ emission increases slowly, this indicates that the emission is almost constant. The emission increases rapidly from that point through the fuel rich region. The highest SO$_2$ emission was produced by swirler vane angle of 30° that is 62 ppm while the lowest SO$_2$ emission was produced by swirler vane angle of 60° that is 23 ppm. Downstream injection shows lower emission results for all swirler vane angle compared to upstream injection at the same orifice plate configuration.

6.3.3 Temperature Profile in Accordance to Equivalence Ratio along the Combustion Chamber Using Orifice Plate of 25mm with Downstream Injection

The next four figures shows the temperature profile in accordance to equivalence ratio along the combustion chamber for four different swirler vane angle of 30°, 40°, 50° and 60° using orifice plate of 25mm with downstream injection.
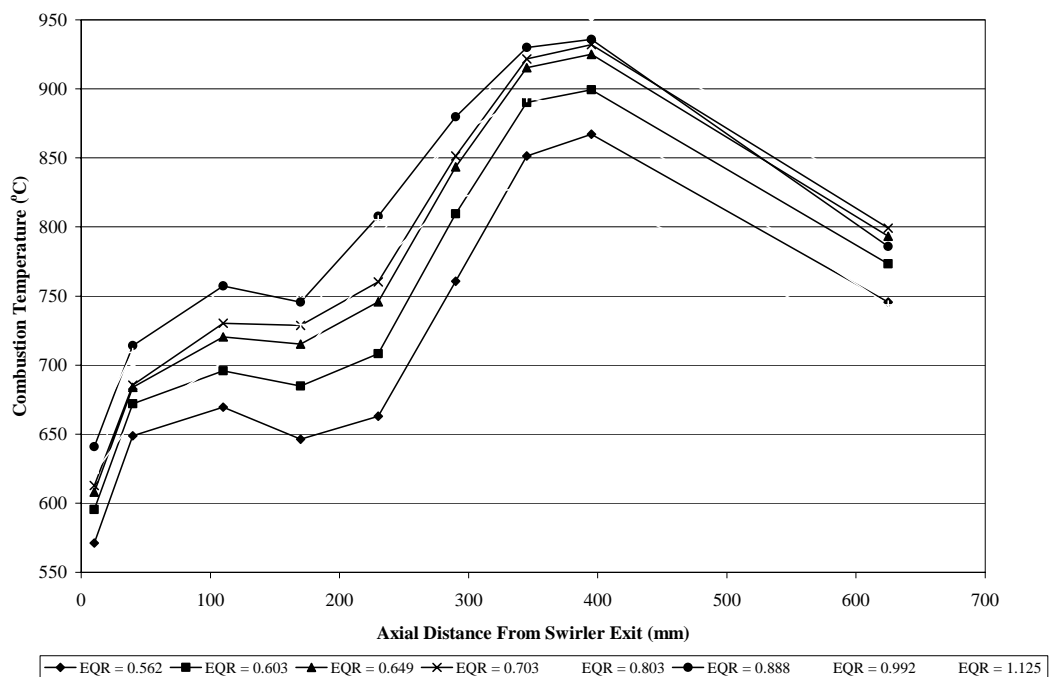
Figure 6.29: Combustion Temperature vs. Axial Distance from Swirler Exit for flames at Different Equivalence Ratios Using Swirler Vane Angle of 30° and Orifice Plate of 25mm with Downstream Injection

Figure 6.29 shows the temperature profile for swirler vane angle of 30° using orifice plate of 25mm with downstream injection. The temperature increases and decreases along the combustion chamber. The highest temperature was shown further downstream at distance of 395mm compared to upstream injection configuration where upstream injection configuration mostly shows the peak at distance of 230mm from the swirler exit. Actually, the flame was shorter in downstream injection configuration compared to upstream injection configuration. This conclusion was taken based on visual observation throughout the experimental testing. The above phenomena occurs because of the flame was shifted further downstream as the injector position was in the combustion chamber. Besides that, the highest

temperature point occurs at the flame tail for downstream configuration while for upstream configuration, the highest temperature point occur at the core of the flame, just after the flame middle portion. The detail of the flame highest temperature point was shown in Figure 6.30 and Figure 6.31 for upstream injection and downstream injection respectively. The highest temperature was produced by flame with equivalence ratio of 0.803. The lowest temperature at the combustion chamber exit was shown by fuel rich flame.

Figure 6.30: Upstream Flame Profile

Figure 6.31: Downstream Flame Profile
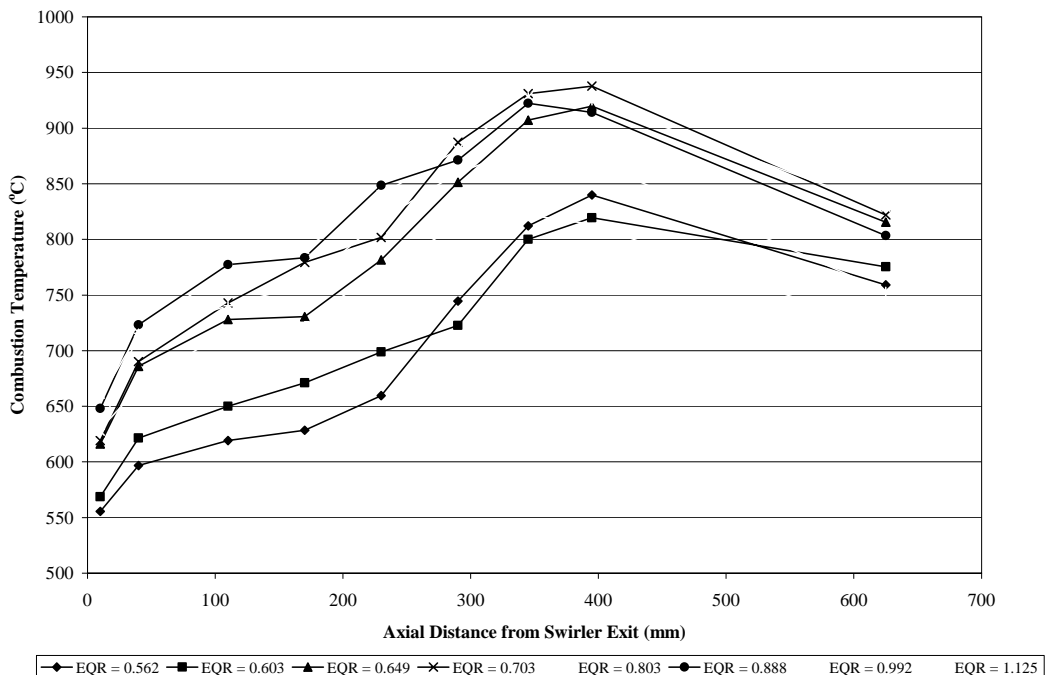
Figure 6.32: Combustion Temperature vs. Axial Distance from Swirler Exit for flames at Different Equivalence Ratios Using Swirler Vane Angle of 40° and Orifice Plate of 25mm with Downstream Injection

As shown in Figure 6.32, this is the temperature profile for swirler vane angle of 40°, the temperature increases steadily along the combustion chamber until the distance of 395mm from the swirler exit and decreases at the chamber end. The lowest temperature at the end of combustion chamber was shown by flame with equivalence ratio of 1.125. The highest temperature was produced by flame with equivalence ratio of 0.703, while flame with equivalence ratio of 0.803 produces highest temperature at the chamber end.
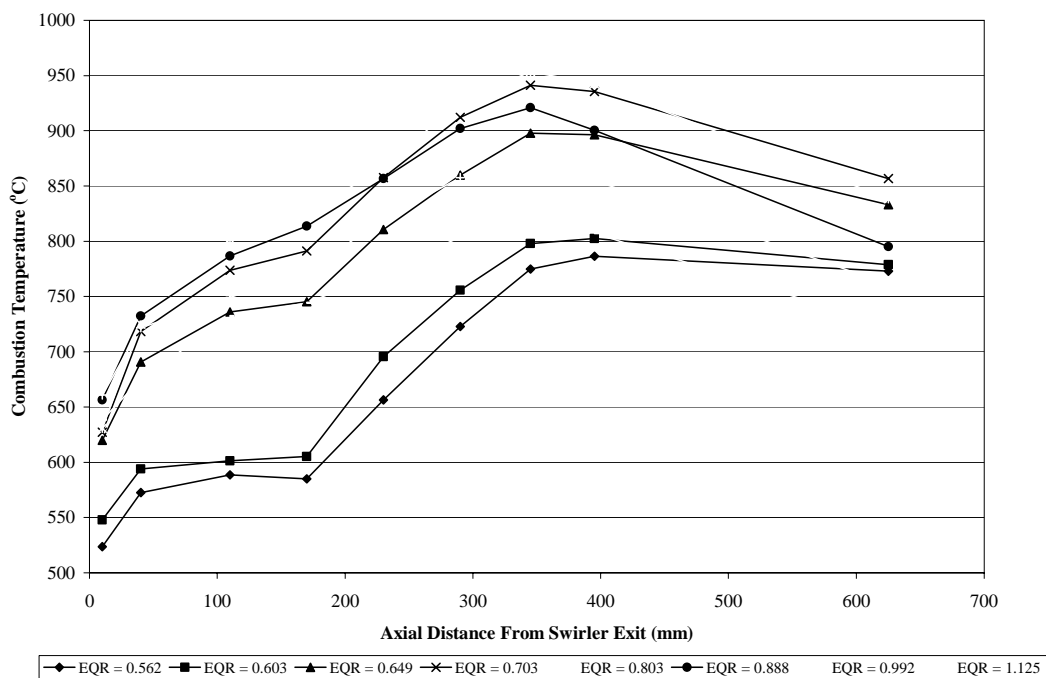
Figure 6.33: Combustion Temperature vs. Axial Distance from Swirler Exit for flames at Different Equivalence Ratios Using Swirler Vane Angle of 50° and Orifice Plate of 25mm with Downstream Injection

Figure 6.33 shows the temperature profile for swirler vane angle of 50° using orifice plate of 25mm with downstream injection. Near the swirler exit, flame with equivalence ratios of 0.562 and 0.603 produce temperature of less than 550°C. The peak area falls at the distance of 345mm from the swirler exit. This distance is more upstream compared to two earlier temperature profiles. The highest temperature was shown by flame with equivalence ratio of 0.803. Meanwhile highest temperature at the chamber exit was exhibited by flame with equivalence ratio of 0.703. Once again, the lowest temperature at the chamber end was exhibited by fuel rich flame.
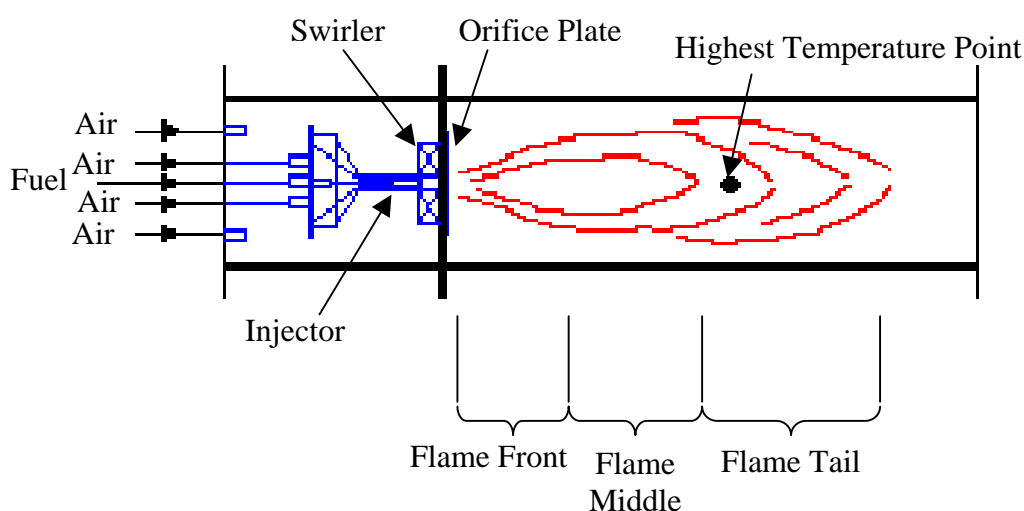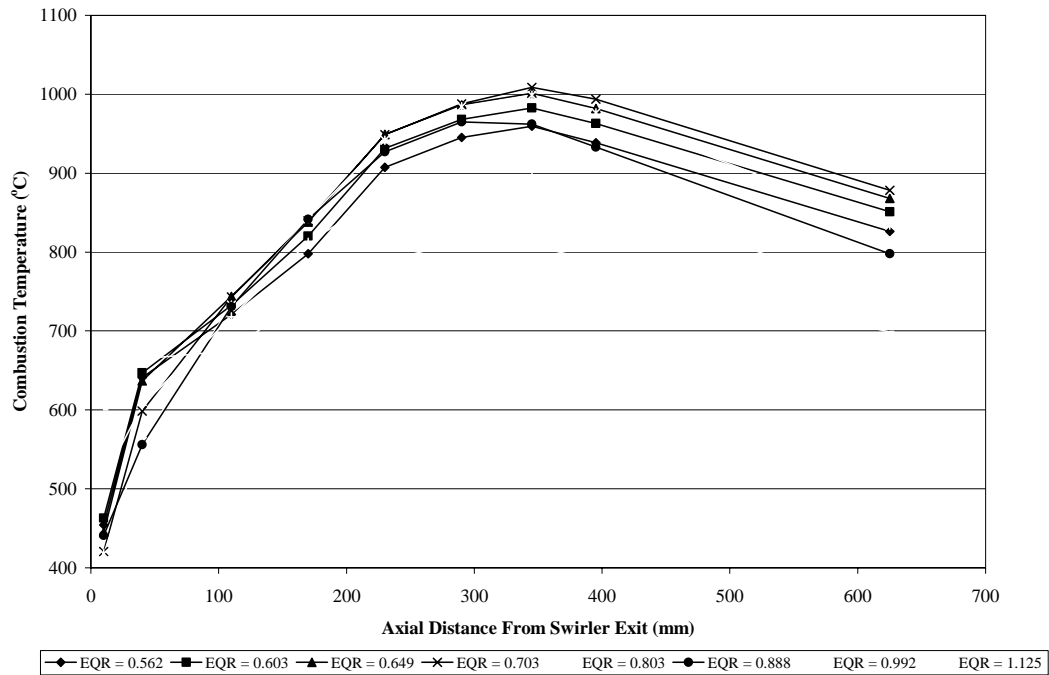
Figure 6.34: Combustion Temperature vs. Axial Distance from Swirler Exit for flames at Different Equivalence Ratios Using Swirler Vane Angle of 60° and Orifice Plate of 25mm with Downstream Injection
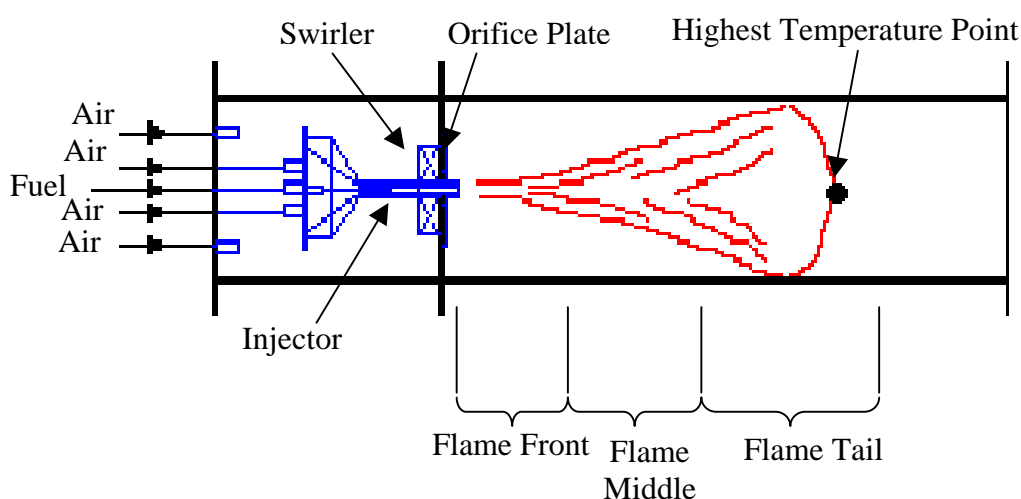
Figure 6.34 shows the temperature profile for swirler vane angle of 60° using orifice plate of 25mm with downstream injection. Excluding the flame with equivalence ratios of 0.992 and 1.125, other flames produce temperatures of less than 500°C at the front portion of the flame. This is the lowest temperature produced compared to other swirler vane angles. The temperature increases steadily until the distance of 345mm from the swirler exit and reduces towards the exit. Flame with equivalence ratio of 1.125; produce highest temperature near the swirler exit and lowest temperature at the exit of combustion chamber. The different between these two temperatures was about 100°C. The highest temperature was found at the distance of 345mm from the swirler exit by flame with equivalence ratio of 0.703. This temperature did exceed 1000°C. The same flame exhibits highest temperature at the exit of combustion chamber.

6.3.4 Emission Investigation Using Orifice Plate of 25mm with Downstream Injection
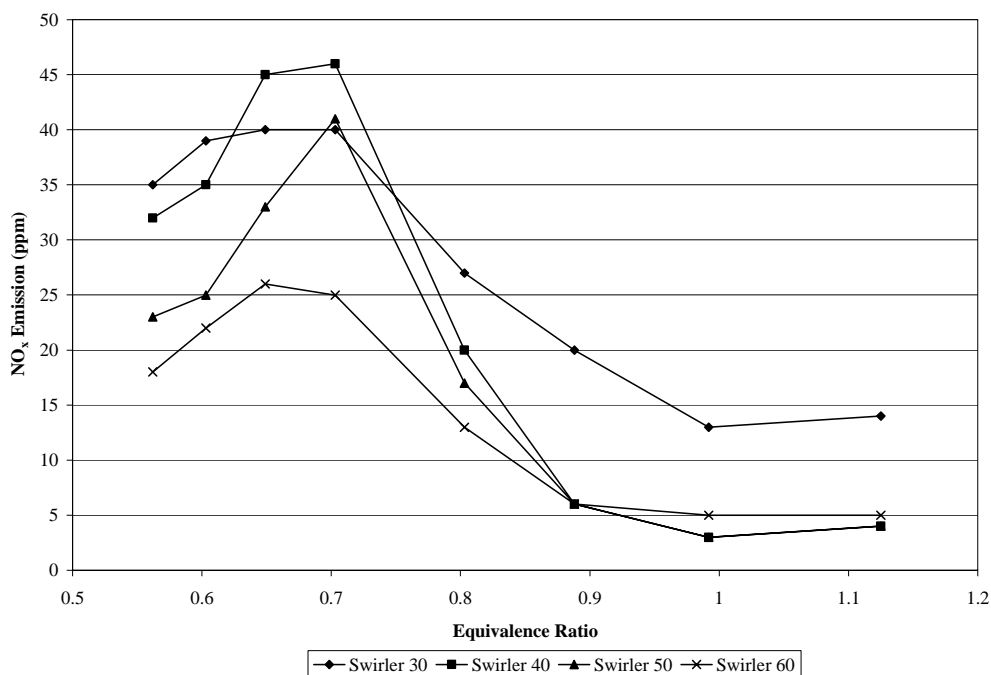
Figure 6.35: NO_x Emission vs. Equivalence Ratio for Various Swirlers Using Orifice Plate of 25mm with Downstream Injection

Figures 6.35, 6.37 and 6.38 shows NO_x, CO and SO_2 emission investigation using orifice plate of 25mm with upstream injection for 4 different swirler vane angles of 30°, 40°, 50° and 60°. The emission pattern is almost the same as for orifice plate of 30mm. However, the NO_x emission was quite deteriorated for swirler vane angle of 30°, 40° and 50° indicating that the flame is not stable for those swirler vane angles setting. The flame is quite stable for swirler vane angle of 60° that produces stable emission results. However, the NO_x emission for this swirler vane angle at fuel rich region does not show any reduction. NO_x emission reduction of about 26 percent was achieved for swirler vane angle of 40° compared to swirler vane angle of 30°. The emission was then further reduced about 20 percent for swirler vane angle of 50°. NO_x emission once again shows reduction of about 24 percent when swirler vane angle was increased to 60°. Once again, comparison was taken at equivalence ratio of 0.803. Comparison was taken after the highest temperature point because lower emission results were spotted at this stage. The purpose of the study was to produce low emission with high power. Even though, equivalence ratio of .888 would produce high power with lower temperature which would produce lower NO_x

emission with high CO emission. So, ideal equivalence ratio of 0.803 was chosen for comparison. Equivalence ratio of 0.803, probably produce higher NO_x emission with lower CO emission. Detail was shown in Figure 6.36.
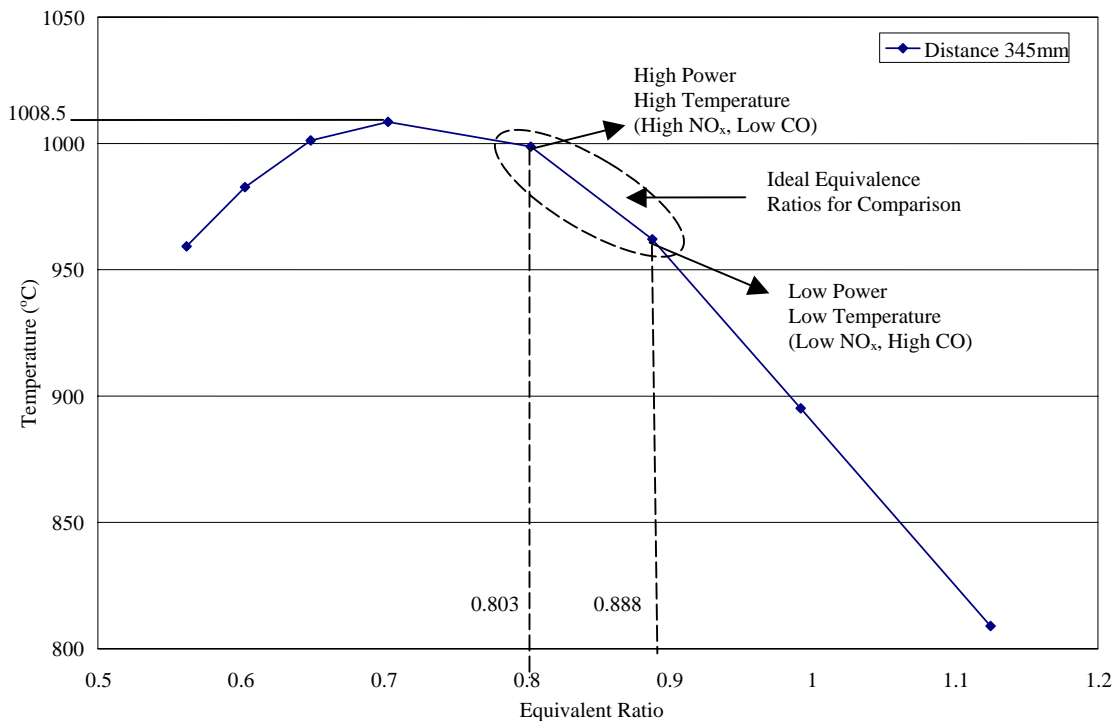
Figure 6.36: Temperature Profile for Various Equivalence Ratios
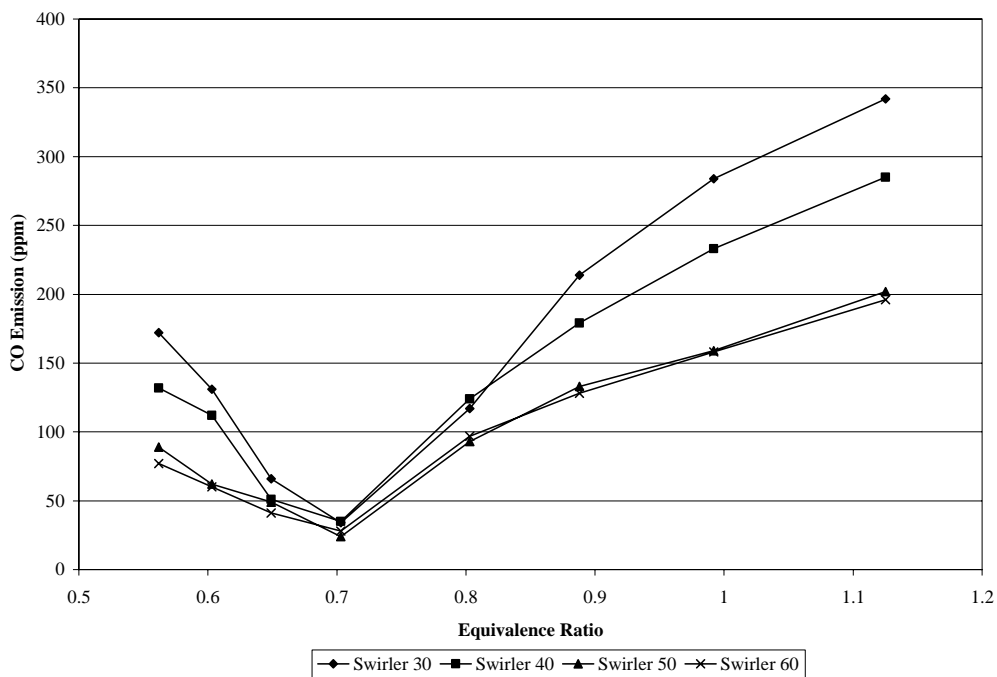
Figure 6.37: CO Emission vs. Equivalence Ratio for Various Swirlers Using Orifice Plate of 25mm with Downstream Injection

Even though, CO emission for this orifice plate configuration with downstream injection shows not much different between swirler vane angles of 50° and 60°, but, as for overall, these results were much lesser compared to upstream injection results. The highest CO emission produced by swirler vane angle of 60° for this orifice plate configuration with downstream injection is 196 ppm that is at fuel rich region. Swirler vane angle of 30° generates highest CO emission among all swirler vane angles. There is not much different in CO emission results between all swirler vane angles in the region of 0.65 to 0.75 equivalence ratios. The emission decreased from swirler vane angle of 30° to 50° but increased for swirler vane angle of 60°. However, as mentioned earlier the increase was small that is about 4 percent for swirler vane angle of 60° compared to swirler vane angle 50°. Meanwhile, emission reduction of about 25 percent was achieved for swirler vane angle of 50° compared to swirler vane angle of 40°. Comparison was again performed at equivalence ratio of 0.803.
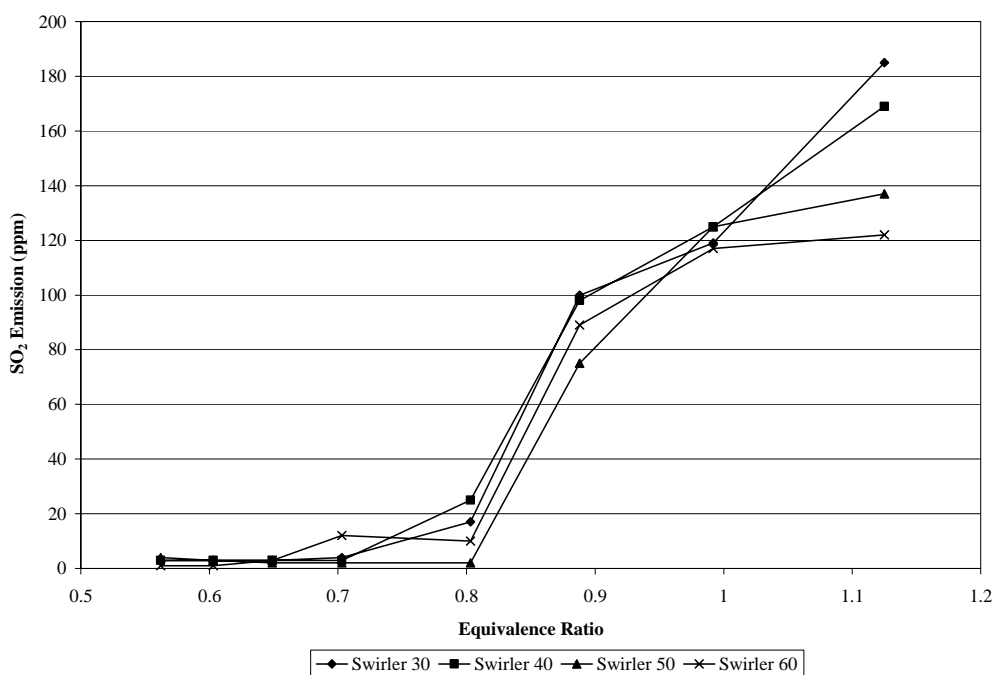
Figure 6.38: SO_2 Emission vs. Equivalence Ratio for Various Swirlers Using Orifice Plate of 25mm with Downstream Injection

Meanwhile, SO_2 emission was almost constant until the equivalence ratio of 0.8 and increases rapidly from that equivalence ratio through to the fuel rich region. As the flame was not stable, the emission results also vary. Even though swirler vane

angle of 30° produces highest emission in fuel rich region, but most of the time, swirler vane angle of 40° shows higher emission. Meanwhile, lowest emission was shown by the 50° swirler vane angle rather than swirler vane angle of 60°. Only in the fuel rich region, swirler vane angle of 60° shows better SO_2 emission results.

6.3.5 Temperature Profile in Accordance to Equivalence Ratio along the Combustion Chamber Using Orifice Plate of 20mm with Downstream Injection
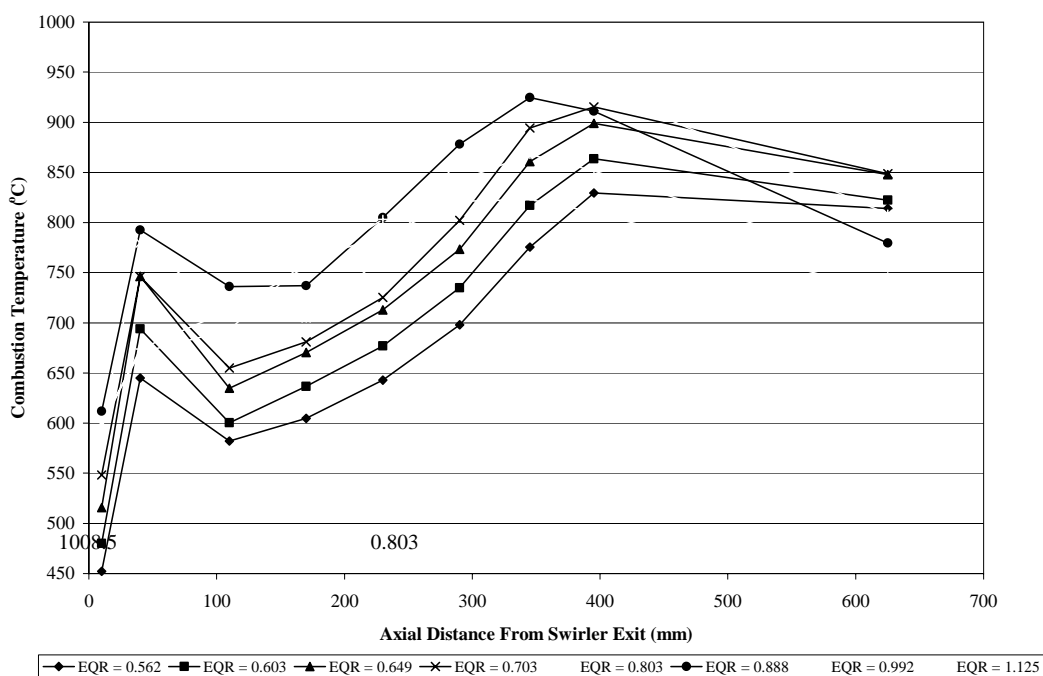
Figure 6.39: Combustion Temperature vs. Axial Distance from Swirler Exit for flames at Different Equivalence Ratios Using Swirler Vane Angle of 30° and Orifice Plate of 20mm with Downstream Injection

Figure 6.39 shows the temperature profile for swirler vane angle of 30° using orifice plate of 20mm with downstream injection. The highest temperature was produced at the distance of 395mm for flames with equivalence ratio of less than 0.8 while the highest temperature at distance of 345mm was produced for flames with equivalence ratio higher than 0.8. Flame with equivalence ratio higher than 0.8 produce bigger pressure drop which forces the flame becomes wider. Meanwhile, its counterpart produces narrower flame profile and pushes the flame longer. Overall

temperature of less than 1000°C was shown in this figure. The highest temperature at the flame front was shown by the flame with equivalence ratio of 0.888. The lowest temperature at the flame front was shown by the flame with equivalence ratio of 0.562.

Figure 6.40: Combustion Temperature vs. Axial Distance from Swirler Exit for flames at Different Equivalence Ratios Using Swirler Vane Angle of 40° and Orifice Plate of 20mm with Downstream Injection

Scattered temperature profile was shown by swirler vane angle of 40° using orifice plate of 20mm with downstream injection. Lowest temperature was once again found near the swirler exit by flame with equivalence ratio of 0.562 as shown in Figure 6.40. Highest temperature at the exit of combustion chamber was produced by flame with equivalence ratio of 0.649 while lowest temperature at the same spot was shown by flame with equivalence ratio of 1.125. Flames with equivalence ratio of 0.562 and 0.603, exhibit highest temperature at the distance of 395mm from the swirler exit. Flames with equivalence ratios of 0.649, 0.703, 0.803 and 0.888 exhibit highest temperature further upstream at distance of 345mm from the swirler exit. Meanwhile, flames with equivalence ratio of 0.992 and 1.125 exhibit highest temperature furthest upstream at 230mm from the swirler exit. The causes of the above phenomena have been discussed in section 6.4.3.
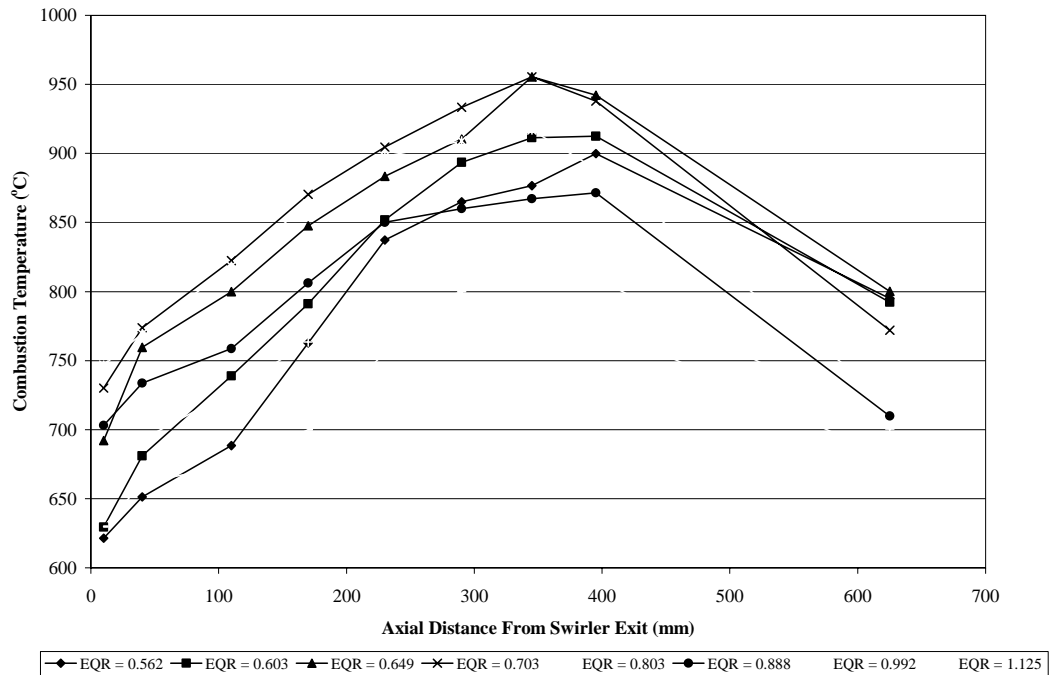
Figure 6.41: Combustion Temperature vs. Axial Distance from Swirler Exit for flames at Different Equivalence Ratios Using Swirler Vane Angle of 50° and Orifice Plate of 20mm with Downstream Injection

As shown in Figure 6.41, flame with equivalence ratio of 1.125 produces overall lowest temperature along the combustion chamber except at the ignition point where at this point, flame with equivalence ratio of 0.562 produces lowest temperature. Flames with equivalence ratios of 0.649 and 0.703 share same highest temperature at the distance of 345mm from the swirler exit. However, highest temperature at the combustion chamber exit was shown by flame with equivalence ratio of 0.649.
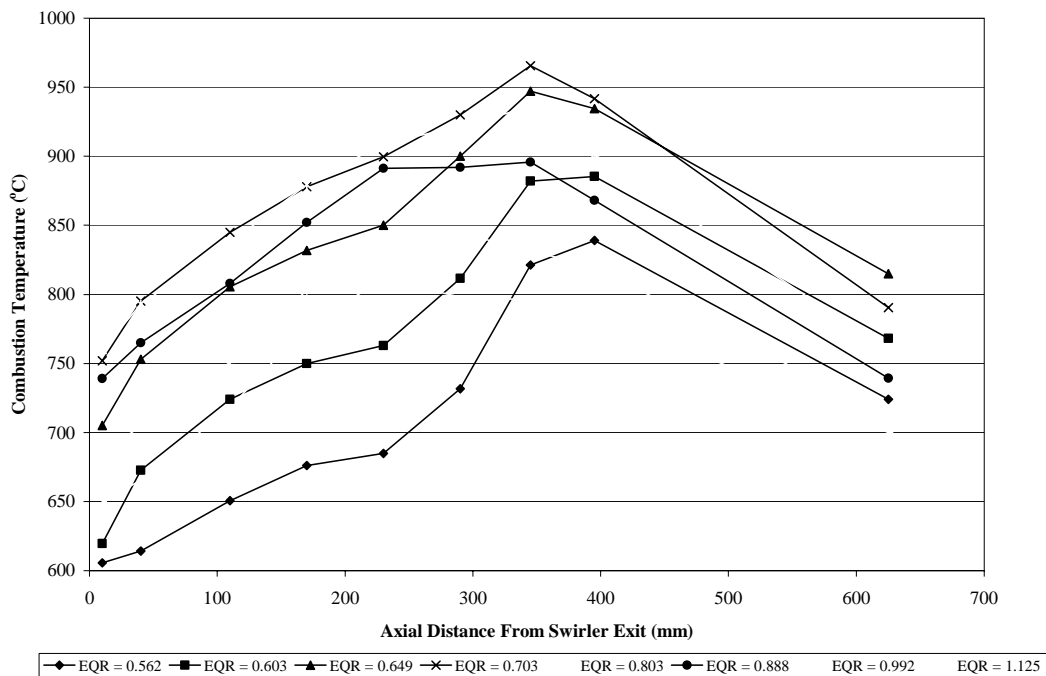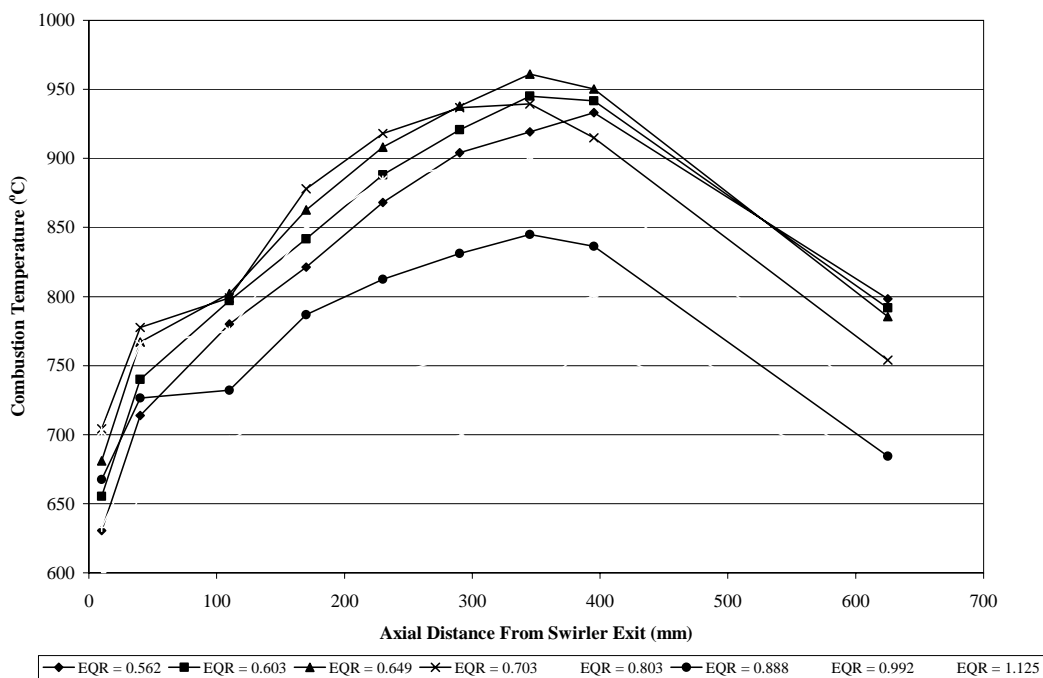
Figure 6.42: Combustion Temperature vs. Axial Distance from Swirler Exit for flames at Different Equivalence Ratios Using Swirler Vane Angle of 60° and Orifice Plate of 20mm with Downstream Injection

Figure 6.42 shows combustion temperature in accordance to equivalence ratio for swirler vane angle of 60° using orifice plate of 20mm with downstream injection. Along the combustion chamber, the fuel rich flame exhibits lowest temperature. At the distance of 345mm form the swirler exit, the lower equivalence ratio flames produce higher temperature compared to the higher equivalence ratio flames. However, flames with equivalence ratios of 0.562 and 0.603 exhibit lower temperatures compared to flame with equivalence ratios of 0.649. The highest temperature was found at the distance of 345mm by flame with equivalence ratio of 0.649. This shows that the flame speed was the highest at this equivalence ratio for current setting. Meanwhile, highest temperature at the chamber exit was shown by flame with equivalence ratio of 0.562. The configuration using orifice plate of 20mm with downstream injection shows highest temperature at equivalence ratio of 0.649 which is lower than most other downstream settings at 0.703 equivalence ratio.

6.3.6 Emission Investigation Using Orifice Plate of 20mm with Downstream Injection
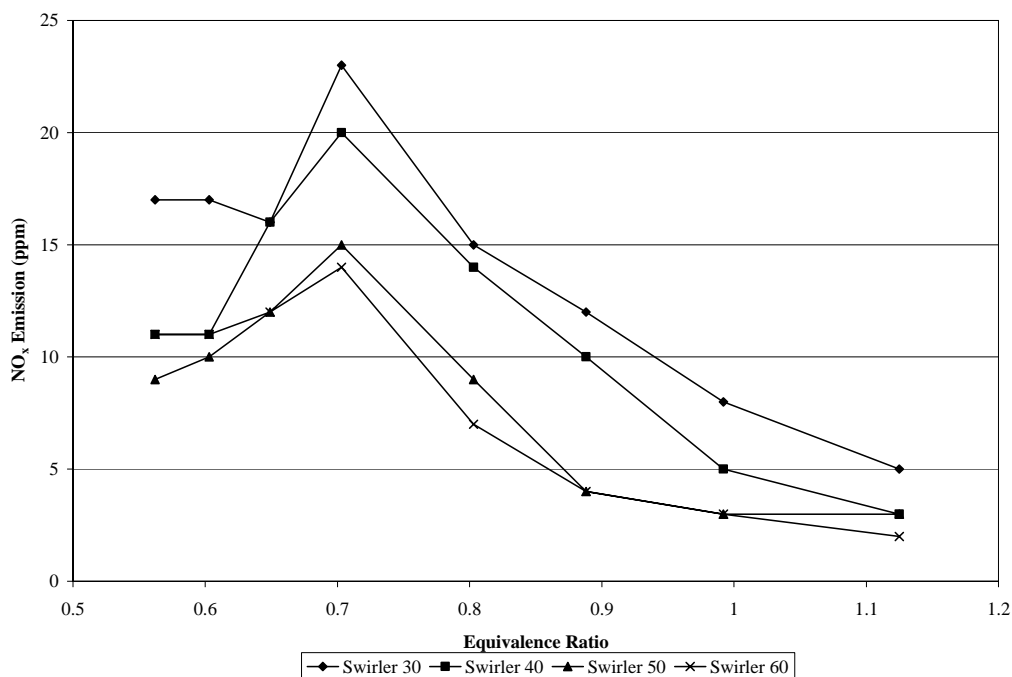
Figure 6.43: NO_x Emission vs. Equivalence Ratio for Various Swirlers Using Orifice Plate of 20mm with Downstream Injection

Figure 6.43 shows NO_x emission versus equivalence ratio for 4 different swirler vane angles using orifice plate of 20mm with downstream injection. NO_x emission of less than 25 ppm was achieved for this setting. Swirler vane angle of 30° produced highest NO_x emission for the entire equivalence ratios. The NO_x emission decreased as swirler vane angle was increased to 40°. The emission was further reduced as swirler vane angle was increased to 50° and 60°. In this setting, even though, swirler vane angle of 60° generates lowest emission, the emission different between swirler vane angle 60° and 50° is only about 2 ppm at equivalence ratio of 0.803. There was only 1 ppm reduction for swirler vane angle of 40° compared to swirler vane angle of 30°. At this equivalence ratio, highest reduction occurs for swirler vane angle of 50° that is about 36 percent compared to swirler vane angle of 40°.
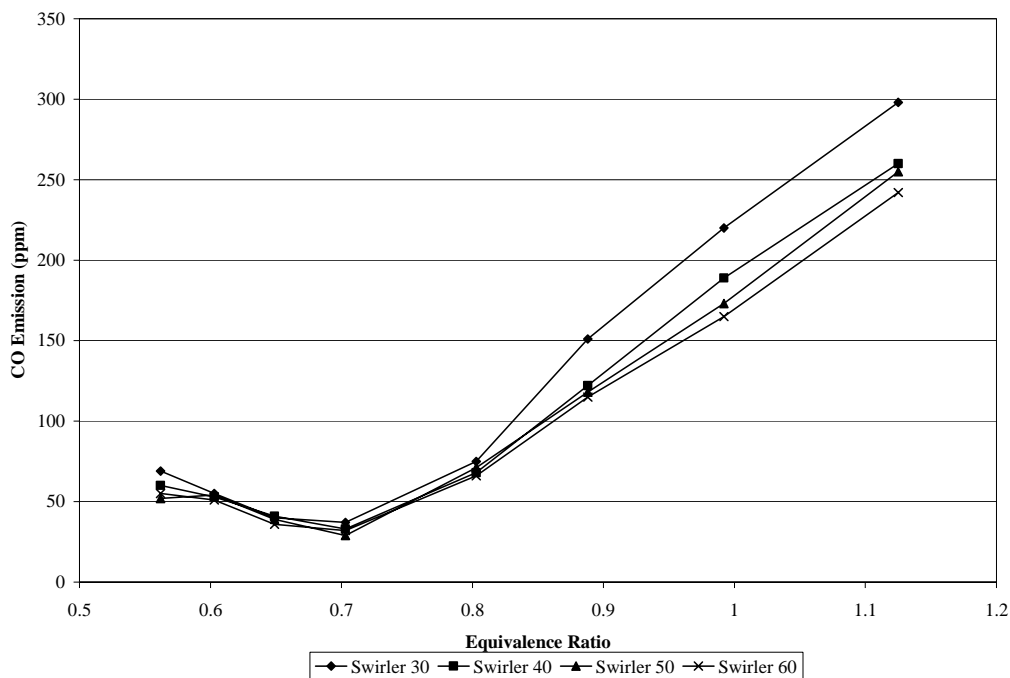
Figure 6.44: CO Emission vs. Equivalence Ratio for Various Swirlers Using Orifice Plate of 20mm with Downstream Injection

CO emission versus equivalence ratio for 4 different swirler vane angles of 30°, 40°, 50° and 60° using orifice plate of 20mm with downstream injection was shown in Figure 6.44. CO emission result decreases with respect to equivalence ratio from equivalence ratio of 0.562 until 0.7, and then increases with respect to equivalence ratio from equivalence ratio of 0.7 to 1.125. Lowest CO emission and highest NO_x emission appear at equivalence ratio of 0.7 for all swirler vane angles for most of the settings. There is no significant CO emission difference between swirler vane angles of 40°, 50° and 60° for the entire equivalence ratio. This was similar for swirler vane angle of 30° except at fuel rich region where swirler vane angle of 30° shows slightly higher CO emission.
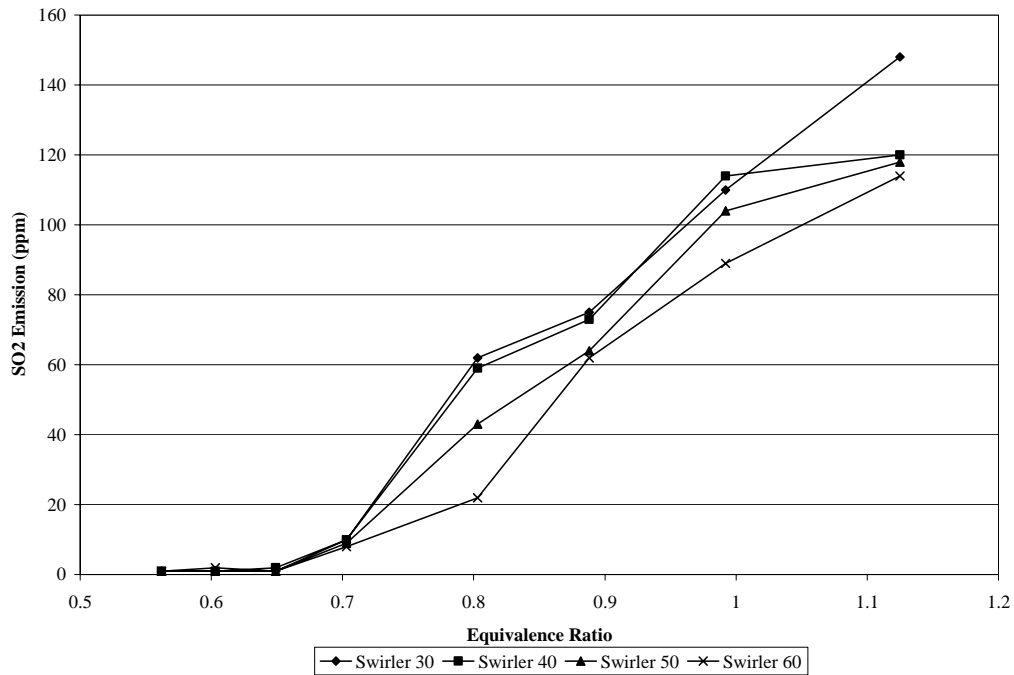
Figure 6.45: SO_2 Emission vs. Equivalence Ratio for Various Swirlers Using Orifice Plate of 20mm with Downstream Injection

SO_2 emission of less than 10 ppm is generated in fuel lean region below 0.8 equivalence ratio for all swirler vane angles as shown in Figure 6.45. The emission increases rapidly from the equivalence ratio of 0.7 to 1.125. SO_2 emission of less than 160 ppm was produced for all swirler vane angles. The emission reduction between swirler vane angles of 60° and 30° was 40 ppm that contributes about 67 percent of reduction. The decrease was small for swirler vane angle of 40° compared to swirler vane angle of 30° that is only 3 ppm. The emission was reduced about 37 percent for swirler vane angle of 50° compared to swirler vane angle of 40°. Further increase in swirler vane angle to 60° reduces the SO_2 emission about 49 percent. These results of 60° swirler vane angle show lowest SO_2 emission compared to other settings.

6.3.7 Temperature Profile for Various Swirlers Using Orifice Plate of 30mm with Upstream Injection at Equivalence Ratio of 0.803
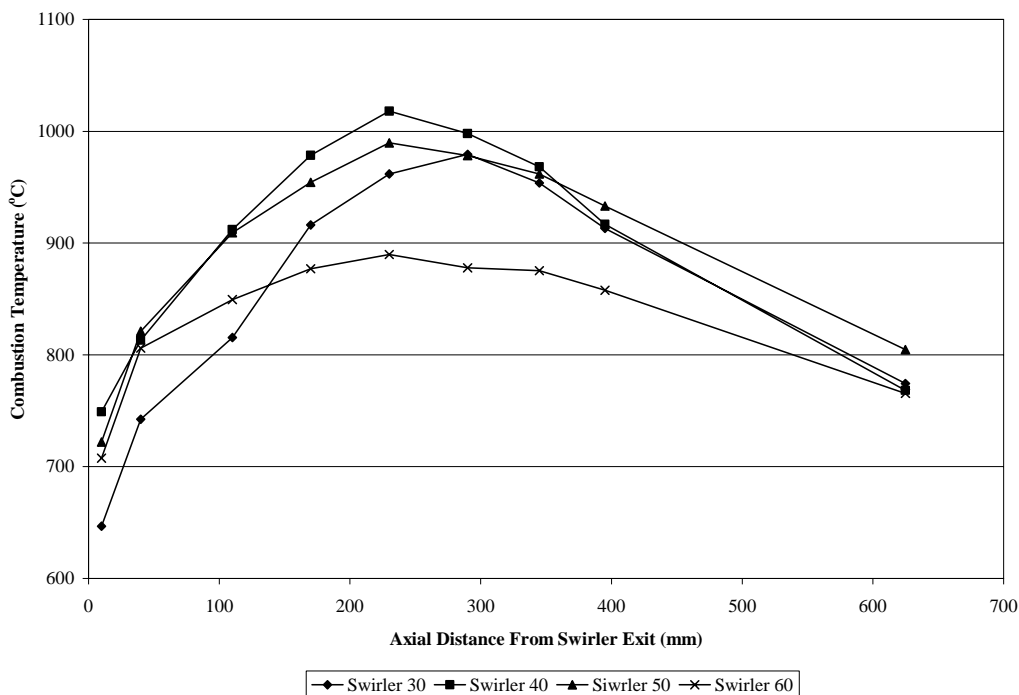
Figure 6.46: Combustion Temperature vs. Axial Distance from Swirler Exit for Various Swirler Using Orifice Plate of 30mm with Upstream Injection at Equivalence Ratio of 0.803

Referring to Figure 6.46, combustion temperature increases with respect to axial distance from swirler exit and decreases at 230mm from swirler exit towards the combustor exit. Temperature profile for swirler vane angle of 30° shows lowest temperature at near the swirler exit. Meanwhile, swirler vane angle of 60° shows lowest temperature at the combustor exit. This is mainly because swirler vane angle of 30° produces longer flame compared to swirler vane angle of 60°. Generally, swirler vane angle of 40° shows highest temperature along the combustion chamber. However, higher temperature was shown by swirler vane angle of 50° at the combustor exit. Swirler vane angle of 60° produces the lowest temperature range where the range of temperature was about 200^oC between lowest temperature and highest temperature for the swirler using orifice plate of 30mm with upstream injection.

Meanwhile, from the flame observation, swirler vane angle of 60° produces wider and shorter flame compared to the other swirler vane angles. Swirler vane

angle of 30° produces most narrow and longest flame length. All the swirler vane angles produce yellow reddish flame.

6.3.8 Temperature Profile for Various Swirlers Using Orifice Plate of 25mm with Upstream Injection at Equivalence Ratio of 0.803

Figure 6.47: Combustion Temperature vs. Axial Distance from Swirler Exit for Various Swirler Using Orifice Plate of 25mm with Upstream Injection at Equivalence Ratio of 0.803

Generally, orifice plate of 25mm produces lower combustion temperature compared to orifice plate of 30mm except for swirler vane angle of 60° as shown in Figure 6.47. Swirler vane angle of 60° shows highest combustion temperature at the flame front which is about 300mm from the swirler exit. However, combustion temperature for this setting decreases drastically since then towards the combustor exit where it shows lowest temperature at the end compared to the other swirler vane angles. Swirler vane angle of 40° shows lowest combustion temperature from the distance of 100mm from the swirler exit until the distance of 300mm from the swirler exit and highest combustion temperature since then towards the combustor

exit. At the flame front, swirler vane angle of 30° exhibit the lowest combustion temperature.

Meanwhile, from the flame observation, once again swirler vane angle of 60° produces wider and shorter flame length compared to the other swirler vane angles. Swirler vane angle of 30° produces most narrow and longest flame length. All the swirler vane angles produced yellow reddish flame. However, the flame length is shorter and wider compared to that using orifice plate of 30mm. The flame is more stable compared to orifice plate of 30mm.

6.3.9 Temperature Profile for Various Swirlers Using Orifice Plate of 20mm with Upstream Injection at Equivalence Ratio of 0.803
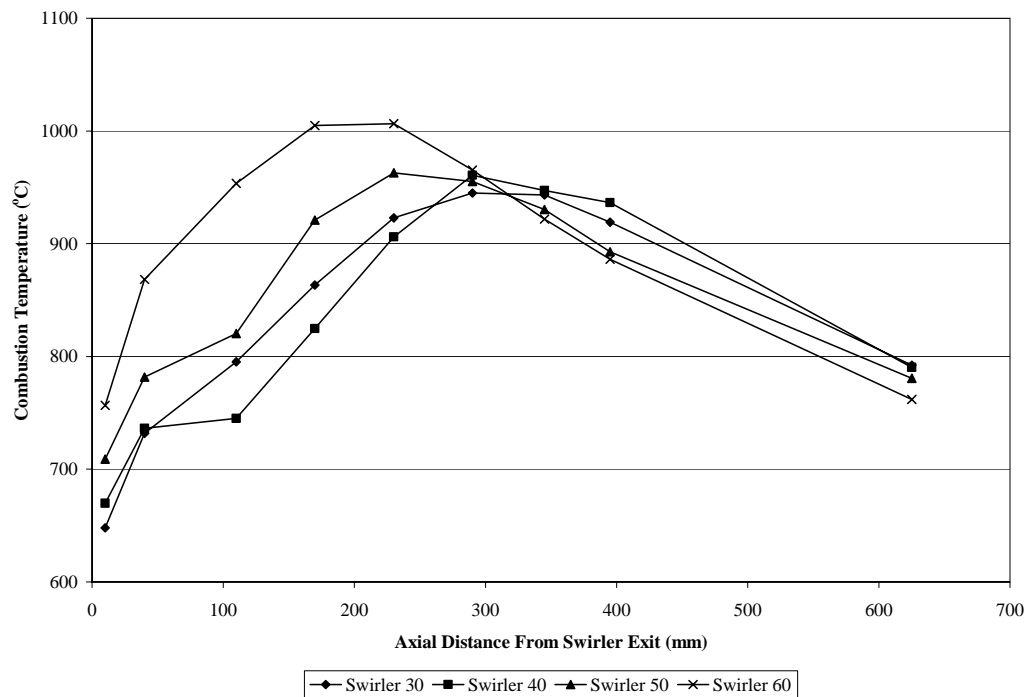

Figure 6.48: Combustion Temperature vs. Axial Distance from Swirler Exit for Various Swirler Using Orifice Plate of 20mm with Upstream Injection at Equivalence Ratio of 0.803

Orifice plate of 20mm produces lowest combustion temperature for all swirler vane angles with upstream injection. The temperature of lower than 1000^oC was produced for this setting as shown in Figure 6.48. The highest temperature for

all swirler vane angles using any investigated orifice plate with upstream injection was basically falls at the distance of 230mm from the swirler exit. The major factor of this circumstance was because of narrow flame and highest flame speed at the distance of 230mm from the swirler exit. In the flame front, swirler vane angles of 30° and 40° produce almost same combustion temperature. Meanwhile, swirler vane angles of 50° and 60° produce about the same temperature in the flame front. Swirler vane angle of 60° shows lowest combustion temperature at the flame tail. Meanwhile, swirler vane angle of 30° shows highest combustion temperature at the flame tail.

Meanwhile, from the flame observation, swirler vane angle of 60° produces wider and shorter flame length compared to the other swirler vane angles. Swirler vane angle of 30° produces most narrow and longest flame length. All the swirler vane angles produce yellow flame except the swirler vane angle of 30° which produces yellow reddish flame. Yellow flame rather than yellow reddish flame indicates better fuel and air mixing. Stable flame was produced where the movement of the flame is minimized. The flame is also shorter and wider compared to the two earlier orifice plate configurations.

6.3.10 Temperature Profile for Various Swirlers Using Orifice Plate of 30mm with Downstream Injection at Equivalence Ratio of 0.803

Figure 6.49: Combustion Temperature vs. Axial Distance from Swirler Exit for Various Swirler Using Orifice Plate of 30mm with Downstream Injection at Equivalence Ratio of 0.803
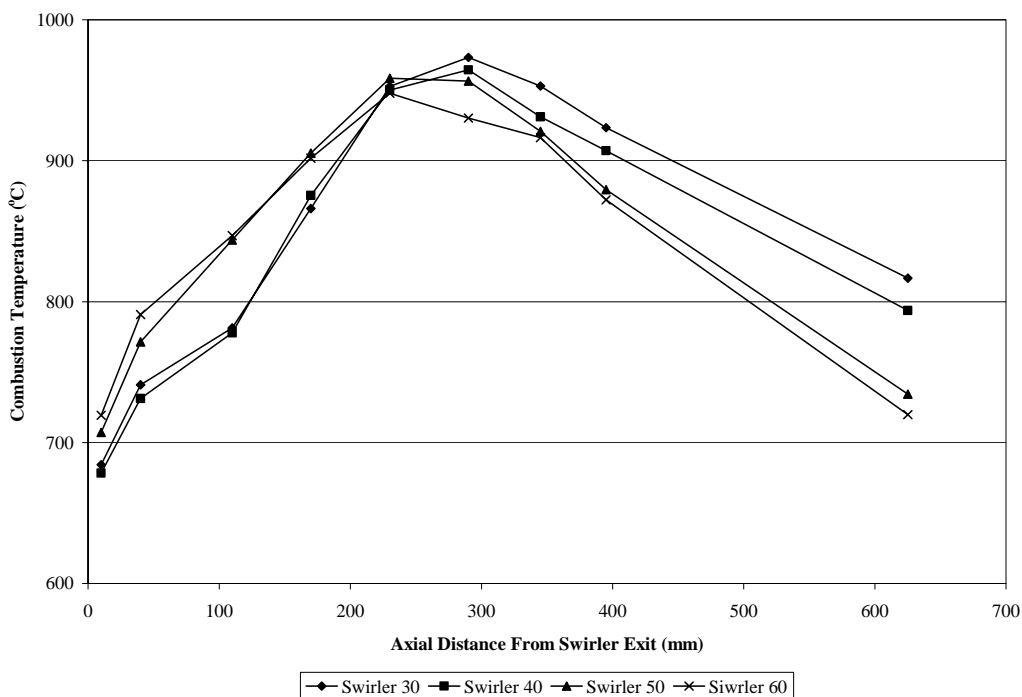
Figure 6.49 shows combustion temperature as a functional of the axial distance from swirler exit. The figure shows relationship of combustion temperature between swirler vane angles of 30°, 40°, 50° and 60° using orifice plate of 30mm with downstream injection. Temperature of less than 1000^oC was exhibited in this figure for all swirler vane angles indicating that thermal NO mechanism for NO_x formation was prevented. Swirler vane angle of 30° produces highest temperature along the chamber. This is followed by swirler vane angles of 40° and 50° at the flame front. At the flame front, lowest temperature was exhibited by swirler vane angle of 60°. Meanwhile, swirler vane angle of 40° shows lowest temperature at the combustor exit. The highest temperature point for all swirler vane angles is shifted to the distance of about 350mm from the swirler exit using downstream injection configuration. The circumstances of these phenomena were explained in section 6.4.3. However, for swirler vane angles of 50° and 60°, highest temperature was exhibited at the distance of about 400mm from the swirler exit.

Meanwhile, from the flame observation, once again swirler vane angle of 60° produces better flame shape. Even though swirler vane angle of 30° produces longer flame, but this flame is shorter compared to that for upstream injection. A yellow flame was observed during experimental testing showing that the mixing of fuel and air was better compared to the setting with upstream injection. The flame from swirler vane angle of 50° shows better shape compared to flame with swirler vane angle of 40°. A yellow bluish flame was observed for swirler vane angles of 50° and 60°.

6.3.11 Temperature Profile for Various Swirlers Using Orifice Plate of 25mm with Downstream Injection at Equivalence Ratio of 0.803
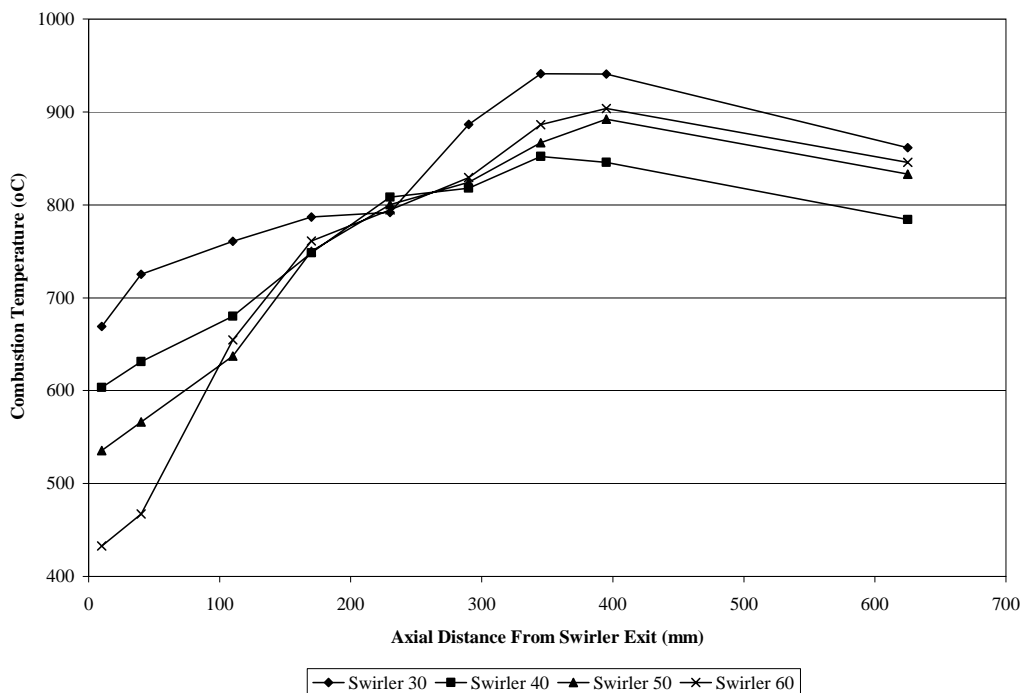

Figure 6.50: Combustion Temperature vs. Axial Distance from Swirler Exit for Various Swirler Using Orifice Plate of 25mm with Downstream Injection at Equivalence Ratio of 0.803

Figure 6.50 shows temperature profile for swirler vane angles of 30°, 40°, 50° and 60° using orifice plate of 25mm with downstream injection at equivalence ratio of 0.803. Temperature of about 400^oC was produced near the swirler exit for swirler vane angle of 60°. The temperature gradient is very steep for this setting where

within the next 200mm from the swirler exit, the temperature rises to 800$^\text{o}$C. The highest temperature is exhibited at distance of 345mm from the swirler exit which is 998.8$^\text{o}$C for swirler vane angle of 60$^\text{o}$. The lowest temperature at the combustor exit was produced by swirler vane angle of 30$^\text{o}$ which is 816.8$^\text{o}$C. However, the different is small between the highest and lowest temperature at this point that is 21.7$^\text{o}$C. Swirler vane angle of 30$^\text{o}$ produces lowest temperature along the combustion chamber except at the distance of about 350mm to 400mm from the swirler exit, where the temperature for this swirler is slightly higher than swirler vane angles of 40$^\text{o}$ and 50$^\text{o}$. Lowest temperature was shown by swirler vane angle of 40$^\text{o}$ at this distance.

Meanwhile, from the flame observation, swirler vane angle of 30$^\text{o}$ produces short and wide flame. However, a shorter flame was produced by other swirler vane angles in this setting. Swirler vane angle of 60$^\text{o}$ produces shortest and widest flame followed by swirler vane angles of 50$^\text{o}$ and 40$^\text{o}$. A bluish flame was observed during the experimental testing.

6.3.12 Temperature Profile for Various Swirlers Using Orifice Plate of 20mm with Downstream Injection at Equivalence Ratio of 0.803
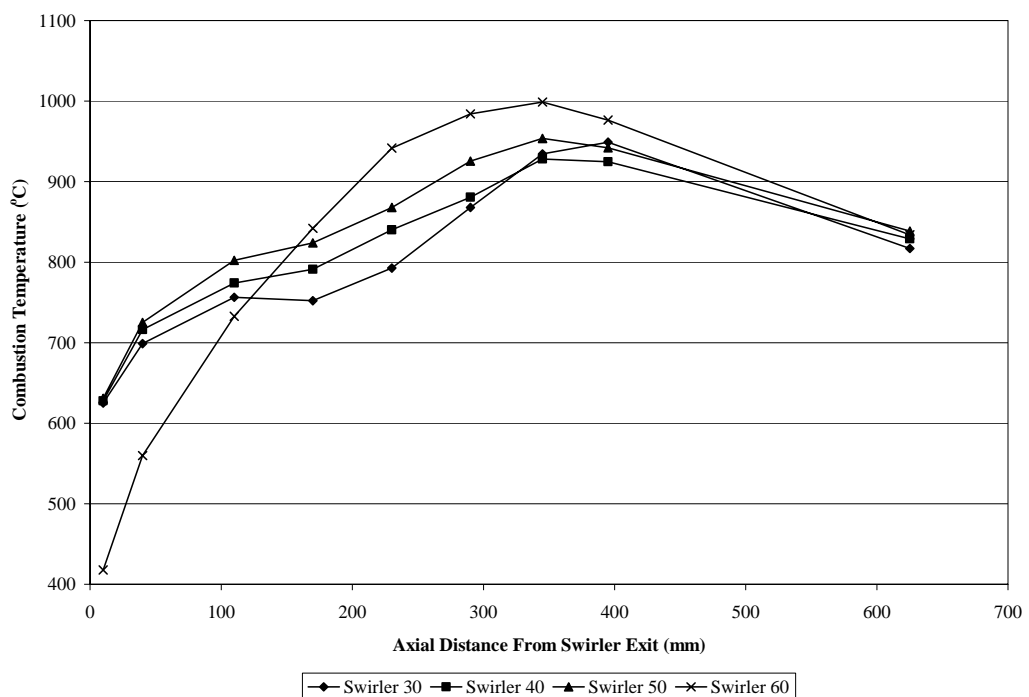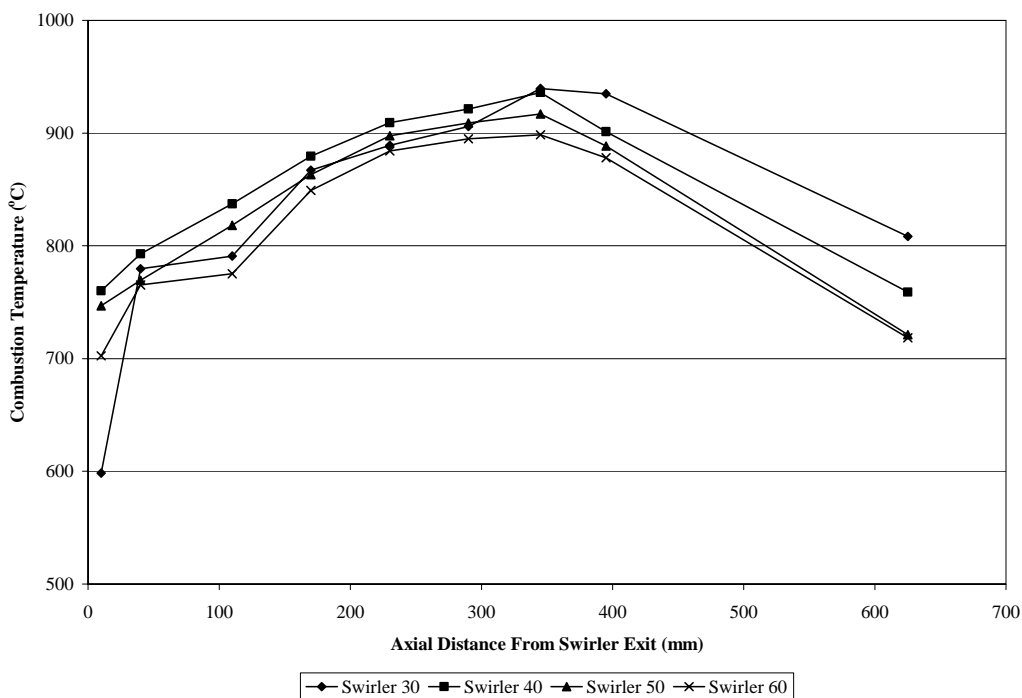

Figure 6.51: Combustion Temperature vs. Axial Distance from Swirler Exit for Various Swirler Using Orifice Plate of 20mm with Downstream Injection at Equivalence Ratio of 0.803

For this setting, swirler vane angle of 60° shows lowest combustion temperature along the combustion chamber except at the distance of 10mm from the swirler exit, where swirler vane angle of 30° produces lowest temperature. Producing lower temperature was good in term of preventing the risk of thermal NO_x formation. However, low temperature also could be because of less homogeneous mixing of fuel and air. However, in present situation, the lower temperature was caused by uniform distribution of air and fuel mixing which reduces the flame speed at highest temperature point. This is because less homogeneous mixing of air and fuel would generate high CO emission which is contradictory with these experimental results. At the flame front, swirler vane angle of 30° produces lower temperature compared to swirler vane angle of 50°. Meanwhile, swirler vane angle of 40° shows highest temperature at the flame front. About 300mm from the combustor exit, temperature for swirler vane angles of 30° and 40° shifted place where swirler vane angle of 30° produces highest temperature among all other swirler vane angles. Once again the

highest temperature for all swirler vane angles located at distance of 345mm from swirler exit.

Meanwhile, from the flame observation, swirler vane angle of 60° produces the shortest and widest flame. It could be concluded that, the flame for swirler vane angle of 60° using orifice plate of 20mm with downstream injection was the shortest and widest compared to all other settings. Swirler vane angle of 30° produces longer and narrower flame in this setting. However, the flame is much shorter compared to the other settings that were discussed before. The flame was also blue in colour indicating that the best fuel and air mixing was produced by swirler vane angle of 60° using orifice plate of 20mm with downstream injection. Swirler vane angle of 50° produces shorter and wider flame compared to swirler vane angle of 40°.

6.4   Discussion on Combustion Temperature Profile

As shown previously, combustion temperature was highest at the middle section of the combustion chamber. Generally for swirler vane angle of 30°, the highest temperature point exist further downstream of the combustion chamber compared to the other swirler vane angles for all setting. This is followed by swirler vane angles of 40°, 50° and 60°, respectively. The highest peak temperature for swirler vane angle of 60° was the nearest to the swirler exit. This shows that swirler vane angle of 60° produces shortest flame amongst all, meanwhile swirler vane angle of 30° produces longest flame amongst all. This is due to better mixing of fuel and air produced in higher swirler vane angle. Higher swirler vane angle generates bigger reverse flow zone and widen the flame angle which in turn reduce the flame length (Morcos, V.H. and Abdel-Rahim, Y.M., 1999). Besides that, swirler vane angle of 60° produces lowest discharge temperature compared to other swirler vane angles. This is followed by swirler vane angles of 50°, 40° and 30°. This shows that bigger swirler vane angles do reduce the overall flame temperature.

Orifice plate insertion does not show any significant different on the flame length even though smaller orifice plate exhibit shorter and wider flame due to bigger

swirler pressure drop at the swirler outlet phase which maximizes the swirler outlet shear layer turbulence (Escott, N.H., 1993). However, smaller orifice plate configuration did reduce the peak temperature of the flame. Even though this does not apply for all settings, it does apply for most of the settings. Orifice plate of 30mm with upstream injection exhibit high peak temperature exceeding 1000°C for all swirler vane angles except for swirler vane angle of 60° which produces highest peak temperature of 950.1^{o}C. Meanwhile, for upstream injection, other orifice plate configurations produce flame temperature of less than 1000°C for all swirler vane angles except for swirler vane angle of 60° with orifice plate of 25mm which shows highest peak temperature of 1010.5^{o}C. For downstream injection, all swirler vane angles with orifice plate of 20mm and 25mm produce flame temperature of less than 1000°C. Flame temperature of more than 1000°C was exhibited for swirler vane angle of 60° with orifice plate of 25mm and 30mm. Smaller orifice plates exhibit higher flame temperature compared to the bigger ones. This was aligned with Kim's (1995) suggestion. However, in upstream injection, orifice plate of 20mm shows lower temperature than orifice plate of 25mm.

Beside these two aspects, equivalence ratio does play the key role on the flame length characteristic. Even though the peak temperature was almost the same for all equivalence ratios for a particular setting, but fuel lean equivalence ratios produce shorter flame length. This could be because of more air is present in the chamber which completes the combustion earlier compared to fuel rich equivalence ratios. Fuel rich equivalence ratios produce longest flame length because more fuel and less air exist in the combustion chamber forces the flame to increase its length to complete its combustion outside the chamber. At fuel lean equivalence ratio below 0.8, the flame was short and narrow. The flame then gets wider with gradual increase in flame length with the increase of equivalence ratio. Once the flame reaches it peak temperature limit, further increase of equivalence ratio shows decrease of flame angle and rapid increase in flame length.

Besides that, downstream injection also shows shorter flame length compared to upstream injection. Downstream injection exhibit lower peak temperature compared to upstream injection. More complete combustion was exhibited with downstream injection rather than upstream injection as the flame produced was blue

in colour shows fuel was burned completely. Yellow and reddish flame as exhibited in upstream injection indicated that there are some fuel was left unburned. Wider flame was also exhibited with downstream injection. This might be because of downstream injection provides steeper boundary of velocity gradients and higher intensity turbulence between the forward flow and the reverse flow zone that promotes high entrainment rates and rapid mixing between the fuel and air.

However, all variation that has been studied does share the same factor to improve both fuel atomization process and mixing between fuel and air, causing intensive combustion with short flame.

6.5   Comparison on Varying Orifice Plate Diameter and Injection Position

Orifice plate of 20mm with downstream injection produces lowest emissions compared to the other settings. The NO_x emission was reduced about 17 percent for orifice plate of 20mm with upstream injection compared to orifice plate of 25mm with same injection position. Orifice plate of 30mm with upstream injection exhibit lower NO_x emission compared to orifice plate of 25mm with upstream injection at equivalence ratio of 0.803. However, this result does not reflect the overall comparison. NO_x emission was higher with orifice plate of 30mm compared to the orifice plate 25mm for all of the equivalence ratios except at equivalence ratios of 0.803 and 0.888. NO_x emission at equivalence ratio of 0.888 was the same for both orifice plates.

CO emission was reduced about 23 percent and 29 percent for orifice plates of 25mm and 20mm with upstream injection respectively compared to orifice plate of 30mm with upstream injection. The CO emission reduction of less than 10ppm was obtained between orifice plate of 25mm and 20mm with upstream injection.

Same pattern of emission results was shown in SO_2 emission where orifice plate of 30mm exhibits highest emission while orifice plate of 20mm exhibits lowest emission in upstream injection position. Orifice plate of 30mm with upstream

injection produces 71 ppm of SO_2 emission, which was reduced to 66 ppm when orifice plate of 25mm with upstream injection was used. The emission was further reduced about 24 percent when replaced with orifice plate of 20mm at the same injection point.

In downstream injection, NO_x emission was reduced about 24 percent for orifice plate of 25mm compared to orifice plate of 30mm. Meanwhile, NO_x emission reduction about 59 percent was achieved for orifice plate of 20mm compared to orifice plate of 30mm. Lowest NO_x emission was achieved by this setting that is 7 ppm.

CO emission also shows emission improvement when smaller orifice plate was used. CO emission of less than 100 ppm was obtained using orifice plates of 25mm and 20mm for both injection positions. CO emission decreased about 33 percent for orifice plate of 25mm with downstream injection compared to orifice plate of 30mm with downstream injection. Further decrease in orifice plate diameter to 20mm reduced CO emission to 66 ppm.

Meanwhile, SO_2 emission in downstream injection shows 2 ppm rise in emission for orifice plate of 25mm compared to orifice plate of 30mm at equivalence ratio of 0.803. This was apparent for all equivalence ratios. Further decrease in orifice plate diameter increases the SO_2 emission. In downstream injection, highest SO_2 emission was shown by orifice plate of 20mm that is 22 ppm.

Meanwhile from the point of injection position, for orifice plate of 30mm, CO emission and SO_2 emission show reduction in emission results while NO_x emission shows rise in emission results. When using orifice plate of 30mm, CO emission and SO_2 decrease about 16 percent and 89 percent respectively for downstream injection compared to upstream injection. The NO_x emission rise was 4 ppm for orifice plate of 30mm with downstream injection compared to orifice plate of 30mm with upstream injection. However, NO_x emission actually decreases for all other equivalence ratios for orifice plate of 30mm with downstream injection compared to orifice plate of 30mm with upstream injection except for equivalence ratio of 0.803.

NO_x emission was also reduced about 28 percent for orifice plate of 25mm with downstream injection compared to orifice plate of 25mm with upstream injection. The CO emission for this orifice plate was almost the same where upstream injection configuration shows CO emission of 90 ppm while downstream injection configuration shows higher 7 ppm at 97 ppm of CO emission. At equivalence ratios from 0.649 to 0.803, orifice plate of 25mm with upstream injection produces lower CO emission compared to orifice plate of 25mm with downstream injection. Meanwhile SO_2 emission dropped about 85 percent for orifice plate of 25mm with downstream injection compared to orifice plate of 25mm with upstream injection. The SO_2 emission different between these two settings was 56 ppm.

Downstream injection configuration shows lower NO_x emission compared to upstream injection configuration for orifice plate of 20mm. NO_x emission was reduced about 53 percent for orifice plate of 20mm with downstream injection compared to the upstream injection. CO emission was reduced to 66 ppm from 88 ppm, which is about 25 percent reduction for downstream injection compared to upstream injection for orifice plate of 20mm. Meanwhile, SO_2 emission was reduced about 56 percent for orifice plate of 20mm downstream injection compared to orifice plate of 20mm with upstream injection.

CHAPTER VII

CONCLUSION AND RECOMMENDATION
FOR FUTURE WORK

7.1   General Conclusions

Swirler could support combustion over a wide range of operating conditions through the generation of central recirculation zone that is formed when the vortex breakdown occur. Turbulence effect in the combustion chamber also could be generated by increasing the blockage or pressure drop of the swirler (Kim, M.N., 1995). Swirlers produce rapid fuel and air mixing which also creates turbulence effect in the combustion chamber. Swirling flow induces a highly turbulent recirculation zone which stabilizes the flame resulting in better mixing and combustion. Another effect of swirl is to decrease the velocity gradient at the exit of burner thus causing a faster decay of the velocities in the flow field with increase the swirl flow (Kim, M.N., 1995). Besides that, swirl reduces both flame lengths and flame attachment lengths and consequently shortens the combustion chamber length necessary for complete combustion. Swirl also promotes high combustion efficiency, easy ignition, reactant recirculation zone residence time, pollutant optimisation potential, widened stability and blow off (Escott, N.H. 1993). Besides that, recirculation vortex produced by swirl acts as a heat source forcing combustion product to move upstream and mix with the partially premixed reactant. This increases the amount of contact between fuel, air and hot combustion products.

Orifice plate, on the other hand, reduces the pressure at the swirler outlet phase, so that the swirler outlet shear layer turbulence was maximized to assist in mixing of fuel and air. Outlet orifice or swirler shroud also creates the flow pressure loss at the outlet plane rather than in the vane passage which maximizes the shear layer turbulence. Orifice plate insertion also increases the total pressure loss and thus for a specific orifice plate the airflow was reduced with decreasing orifice diameter. Smaller orifice sizes enhance better mixing due to improved upstream mixing. Beside that, orifice plate insertion helps to prevent fuel from entraining into the corner recirculation zone that will create local rich zone thus generates lower NO_x emission by eliminating locally rich region (Al-Kabie, H.S., 1989). Locally rich region tends to generate locally high NO_x emission that contributes to overall high NO_x emission. Smaller orifice plates outlet do increase the velocity of the air and fuel at the swirler shroud thus reduce the risk of flashback. However, this velocity should not be to high as lift off could occur and cause blow off of combustion. The increase in velocity also would increase the Reynolds number which increases the strength of turbulence effect and thus reduces the combustions residence time. Other than that, from the aerodynamic factor, air and fuel mixing rate increases as the pressure drop in the swirler outlet increases (Escott, N.H., 1993).

Meanwhile, proper injection positions assist in more complete combustion. Better mixing of fuel and air was enhanced in the downstream injection as the fuel, which enters the combustor, was in turbulence flow. Meanwhile in upstream injection, the fuel goes through a laminar flow before changing to turbulence flow. Downstream injection provide steeper boundary of velocity gradients and higher intensity turbulence between the forward flow and the reverse flow zone, that promotes high entrainment rates and rapid mixing between the fuel and air. Due to high entrainment and increased mixedness of the jets, flame length was reduced while increasing the diameter of the flame. This resulted in a more complete combustion (Escott, N.H., 1993).

7.2   Conclusion on Combustion Performance

From the results obtained, orifice plate of 20mm produced best emission results compared to orifice plates of 25mm and 30mm. This proved that orifice plate does help to create the swirler pressure loss at the swirler outlet so that the swirler outlet shear layer turbulence was maximized to assist in mixing of fuel and air. Smaller orifice plate produces better emission results compared to the larger one. Larger orifice plates produces higher local rich region near the fuel injector outlet, which in turn generate more emissions. Smaller orifice helps to prevent fuel from entraining into the corner recirculation zone that will create local rich zone (Kim, M. N., 1995). Small orifice plate size enhances better mixing than the larger ones due to improved upstream mixing. This once again could be attributed to good mixing resulted from the smaller area that generates higher turbulence due to increased swirling of the fuel and air mixture prior to combustion.

Besides the orifice plate effects, varying swirler vane angle also does helps in mixing the fuel and air thoroughly prior to ignition and hence reduces emissions. Swirler vane angle of 60° exhibit better emission results compared to other swirler vane angles. Increasing the swirler vane angles increases the swirl intensity that helps in promoting the mixing of fuel and air. Besides that, it also increases the reverse flow of hot burned gases back into the burner. The high temperature of this product serves as an energy source for preheating and ignition assistance for the incoming fresh combustible mixture (Al-Kabie, H.S., 1989). The process goes into a cycle and this keep the flame from extinguishing or having to ignite continuously. Varying swirler vane angle does vary its swirl strength which was expressed in terms of swirl number. One way of increasing the swirl number is by increasing the vane angle of the swirler. Increasing swirler vane angle from 30° to 60° would increase the swirl number from 0.706 to 2.534 hence increases the swirl intensity of the flow which increases the recirculation zone length and diameter. Longer recirculation zone provides flame stability and reduction in emissions. Yet, once the recirculation zone achieved a certain length, further increased in swirl number will not have much effect on the length of recirculation zone. At this point it is considered that the central recirculation zone has been well established. However, most of the plotted

graphs do agree with Alkabie's (1989) view stating that there is no significant effect on NO_x emissions by varying the vane angle from 20° to 60°.

Swirl has several important effects on combustion system. Swirler increases the blockage or pressure drop in the combustion chamber. This pressure drop generates turbulence, which supply rapid fuel and air mixing to promote the mixing. Turbulence energy is created from pressure energy dissipated downstream of the stabilizer. The most important effect of swirl in combustion process is that it improves flame stability and extends flammability limit. From the results, higher pressure drop was created by swirler vane angle of 60° which gives most stable flame. This is followed by swirler vane angles of 50°, 40° and 30°. Swirler vane angle of 30° has bigger vane opening which reduces its swirl velocity. Low swirl velocity generates less swirler pressure drop in the chamber (Kim, M.N., 1995).

When air is tangentially introduced into the combustion chamber, it is forced to change its path, which contributes to the formation of swirling flow. Low pressure in the core centre of the swirling flow is retrieving the jet flow in the combustion chamber and thus, produces the not-so-good slope of axial pressure. Meanwhile at the optimum swirler angle, the swirl finds its own direction and as a result, swirl vortex is formed (Nazri, 1997).

The downstream injection shows better emissions results compared to the upstream injection. This is because better mixing of fuel and air was enhanced in the downstream injection as the fuel, which enters the combustor, were in turbulence flow. Meanwhile in upstream injection, the fuel goes through a laminar flow before changing to turbulence flow. Downstream injection provide steeper boundary of velocity gradients and higher intensity turbulence between the forward flow and the reverse flow zone that promotes high entrainment rates and rapid mixing between the fuel and air. Due to high entrainment and increased homogeneous mixing of the jets, flame length was reduced while increasing the diameter of the flame. This resulted in a more complete combustion.

In low fuel lean region, the content of carbon monoxide emission decreases with the increase of equivalence ratio meanwhile the NO_x emission rise with the

increase of equivalence ratio. This was anticipated due to the fact that any measure of decreasing NO_x will tend to increase CO since both emissions were on the different side of the balance.

As for conclusion, swirler vane angle of 60° using orifice plate of 20mm with downstream injection produces the lowest emissions results compared to other settings in this project. Meanwhile, swirler vane angle of 30° using orifice plate of 30mm with upstream injection produces the highest emission results. Higher swirler vane angles with smaller orifice plate configurations show lower emission results. Meanwhile the downstream injection produces lower emission compared to the upstream injection setting.

7.3   Conclusions on Emission Results

Even though three pollutants i.e. NO_x, CO and SO_2 were studied in this project, NO_x emission was the main pollutant that needs to be reduced. CO emission could be minimized by homogeneous mixing of the fuel and air.

The relation between the combustion performance to the swirlers, orifice plates and injection positions has been studied in the present work. All other operating parameters were kept constant such as fuel pressure, swirling air pressure, injection air pressure, injection air flow rate and fuel flow rate. Only swirling air flow rate was varied.

Even though NO_x emission shown by swirler vane angle of 30° using orifice plate of 30mm with upstream injection was low at equivalence ratio of 0.803, for overall, this swirler vane angle produces highest emissions compared to the other setting in the present work. Highest NO_x emissions shown by this setting is 61 ppm at equivalence ratio of 0.603. Lowest NO_x emission was shown by swirler vane angle of 60° using orifice plate of 20mm with downstream injection. As mentioned earlier, higher swirler vane angle with smaller orifice plate size exhibit better emission

results. Meanwhile downstream injection produces lower emission results compared to upstream injection.

7.4 Conclusions on Temperature Profiles

The base emissions formation in the present work is Prompt NO. Thermal NO was prevented as the combustion temperature is below $1300^{o}C$. Fuel NO formation is also prevented as the fuel used in this study is not nitrogen bound fuel.

Higher swirler vane angles with smaller orifice plates produce shorter and wider flame. Higher swirler vane angle with smaller orifice plate reduces flame length that is necessary for complete combustion and generates bigger reverse flow zone which widen the flame diameter (Morcos, V.H. and Abdel-Rahim, Y.M., 1999). Meanwhile smaller orifice, due to improved upstream injection and maximized shear layer turbulence, widen the flame diameter. Wider flame was also exhibited with downstream injection. This is because downstream injection provides steeper boundary of velocity gradients and higher intensity turbulence between the forward flow and the reverse flow zone that promotes high entrainment rates and rapid mixing between the fuel and air. Upstream injection configuration produces yellowish flames indicating that there is some fuel left unburned and incomplete combustion. Meanwhile downstream injection configuration produces bluish flames indicating more complete combustion occur in this phase. The highest temperature point or peak temperature occurs further downstream of combustion chamber for orifice plate of 30° compared to other swirler vane angles. Peak temperature for swirler vane angle of 60° was the nearest to swirler outlet. Smaller orifice plate also does reduce the peak temperature thus reduce the NO_x emission. NO_x emission increases parallel with temperature rise.

7.5   Recommendation for Future Work

The present work shows higher swirler vane angle produces better emission results. However, past researchers do agree that there is an optimum swirler vane setting where further increase in swirler vane angle increases the emissions. More swirler vane angles should be studied to investigate this optimum setting such as 70° and 80°. Besides that, more precise swirler vane angle degree should take into consideration. Rather than studies between swirler angle of 50° and 60°, swirler vane angles of 51°, 52°, 58°, 59° should also be considered to produce optimum swirler vane setting. Besides that, varying the swirler vane depth would also provide some extra advantages on emission reduction.

Meanwhile, from the injection mode, present work employs a single 1mm hole. Smaller diameter holes should also be considered to produce smaller fuel droplet and atomization of fuel could easily be established. Besides that, comparison between single and multiple injector holes could also be studied. Wall injection and vane passage injection may also be considered in the future work.

The measurement of local velocity profiles and the turbulent intensities of the combustor flow field especially that near the swirler outlet will add crucial information to the present experimental and theoretical results.

REFERENCES

Ahmad, N.T., Andrews, G.E., Kowkabi, M. and Sharif, S.F. (1986). *International Journal Turbo and Jet Engines*, 3, pp. 319-329.

Al-kabie, H.S., Andrews, G.E. & Ahmad, N.T. (1988). Lean Low NO_x Primary Zones using Radial Swirlers. *ASME*. 88-GT-245.

Al-Kabie, H.S. (1989). *Radial Swirlers for Low Emissions Gas Turbine Combustion*. University of Leeds, Dept. of Fuel & Energy: PhD.

Aurther H. Lefebvre. (1983). *Gas Turbine Combustion*. Hemisphere Publishing Corporation.

Beer,J.M. and N.A. Chigier. (1972). *Combustion Aerodynamics*. Applied Science Publishers Ltd.

Blas, Luis Javier Molero de. (1998). *Pollution Formation and Interaction in the Combustion of Heavy Liquids Fuels.* University of London, England. PhD.

Blazowski, W.S. and Walsh, D.E. (1975). *Catalytic* Combustion: An Important Consideration for Future Applications. *Combustion Science Technologies*. Vol. 10. pp. 233-244.

Chervinskey, A. and Manheimertiment, Y. (1968). Effect of Swirl on Flame Stabilization. *Israel Journal of Technology*. Vol. 6. No. 2. pp 25-31.

Claypole, T.C., and Syred, N. (1981). The Effect of Swirl Burner Aerodynamics on NO_x Formation. *Eighteenth Symposium (International) on Combustion*, pp.81-89.

Clements, T.R. (1976). *Effects of Swirling Flow on Augmentor Performance, Phase 1 and 2*, NASA-CR-135024.

Collete, R.J. (1985). *Update* on NO_x Emission Control Technology at Combustion Engineering. *Joint Symposium on Stationery Combustion NO_x Control.* EPRI.

Cremer, M.A., Adams, B.R., Boll, D.E. and O'Connor, D.C. (2002). Demonstration of Rich Reagent Injection for NO_x Control in AmerenUE's Sioux Unit 1. *Reaction Engineering International.* Salt Lake City.

Crutzen, P. J. (1970). The Influence of Nitrogen Oxides on the Atmospheric Ozone Content. *Quarterly Journal of the Royal Meteorological Society*. Vol. 96. pp. 320-325.

Escott, N.H. (1993). *Ultra Low NO$_x$ Gas Turbine Combustion Chamber Design*. University of Leeds, Dept. of Fuel & Energy: PhD.

Fenimore, C.P. (1970). Formation of Nitric Oxide in Premixed Hydrocarbon Flames. *13th Symposium (International) on Combustion*. The Combustion Institute. Pittsburgh. Pp. 373-380.

Flagan, R.C. & Seinfeld, J.H. (1988). *Fundamental of Air Pollution Engineering*. Prentice Hall.

Fricker, N. & Leuckel, W. (1976). The characteristic of Swirl Stabilized Natural Gas Flames Part 3 ; The effect of Swirl and Burner Mouth Geometry on Flame Stability. *Journal of the Institute of Fuel*. pp 152-158.

Goddard, P.R. (1996). *Reburning*. University of Leeds, Dept. of Fuel & Energy: PhD.

Hoe, Y.M. (2000). *Fuel Injection Design and Development for a Combustor*. Universiti Teknologi Malaysia. B. Eng.

Jamieson, J.B. (1990). Twenty-first Century Aero Engine Design: The Enviromental Factor. *Proc. Inst. Mech. Engrs*. Vol. 204. pp. 119-134.

Jeffs, E. (1992). Gas Turbine Show: ASME Stresses Low Emissions and High Efficiency. *Turbomachinery International*.

Kaiman Lee. (1973). *Air Pollution: Its Effect on The Urban Man And His Adaptive Strategies*. Bolton. Environmental Design and Research Centre.

Kim, M.N. (1995). *Design Of Low NOx Gas Turbine Combustion Chamber*. University Of Leeds, Dept. of Fuel & Energy: PhD.

Krill, W.V., Kesselring, J.P. and Chu, E.K. (1979). Catalytic Combustion for Gas Turbine Applications. *ASME paper 70-GT-188: Gas Turbine Conference Exhibit and Solar Energy Conference*. San Diego.

Leuckel, W. (1967). Swirl Intensities, Swirl Types and Energy losses of Different Swirl Generating Devices. *IFRF Document*. No. GO2/a/16

Leonard, G. and Stegmaier, J. (1993). Development of an Aeroderivative Gas Turbine Dry Low Emissions Combustion System. *ASME Paper 93-GT-288*.

Lyon, R.K. (1975). U.S. Patent No. 390000554.

Masataka Arai. (2000). Flue Gas Recirculation for Low NO$_x$ Combustion System. *2000 International Joint Power Generation Conference*. Florida.

McLaughlin, B.R., Jones Jr., E.A. and Lewis, E.C. (1997). Selective Catalyst Reduction (SCR) Retrofit at San Diego Gas and Electric Company South Bay

Generation Station. *EPRI-DOE-EPA Combined Utility Air Pollution Control Symposium.* Washington.

Mellor, A. M., Anderson, R, D., Altenkirch, R. A. and Tuttle, J. H. (1972). Emissions From and Within an Allison J-33 Combustor. *Combustion Science Technology*. Vol. 6. pp. 169-176.

Mellor, A.M. (1990). *Design of Modern Turbine Combustor*. Nashville, USA. Academic Press Limited.

Mestre, A. (1974). Efficiency and Pollutant Formation Studies in a Swirling Flow Combustor*, The American Society of Mech.Engineers*, New York.

Mikus, T. and Heywood, S.B. (1971). The Automotive Gas Turbine and Nitric Oxide Emissions. *Combustion Science Technology*. Vol 24. pp. 149-158.

Mohammad Nazri. (1997). Emissions from Gas Burners, Their Impact on the Environment and Abatement Techniques. *Jurnal Mekanikal*. Jilid I. pp. 50-70.

Morcos, V.H. and Abdel-Rahim, Y.M. (1999). Parametric Study of Flame Length in Straight and Swirl Light Fuel oil Burners. *Journal of the Institute of Fuel*. Pp. 979-985.

Ralph D. Bent & James L. Mckinlay. (1985). *Aircraft Power Plants 5th Edition*. McGraw Hill Book Company.

Sothern, A. (1979). *Emission from Gas Turbine Lecture prepared for a short course on Emission from Combustion Processes*. Leeds. University of Leeds.

Syred, N. and Dahman, K.R. (1965). Effect on High Confinement upon the Aerodynamics of Swirl Burners. *Journal of Energy*. pp 111-127

Syred, N. and Beer, J.M. (1974). Combustion in Swirling Flows: A Review. *Combustion and Flame*. Vol. 23. pp. 143-201.

Treager, I.E. (1995). *Aircraft Gas Turbine Engine Technology*. 3rd Ed. Glencoe McGraw-Hill, Inc.

Willis, J.D., Toon, I.J., Schweiger, T. and Owen, D.A. (1993). Industrial RB211 Dry Low Emission Combustion. *ASME Paper 93-GT-391*.

Wu, H. L. and Fricker, N. (1976). The Characteristic of Swirl Stabilized Natural Gas Flames Part 2; The Behaviour of Swirling Jet Flames in a Narrow Cylindrical Furnace. *Journal of the Institute of Fuel*. pp. 144-151.

Appendix A

Relative Merits of Various Types of Fuel Injectors (Mellor, A.M., 1990)

Type	Description	Advantages	Drawbacks	Application
Pressure Atomizer	Plain Orifice	1. Simple, cheap 2. Rugged	1. Narrow spray angle 2. Solid spray cone	Afterburners, torch igniters
	Simplex	1. Simple, cheap 2. Wide spray angle	1. Needs high fuel pump pressure 2. Excessive soot formation at high combustion pressure 3. Fuel distribution and exit pattern varies with fuel flow rate	Engines of low fuel flow range
	Duplex	1. Simple, cheap 2. Wide spray angle 3. Good atomisation over wide range of fuel flows	1. Needs high fuel pump pressure 2. Excessive soot formation at high combustion pressure 3. Fuel distribution and exit pattern varies with fuel flow rate	Engines of low to medium pressure ratio

Appendix A

Relative Merits of Various Types of Fuel Injectors (Cont'd)

Type	Advantages	Disadvantages	Applications
Dual Orifice	1. Good atomisation over wide range of fuel flows 2. Wide burning range 3. Mechanically robust 4. Easily modified to facilitate combustor development	1. Needs high fuel pump pressure 2. Excessive soot formation at high combustion pressure 3. Fuel distribution and exit pattern varies with fuel flow rate 4. Complex 5. High manufacturing cost 6. Susceptibility of small passages to blockage by contamination and fuel gumming	Wide range of aircraft and industrial gas turbines; cannot be used on high pressure ratio engines owing to excessive exhaust smoke
Spill Return	1. Simple construction 2. Large holes and flow passage obviate risk of blockage	1. Spray angle varies with fuel flow rate 2. Fuel pump power requirement can be excessive	Good potential application for "dirty" fuels and fuels of low thermal stability
Slinger System	1. Simplicity 2. Low cost	1. Atomisation relatively poor at high altitude relight condition	Small engines of low compression ratio
Rotary Atomizer			

Appendix A
Relative Merits of Various Types of Fuel Injectors (Cont'd)

Type	Advantages	Disadvantages	Applications
	3. Needs only low pressure fuel pump	2. Slow response to changes in fuel flow rate	
Plain-jet Airblast	1. Simple, cheap 2. Low susceptibility to blockage 3. Operates satisfactorily with low fuel pressure	1. Narrow spray angle 2. Atomising performance inferior to perfilming airblast	Few
Perfilming Airblast	1. Operates satisfactorily with low fuel pressure 2. Low soot formation 3. Exit pattern factor fairly insensitive to changes in fuel flow rate 4. Mechanically robust 5. Atomizing performance is superior to all forms of pressure atomizer, specially at high combustion Pressure	1. Narrow burning range 2. Atomizing quality is low for low combustor velocities, such as occur at start up	Wide range of modern high performance, high pressure ratio engines
Twin Fluid Atomizer			

Appendix A

Relative Merits of Various Types of Fuel Injectors (Cont'd)

Piloted or Hybrid	1. Operates satisfactorily with low fuel pressure and mechanically robust 2. Low soot formation 3. Exit pattern factor fairly insensitive to changes in fuel flow rate 4. Atomizing performance is superior to all forms of pressure atomizer, specially at high combustion pressure 5. Easy engine start up 6. Wide burning range	1. Need pilot nozzle	General application to all types of engines
Air Assist	1. Good atomisation	1. Needs external source of high pressure air or steam	Industrial engine

Appendix A

Relative Merits of Various Types of Fuel Injectors (Cont'd)

		Advantages	Disadvantages	Applications
Vaporizer Atomizer	Conventional Vaporizer	1. Operates satisfactorily with low fuel pressure 2. Reduced soot formation due to premixing of fuel and air 3. Pattern factor fairly insensitively to fuel flow rate	1. Requires auxiliary fuel jet for starting 2. Difficult to develop 3. Mechanically suspect, especially at high pressure 4. Fairly narrow burning range 5. Unsuitable for heavy distillate fuels owing to coke deposition	Used on several early aircraft engines of medium pressure ratio
	Lean Premix Prevapourized	1. Very low NOx Emissions 2. No exhaust smoke 3. Very low flame radiation 4. Constant pattern factor	1. Susceptible to auto ignition, flashback and flame blow out 2. Requires sophisticated control system	All types of engines where ultra low pollutant emissions is prime requirement

Appendix B
Swirl Number Calculation (Leuckel Method)

Swirler	α (°)	No. of Vanes (n)	Thickness (s)	Swirler Outlet Area (r₁)	$2\pi r_1$	Cos α	ψ	1- ψ	Tan α	σ
R1	20.00	8.00	0.02	0.1610	1.0116	0.9397	0.1683147	0.8316853	0.3640	0.437666
R2	30.00	8.00	0.02	0.1610	1.0116	0.8660	0.1826389	0.8173611	0.5774	0.706420
R3	40.00	8.00	0.02	0.1610	1.0116	0.7660	0.2064821	0.7935179	0.8391	1.057443
R4	45.00	8.00	0.02	0.1610	1.0116	0.7071	0.2236816	0.7763184	1.0000	1.288131
R5	50.00	8.00	0.02	0.1610	1.0116	0.6428	0.2460568	0.7539432	1.1918	1.580756
R6	60.00	8.00	0.02	0.1610	1.0116	0.5000	0.3163306	0.6836694	1.7321	2.533534
R7	70.00	8.00	0.02	0.1610	1.0116	0.3420	0.4624716	0.5375284	2.7475	5.111358
R8	80.00	8.00	0.02	0.1610	1.0116	0.1736	0.9110903	0.0889097	5.6713	63.787218

Where,

$$\psi = \frac{n.s}{2\pi r_1 . \, Cos \, \alpha}$$

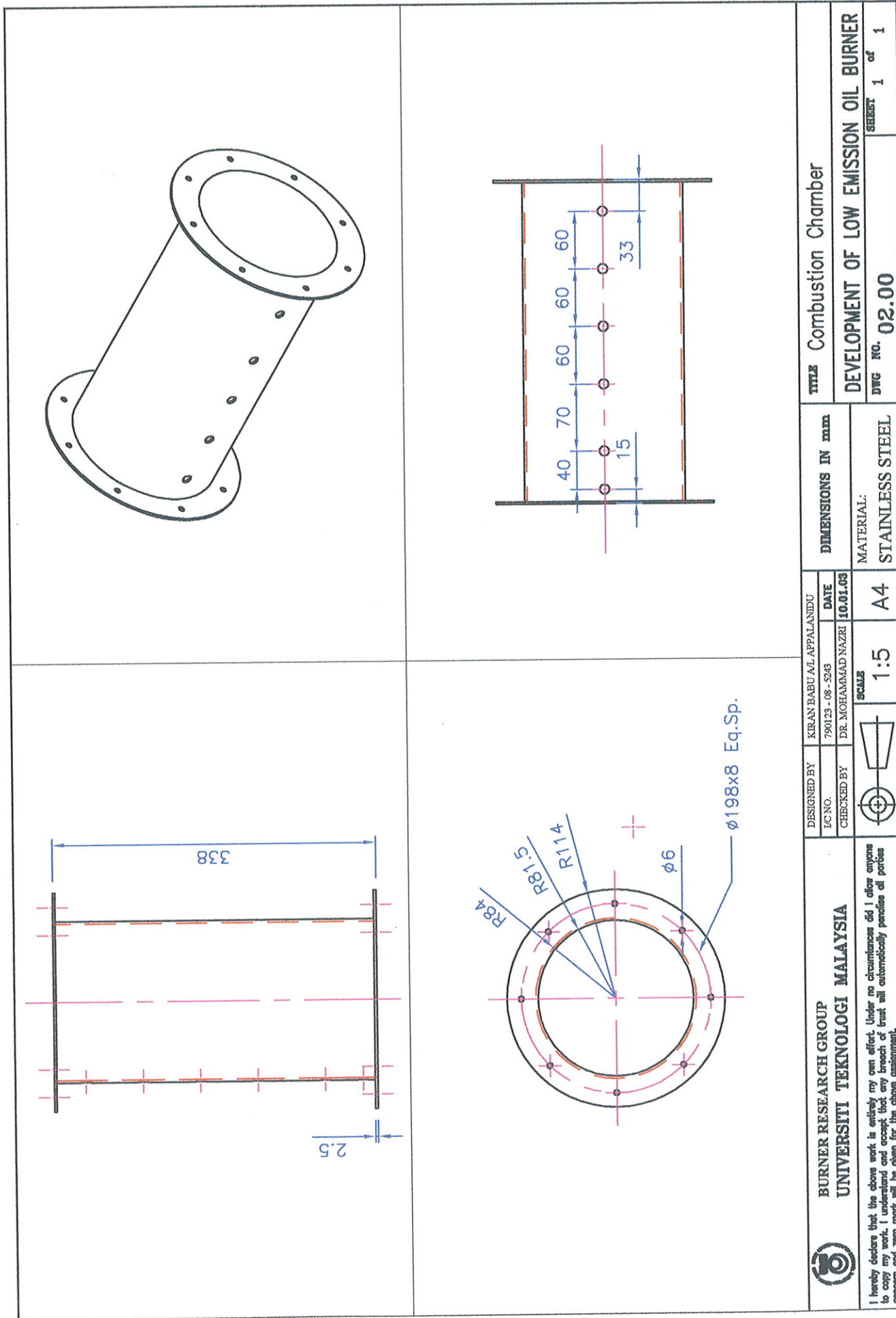$$\sigma = \frac{Tan \, \alpha}{1 - \psi}$$

Appendix C

Experimental Set Up Layout
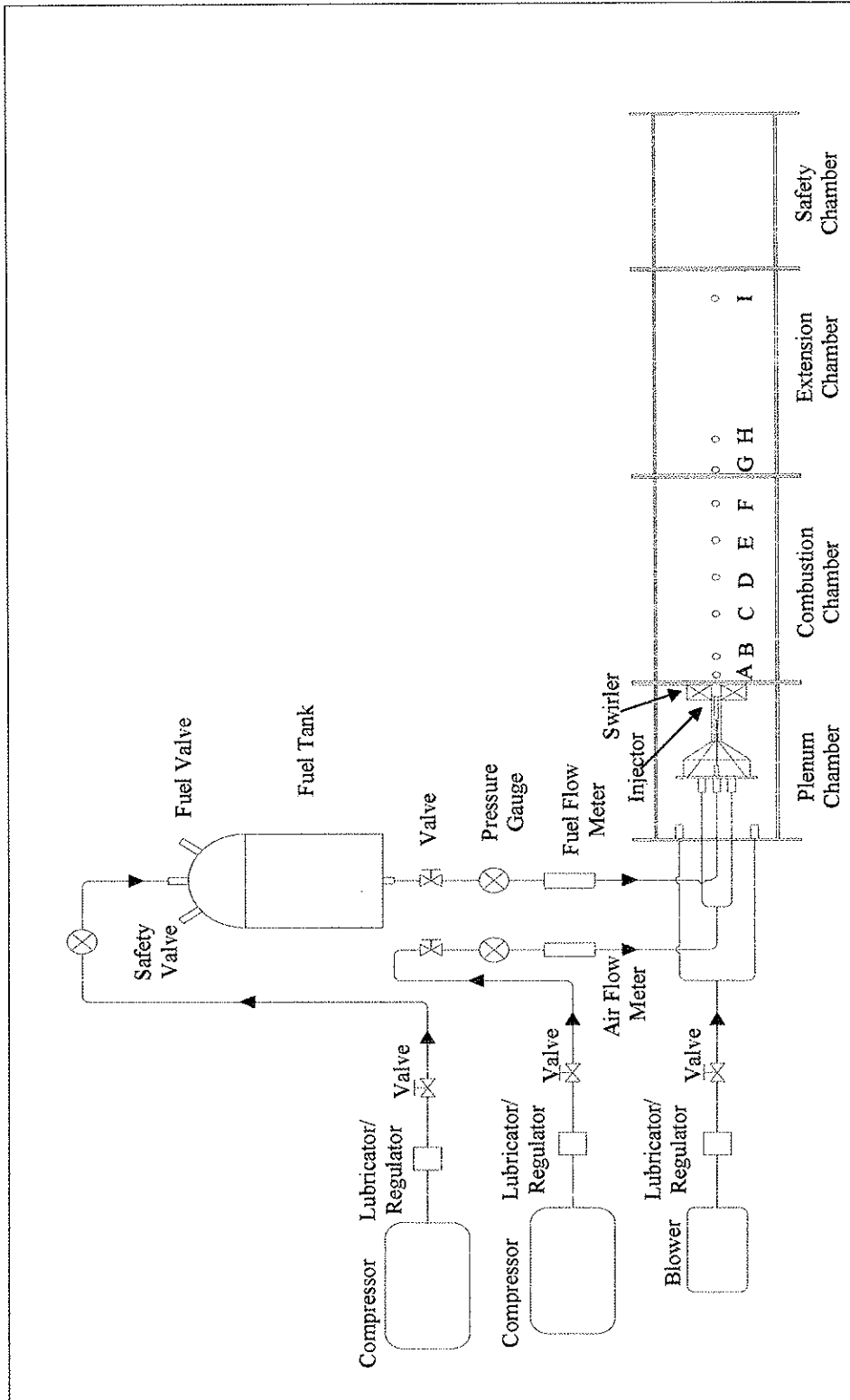
Appendix D

Plenum Chamber Design Drawing

2.5

255

72.5

R4.5

R84

R114

R81.5

Ø6×8 Eq.Sp.

198

BURNER RESEARCH GROUP
UNIVERSITI TEKNOLOGI MALAYSIA

DESIGNED BY KIRAN BABU A/L APPALANIDU
I/C NO. 790123 - 08 - 5243
CHECKED BY DR. MOHAMMAD NAZRI
DATE 10.01.08

SCALE 1:5

A4

DIMENSIONS IN mm

MATERIAL:
STAINLESS STEEL

TITLE Plenum Chamber

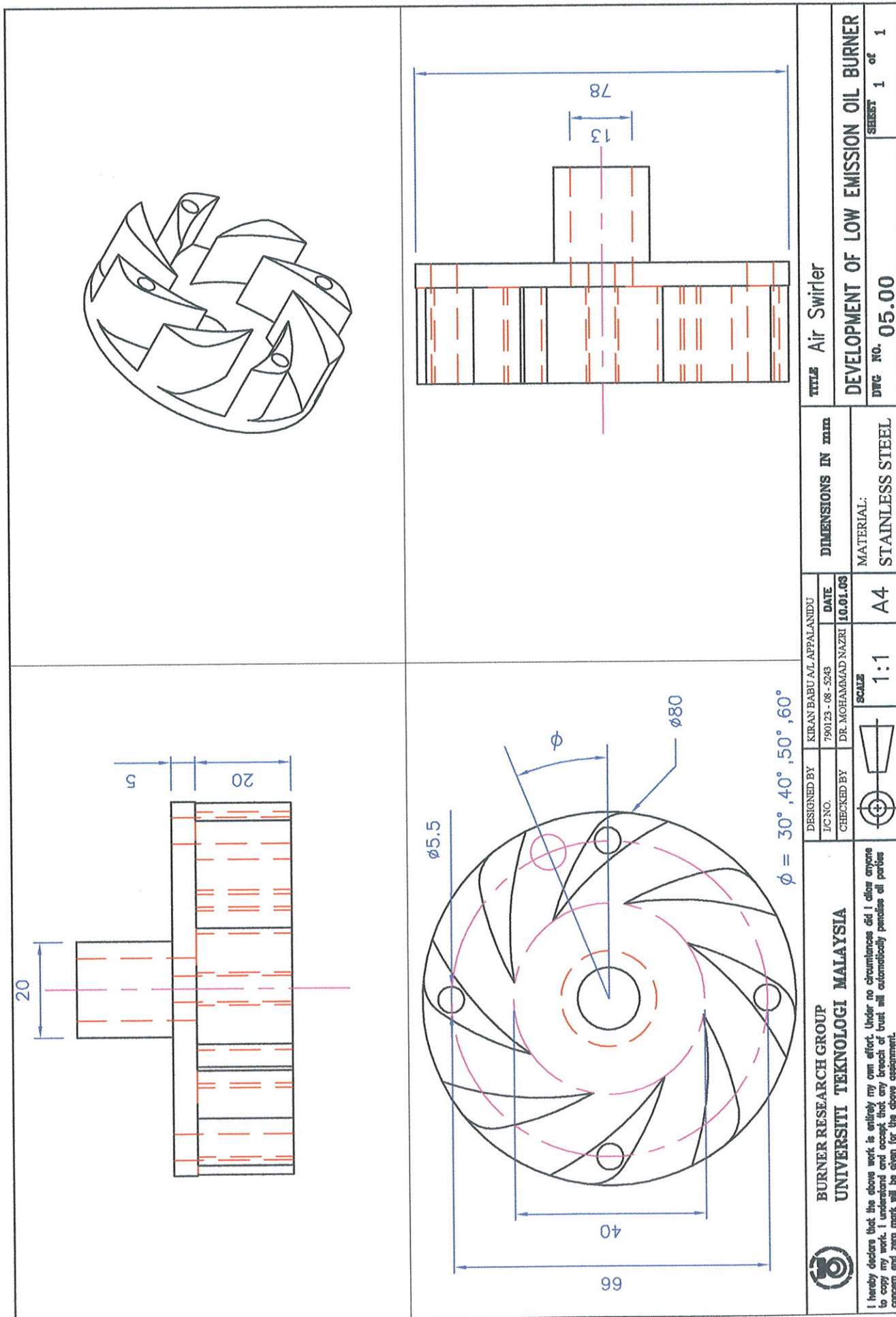DEVELOPMENT OF LOW EMISSION OIL BURNER
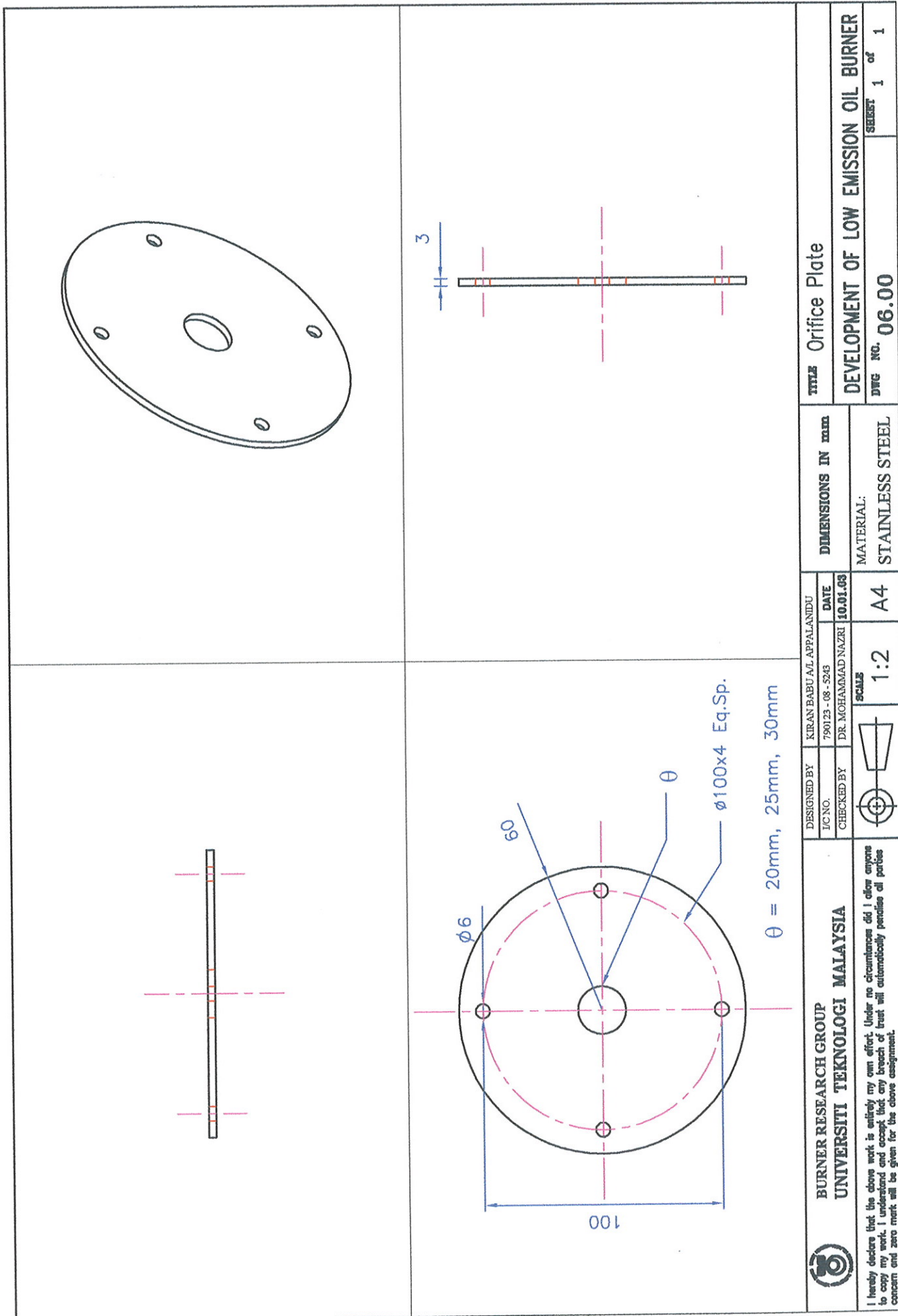
01.00

SHEET 1 of 1

I hereby declare that the above work is entirely my own effort. Under no circumstances did I allow anyone to copy my work. I understand and accept that any breach of trust will automatically penalise all parties concern and zero mark will be given for the above assignment.

Appendix E

Combustion Chamber Design Drawing

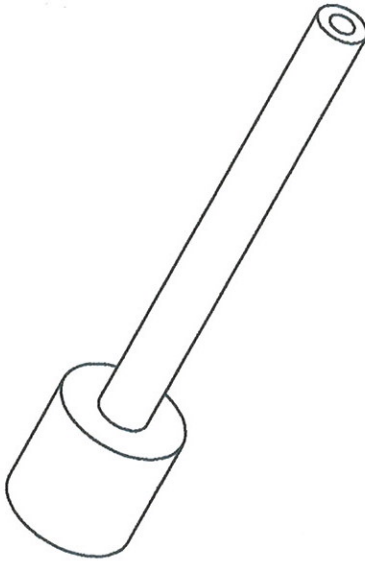|	
60 60	33
60 60	
70	15
40	

338

2.5

R84
R81.5
R114
ø6
ø198x8 Eq.Sp.

BURNER RESEARCH GROUP UNIVERSITI TEKNOLOGI MALAYSIA	DESIGNED BY	KIRAN BABU A/L APPALANIDU			TITLE Combustion Chamber
	I/C NO.	790123 - 08 - 5243			DEVELOPMENT OF LOW EMISSION OIL BURNER
	CHECKED BY	DR. MOHAMMAD NAZRI	DATE 10.01.03	DIMENSIONS IN mm	
	SCALE 1:5	A4	MATERIAL: STAINLESS STEEL		DWG NO. 02.00 SHEET 1 of 1

Appendix F

Extension Chamber Design Drawing

BURNER RESEARCH GROUP	**TITLE** Extension Chamber
UNIVERSITI TEKNOLOGI MALAYSIA	**DEVELOPMENT OF LOW EMISSION OIL BURNER**

DESIGNED BY: KIRAN BABU A/L APPALANIDU
I/C NO.: 790123 - 08 - 5243
CHECKED BY: DR. MOHAMMAD NAZRI — DATE 10.01.03

DIMENSIONS IN mm

MATERIAL: STAINLESS STEEL

SCALE 1:5

A4

DWG NO. 03.00

SHEET 1 of 1

I hereby declare that the above work is entirely my own effort. Under no circumstances did I allow anyone to copy my work. I understand and accept that any breach of trust will automatically penalise all parties concern and zero mark will be given for the above assignment.
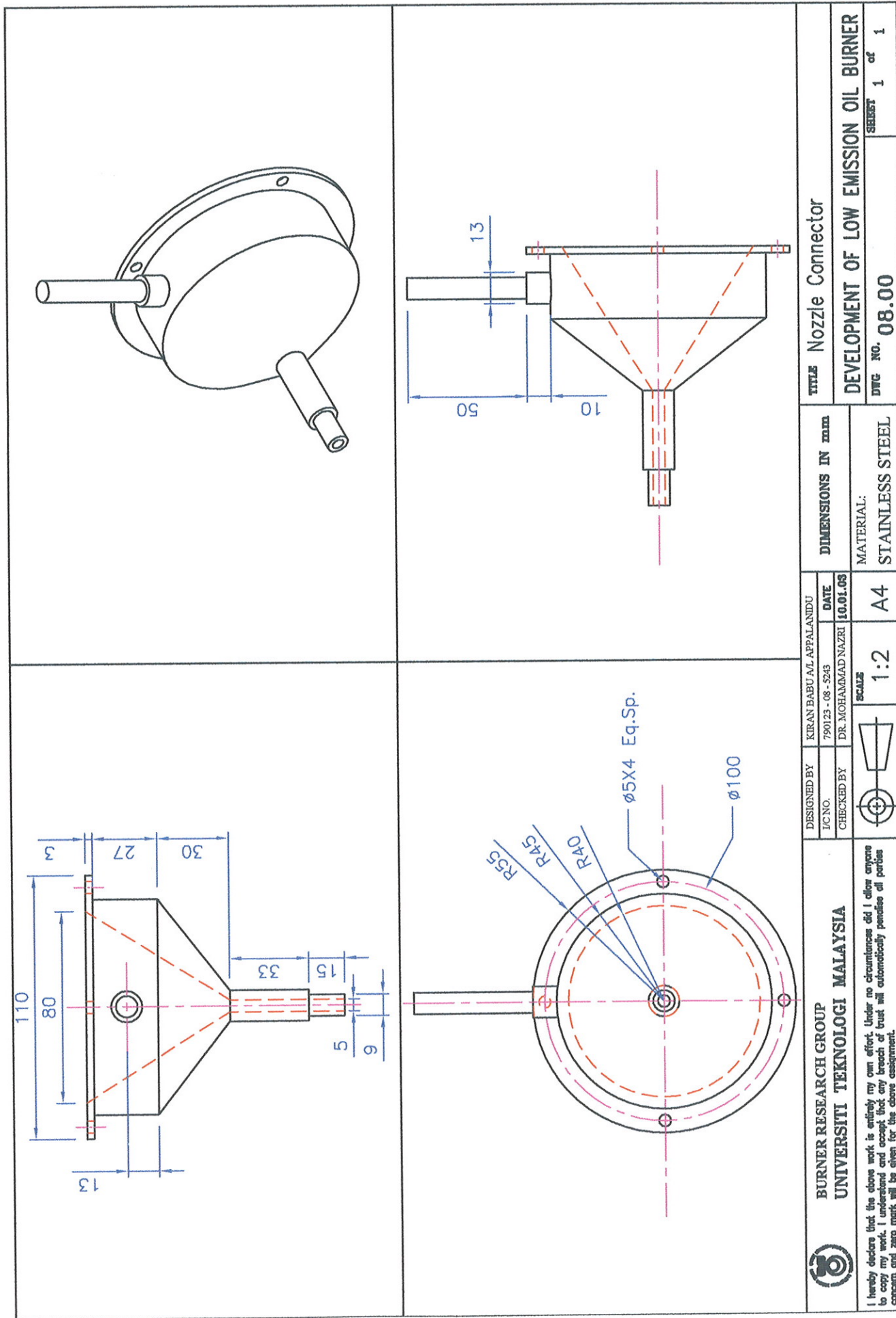
338

2.5

28

230

50

30

Ø198X8 Eq.Sp.

R81.5

R84

R114

Ø6

Appendix G

Safety Chamber Design Drawing

0.5		

255

Ø198x8 Eq.Sp.

R81.5
R114
R84
ø6

DESIGNED BY — KIRAN BABU AL. APPALANIDU
I/C NO. 790123-08-5243
CHECKED BY — DR. MOHAMMAD NAZRI
DATE 10.01.08

SCALE 1:5 A4

DIMENSIONS IN mm

MATERIAL: STAINLESS STEEL

TITLE Safety Chamber

DEVELOPMENT OF LOW EMISSION OIL BURNER

DWG NO. 04.00   SHEET 1 of 1

Appendix H

Swirler Design Drawing

78	13	
5	20	20
φ80	φ5.5	φ
40	66	

φ = 30°, 40°, 50°, 60°

TITLE Air Swirler

DEVELOPMENT OF LOW EMISSION OIL BURNER
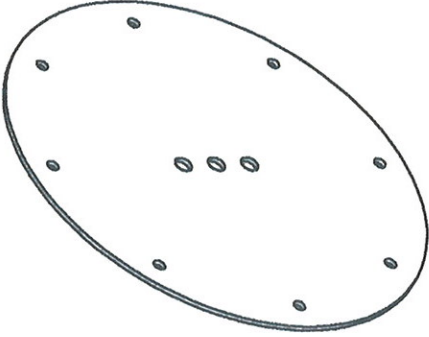
DWG NO. 05.00 SHEET 1 of 1

DIMENSIONS IN mm

MATERIAL: STAINLESS STEEL

DESIGNED BY KIRAN BABU A/L APPALANIDU
I/C NO. 790123-08-5243
CHECKED BY DR. MOHAMMAD NAZRI
DATE 10.01.08

SCALE 1:1 A4

BURNER RESEARCH GROUP
UNIVERSITI TEKNOLOGI MALAYSIA

Appendix I

Orifice Plate Design Drawing
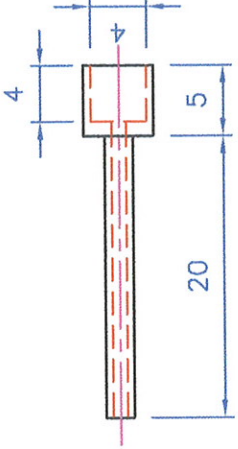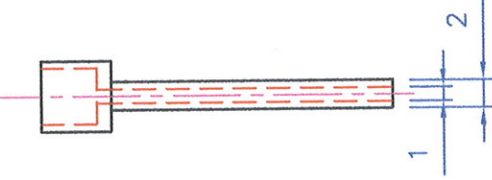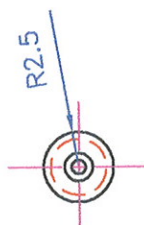
θ = 20mm, 25mm, 30mm

ø100x4 Eq.Sp.

60

ø6

θ

100

3

BURNER RESEARCH GROUP	DESIGNED BY	KIRAN BABU A/L APPALANIDU		TITLE Orifice Plate
UNIVERSITI TEKNOLOGI MALAYSIA	I/C NO.	790123-08-5243	DATE	DEVELOPMENT OF LOW EMISSION OIL BURNER
	CHECKED BY	DR. MOHAMMAD NAZRI	10.01.03	

DIMENSIONS IN mm

SCALE 1:2   A4   MATERIAL: STAINLESS STEEL

DWG NO. 06.00   SHEET 1 of 1

Appendix J

Fuel Nozzle Design Drawing
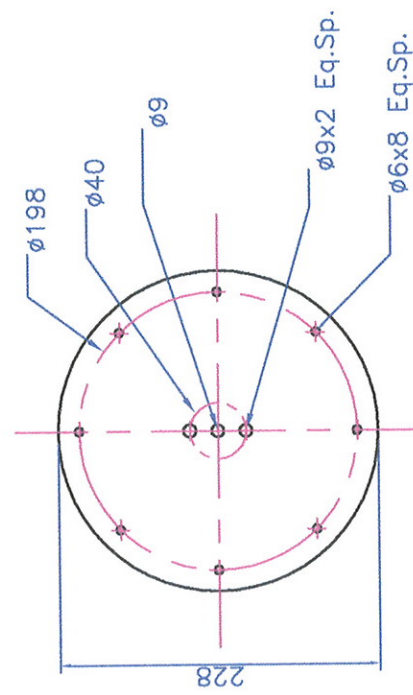
BURNER RESEARCH GROUP	DESIGNED BY	KIRAN BABU A/L APPALANIDU		TITLE Nozzle
UNIVERSITI TEKNOLOGI MALAYSIA	I/C NO.	790123-08-5243	DATE	DIMENSIONS IN mm
	CHECKED BY	DR. MOHAMMAD NAZRI	10.01.08	DEVELOPMENT OF LOW EMISSION OIL BURNER

SCALE 2:1 A4 MATERIAL: STAINLESS STEEL DWG NO. 07.00 SHEET 1 of 1

R2.5
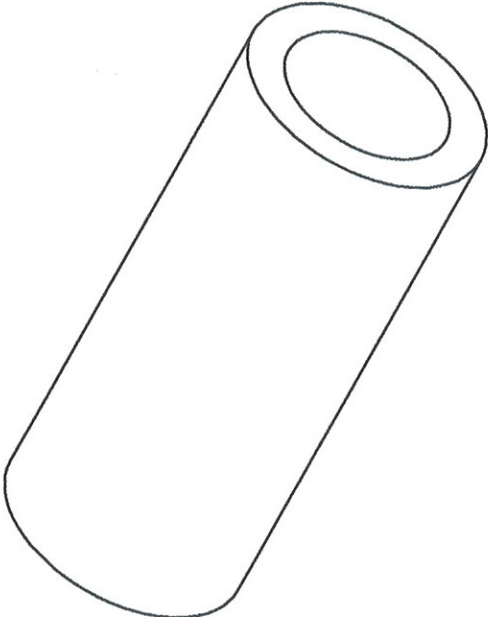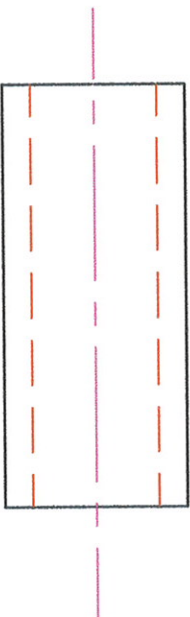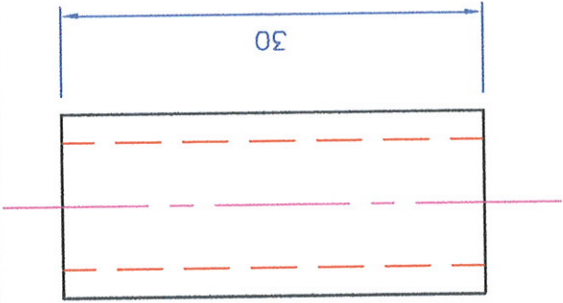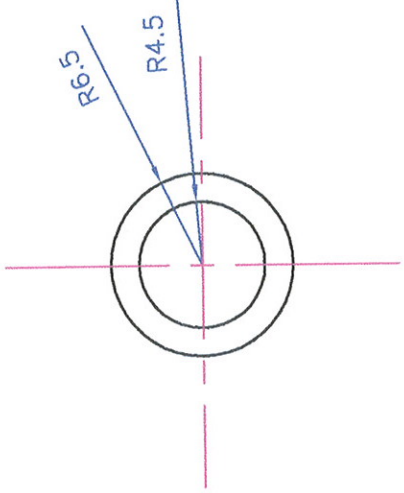
Appendix K

Nozzle Connector Design Drawing

Engineering drawing of Nozzle Connector.

Dimensions shown: 13, 50, 10 (side section view); 3, 27, 30, 33, 15, 5, 9, 110, 80, 13 (left section view); ø5X4 Eq.Sp., ø100, R55, R45, R40 (bottom view).

BURNER RESEARCH GROUP	DESIGNED BY: KIRAN BABU A/L APPALANIDU
UNIVERSITI TEKNOLOGI MALAYSIA	I/C NO. 790123 - 08 - 5243
	CHECKED BY: DR. MOHAMMAD NAZRI DATE 10.01.08

DIMENSIONS IN mm

MATERIAL: STAINLESS STEEL

SCALE 1:2   A4

TITLE: Nozzle Connector

DEVELOPMENT OF LOW EMISSION OIL BURNER

DWG NO. 08.00   SHEET 1 of 1

Appendix L

Fuel Air Nozzle Flange Design Drawing

ø198
ø40
ø9
ø9x2 Eq.Sp.
ø6x8 Eq.Sp.
228
2.5

DESIGNED BY	KIRAN BABU A/L APPALANIDU	DIMENSIONS IN mm	TITLE Fuel-Air Inlet Flange
I/C NO.	790123-08-5243		DEVELOPMENT OF LOW EMISSION OIL BURNER
CHECKED BY	DR. MOHAMMAD NAZRI	MATERIAL:	
	DATE 10.01.03	STAINLESS STEEL	DWG NO. 09.00 SHEET 1 of 1
SCALE 1:5	A4		

BURNER RESEARCH GROUP
UNIVERSITI TEKNOLOGI MALAYSIA

Appendix M

Downstream Injection Extension Design Drawing

BURNER RESEARCH GROUP	DESIGNED BY	KIRAN BABU A/L APPALANIDU		DIMENSIONS IN mm	TITLE Downstream Injection Extension
UNIVERSITI TEKNOLOGI MALAYSIA	I/C NO.	790123 - 08 - 5243	DATE		DEVELOPMENT OF LOW EMISSION OIL BURNER
	CHECKED BY	DR. MOHAMMAD NAZRI	10.01.03	MATERIAL:	DWG NO. 10.00

SCALE 2:1 | A4 | STAINLESS STEEL | SHEET 1 of 1

30

R6.5
R4.5

Appendix N

Swirler -Orifice Plate Attachment Flange Design Drawing

TITLE	Swirler–Orifice Attachment Flange
	DEVELOPMENT OF LOW EMISSION OIL BURNER
DWG NO.	11.00 SHEET 1 of 1

DIMENSIONS IN mm

MATERIAL: STAINLESS STEEL

A4

SCALE 1:5

DESIGNED BY KIRAN BABU A/L APPALANIDU
I/C NO. 790123 - 08 - 5243
CHECKED BY DR. MOHAMMAD NAZRI DATE 10.01.03

BURNER RESEARCH GROUP
UNIVERSITI TEKNOLOGI MALAYSIA

I hereby declare that the above work is entirely my own effort. Under no circumstances did I allow anyone to copy my work. I understand and accept that any breach of trust will automatically penalise all parties concern and zero mark will be given for the above assignment.

Appendix O
Burner Assembly Drawing

Item No. 5 : Used for Downstream Injection
Removed for Upstream Injection

NO	ITEM	MATERIAL	QTY
14	Safety Chamber	Stainless Steel	1
13	Extension Chamber	Stainless Steel	1
12	Thermocouple	Stainless Steel Insulated	9
11	Combustion Chamber	Stainless Steel	1
10	Orifice Plate	Mild Steel	3
9	Swirler-Orifice Attachment Flange	Mild Steel	1
8	Air Swirler	Mild Steel	4
7	Flange	Mild Steel	8
6	Plenum Chamber	Stainless Steel	1
5	Downstream Injection Extension	Mild Steel	1
4	Nozzle Connector	Mild Steel	1
3	Fuel Nozzle	Mild Steel	1
2	Fuel-Air Inlet to Nozzle Connector	Mild Steel	1
1	Fuel-Air Inlet Flange	Mild Steel	1

BURNER RESEARCH GROUP
UNIVERSITI TEKNOLOGI MALAYSIA

DESIGNED BY	KIRAN BABU A/L APPALANIDU		
I/C NO.	790123 - 08 - 5243	DATE	
CHECKED BY	DR. MOHAMMAD NAZRI	10.01.03	

| SCALE | | DIMENSIONS IN mm |
| N/A | A4 | |

MATERIAL:
STAINLESS STEEL

TITLE Combustor Assembly Drawing

DEVELOPMENT OF LOW EMISSION OIL BURNER

DWG NO. 12.00   SHEET 1 of 1

Appendix P

Calibration Chart of Fuel Flow Meter on Diesel Fuel

Graph of Measured Diesel Flow Rate vs Indicator Diesel Flow Rate
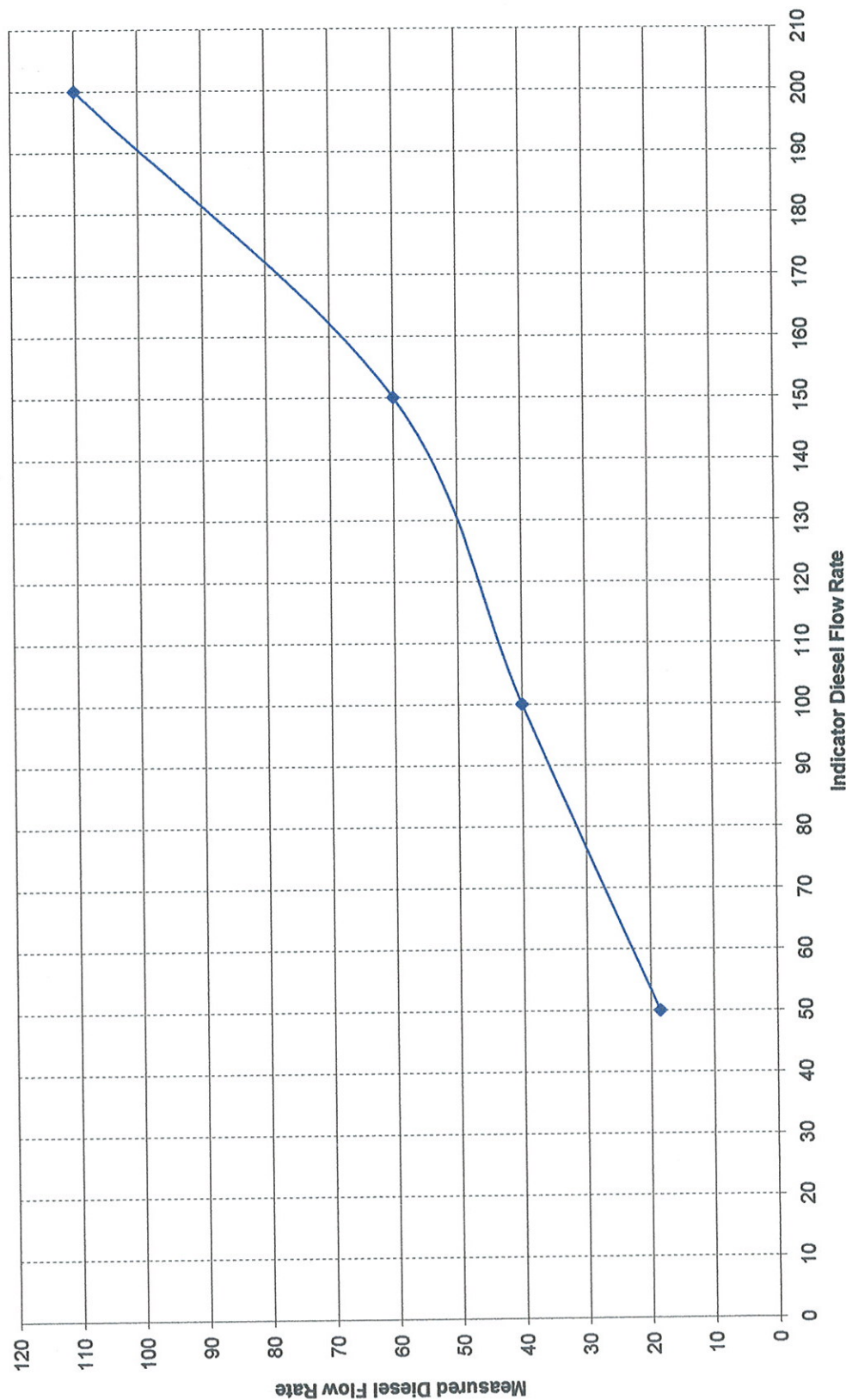
Appendix Q

Calibration Chart of Thermocouples

(Thermocouple Reading with Boiled Water)

Temperature of Boiled Water : 100°C

Channel	Reading 1	Reading 2	Reading 3	Average
1	99.5	99.4	99.7	99.533
2	99.5	99.5	99.5	99.500
3	99.6	99.5	99.5	99.533
4	99.5	99.4	99.5	99.467
5	99.5	99.5	99.5	99.500
6	99.5	99.5	99.4	99.467
7	99.4	99.5	99.6	99.500
8	99.5	99.5	99.4	99.467
9	99.5	99.5	99.5	99.500
10	99.5	99.5	99.5	99.500
11	99.4	99.5	99.4	99.433
12	99.5	99.4	99.5	99.467

(Thermocouple Reading with Ice Cubes)

Temperature of Ice Cubes : 0°C

Channel	Reading 1	Reading 2	Reading 3	Average
1	0.8	0.9	0.8	0.833
2	0.9	1.0	0.9	0.933
3	1.1	1.0	1.1	1.067
4	1.0	0.9	1.1	1.000
5	1.1	1.2	1.0	1.100
6	1.1	1.0	1.0	1.033
7	1.0	1.1	1.0	1.033
8	1.1	1.1	0.9	1.033
9	0.9	0.9	1.1	0.967
10	0.8	0.9	1.0	0.900
11	1.0	1.1	1.1	1.067
12	0.9	0.9	0.9	0.900

Appendix R

Equivalent Ratio Calculation of Fuel and Air

V_f (ml/min)	$Eq\ V_f$ (ml/min)	CFM	LPM Swirling	LPM Atomising air	V_a (LPM)	m_f (kg/s)	m_a (kg/s)	AFR (Stoi)	AFR (act)	FAR (stoi)	FAR (act)	EQR-FAR	Sequence
130	50.000	25	707.925	170	877.925	0.000675	0.017983	14.5	26.641	0.06897	0.03754	0.544	
130	50.000	24	679.608	170	849.608	0.000675	0.017403	14.5	25.782	0.06897	0.03879	0.562	1
130	50.000	23	651.291	170	821.291	0.000675	0.016823	14.5	24.923	0.06897	0.04012	0.582	
130	50.000	22	622.974	170	792.974	0.000675	0.016243	14.5	24.063	0.06897	0.04156	0.603	2
130	50.000	21	594.657	170	764.657	0.000675	0.015663	14.5	23.204	0.06897	0.04310	0.625	
130	50.000	20	566.34	170	736.340	0.000675	0.015083	14.5	22.345	0.06897	0.04475	0.649	3
130	50.000	19	538.023	170	708.023	0.000675	0.014503	14.5	21.485	0.06897	0.04654	0.675	
130	50.000	18	509.706	170	679.706	0.000675	0.013923	14.5	20.626	0.06897	0.04848	0.703	4
130	50.000	17	481.389	170	651.389	0.000675	0.013343	14.5	19.767	0.06897	0.05059	0.734	
130	50.000	16	453.072	170	623.072	0.000675	0.012763	14.5	18.908	0.06897	0.05289	0.767	
130	50.000	15	424.755	170	594.755	0.000675	0.012183	14.5	18.048	0.06897	0.05541	0.803	5
130	50.000	14	396.438	170	566.438	0.000675	0.011603	14.5	17.189	0.06897	0.05818	0.844	
130	50.000	13	368.121	170	538.121	0.000675	0.011023	14.5	16.330	0.06897	0.06124	0.888	6
130	50.000	12	339.804	170	509.804	0.000675	0.010442	14.5	15.470	0.06897	0.06464	0.937	
130	50.000	11	311.487	170	481.487	0.000675	0.009862	14.5	14.611	0.06897	0.06844	0.992	7
130	50.000	10	283.17	170	453.170	0.000675	0.009282	14.5	13.752	0.06897	0.07272	1.054	
130	50.000	9	254.853	170	424.853	0.000675	0.008702	14.5	12.892	0.06897	0.07756	1.125	8

Appendix S
Combustion Calculation

Basic Combustion Chemical Formulation

$$C_aH_bO_cN_d + a_1(O_2 + 3.76N_2) \Longleftrightarrow b_1CO_2 + c_1H_2O + d_1N_2$$
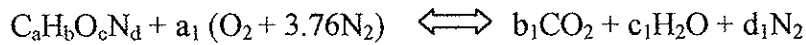
where:

a_1, b_1, c_1, d_1 = molar coefficients

a, b, c, d = fuel components

Combustion Calculation of Fuel Air Equivalence Ratio for Diesel Fuel

Stoichiometric fuel to air can be calculated with:

$$FAR_{stoi} = 1 \text{ mole of fuel}/ a_1(O_2 + 3.76N_2)$$

Flow Rate

1 CFM (Cubic Foot per Minute) = 28.317 LPM (Liter per Minute)

$$V_a = V_{as} + V_{ai}$$

$$m_a = \rho_a V_a$$

$$m_f = \rho_f V_f$$

Appendix S

Combustion Calculation (cont'd)

Air Fuel Ratio (AFR) & Fuel Air Ratio (FAR)

$$AFR_{act} = m_a / m_f \qquad\qquad FAR_{act} = m_f / m_a$$

$$AFR_{stoi} = 14.5 \qquad\qquad AFR_{stoi} = 0.0689$$

Equivalence Ratio Based on Fuel Air Ratio (Φ-FAR)

$$\Phi\text{-FAR} = FAR_{act} / FAR_{stoi}$$

Air Fuel Ratios for Various Fuels

Fuel	Chemical Formula	HHV [kJ/kg] [kg air/kg fuel]	Air/Fuel Ratio Stoichiometric	Fuel/Air Stoichiometric
Methane	CH_4	55,500	17.2	0.05814
Propane	C_3H_8	50,300	15.6	0.06410
Octane	C_8H_{18}	47,900	15.1	0.06623
Methanol	CH_3OH	22,700	6.5	0.15385
Ethanol	C_2H_5OH	29,700	8.99	0.11123
Hydrogen	H_2	141,600	27.2	0.03677
Gasoline	C_8H_{15}	47,300	14.6	0.06849
Diesel	$C_{12.5}H_{22.2}$	44,800	14.5	0.06897

Appendix S

Combustion Calculation (cont'd)

Equivalence Ratio Calculation (Example: Ø = 0.703)

$$\dot{v}_f = 50 m\ell / min$$

$$\dot{v}_f = 0.000833\ell / s$$

$$\dot{v}_f = 0.000000833 kg / s$$

$$\dot{v}_a = \dot{v}_{as} + \dot{v}_{ai}$$

$$\dot{v}_a = (509.706 + 170)\ell / min$$

$$\dot{v}_a = (679.706 / 60)\ell / s$$

$$\dot{v}_a = 11.328433\ell / s$$

$$\dot{v}_a = 0.011328433 m^3 / s$$

$$\rho_f = \dot{m}_f \Big/ \dot{v}_f$$

$$\dot{m}_f = \rho_f \dot{v}_f$$

$$\dot{m}_f = (810)(8.333x10^{-7}) kg / s$$

$$\dot{m}_f = 0.000675 kg / s$$

$$\dot{m}_f = 6.75x10^{-4} kg / s$$

$$\rho_a = \dot{m}_a \Big/ \dot{v}_a$$

$$\dot{m}_a = \rho_a \dot{v}_a$$

$$\dot{m}_a = (1.229)(0.011328433) kg / s$$

$$\dot{m}_a = 0.013923 kg / s$$

$$AFR_{act} = \frac{\dot{m}_a}{\dot{m}_f} = \frac{0.013923 kg / s}{6.75x10^{-4} kg / s} = 20.626$$

$$AFR_{stoi} = 14.5$$

$$FAR_{stoi} = \frac{1}{14.5} = 0.06897$$

$$FAR_{act} = \frac{1}{AFR} = \frac{1}{20.626} = 0.04848$$

$$\phi = \frac{FAR_{act}}{FAR_{stoi}} = \frac{0.04848}{0.06897} = 0.703$$

Appendix T
List of Publications

1. Mohammad Nazri Mohd. Jaafar, Mohd. Shaiful Asrul Ishak, Mohd. Rodzimin Abd. Rahman and Kiran Babu Appalanidu. (April 2002). Emissions Reduction from Oil Burner System Applying Orifice Plate Insertion. *Proceedings of The 4th Asian Science and Technology Congress 2002.*Kuala Lumpur, Malaysia.

2. Mohammad Nazri Mohd. Jaafar, Mohd. Shaiful Ashrul Ishak, Kiran Babu Appalanidu and Mohd. Radzi Md. Yunus. (May 2002). The Effect of Swirler Vane Angle on Reducing Emission from Liquid Fuel Burner. *Proceedings of The 6th Asia Pacific International Symposium on Combustion and Energy Utilization 2002.*Kuala Lumpur, Malaysia.

3. Mohammad Nazri Mohd Jaafar, Mohamad Shaiful Ashrul Ishak and Kiran Babu Appalanidu. (July 2002)..The Effect of Swirler Vane Angle on Reducing Emission from Liquid Fuel Burner. *Proceedings of The 2nd World Engineering Congress.* Sarawak, Malaysia.

4. Mohammad Nazri Mohd Jaafar, Farid Nasir Ani, Kiran Babu Appalanidu, Khandoker Abul Hossain, Ismail Samat and Mohamed Shukri Abdul Mookmin. (October, 2002). The Effect of Swirler Vane Angle on Pollutants Reduction from Liquid Fuel Burner using Downstream injection. *Proceedings of Advances in Malaysian Energy Research 2002.*Kuala Lumpur, Malaysia.

5. Mohammad Nazri Mohd Jaafar, Mohd. Rosdzimin Abdul Rahman, Mohammad Saiful Ashrul Ishak and Kiran Babu Appalanidu. (Disember 2002). Pengaruh Penyelitan Plat Orifis Dalam Mengurangkan Emisi Dari Pembakar. *Proceedings of Jurnal Teknologi Environmental and Process Technology.*Universiti Teknologi Malaysia, Johor, Malaysia.

6. Kiran Babu Appalanidu, Mohammad Nazri Mohd. Jaafar, Farid Nasir Ani and Khandoker Abul Hossain. (February 2003). The Effect of Fuel Injector Position on Emission Reduction from Liquid Fuel Burner. *Proceeding of the Regional Conference on Energy Technology towards a Clean Environment.* Phuket, Thailand.